Impact of Electric Vehicles Penetration on Power System Dynamics

Hengqing Tian

A thesis submitted for the degree of Doctor of Philosophy to Department of Electronic and Electrical Engineering University of Strathclyde

Signed: Hengqing Tian

Date: June 08, 2024

Abstract

In recent years, governments worldwide have been actively advocating for the electrification of the transportation sector to reduce carbon emissions. As a result, the global fleet of electric vehicles (EVs) has undergone significant growth, signifying their increasing importance in the overall power consumption landscape. The unique characteristics of power converters used in EV charging stations have a direct influence on power system dynamics, which necessitates the development of new methods and models to analyse the dynamic performance of distribution networks (DNs) that incorporate EVs.

This thesis presents a novel approach to analysing the dynamic properties of EVs and simulating the dynamic behaviour of EV-rich DNs. These studies focus on two aspects - EV dynamic equivalent modelling and the impact of EVs and their modelling for system-level studies.

From the perspective of dynamic equivalent EV load modelling, this study investigates different charging approaches of EVs, i.e. slow and fast charging. From the perspective of DNs, EVs represent a distinctive type of load characterized by the control loops of interfacing converters. By examining the charging approaches utilized by EVs, this study provides insights into the behaviour of EV loads and their interaction with the distribution networks. It considers the implications of EV charging dynamics on load modelling, recognizing the need to accurately represent the distinctive characteristics of EV loads in power system studies. Through a comprehensive investigation, this research sheds light on the specific features and behaviour of EV loads, facilitating the development of accurate and reliable models for incorporating EVs into distribution network analysis.

On the other hand, this thesis investigates the dynamic characteristics of DNs hosting EVs. As EVs become a part of the overall load in DNs, the research focuses on analysing the dynamic behaviour of the entire network. However, the presence of EVs introduces complicated parameters that influence the system, posing challenges in quantifying differences among extensive simulation results. Consequently, new methods and models are needed to simulate and analyse the dynamic performance of DNs integrated with EVs. Towards this objective, an equivalent model based on variable order

transfer functions, is proposed in this thesis, to analyse the dynamic properties of EVs as well as to simulate the dynamic behaviour of EV-rich DNs. Furthermore, the study quantifies the influence of EV penetration levels on DN dynamics using a set of metrics. This analysis contributes to a better understanding of the effects of increasing EV penetration on the overall network behaviour. Additionally, a parametric analysis is conducted to validate the applicability of the proposed equivalent model for the dynamic analysis of DNs under specific EV penetration levels. Finally, guidelines for the derivation of generic parameters for the developed equivalent model are proposed.

Acknowledgements

This research and thesis are funded by the University of Strathclyde Studentship, and supervised by the primary supervisor Dr. Panagiotis Papadopoulos, and the secondary supervisor Prof. Graeme Burt.

In the past, I held the belief that research primarily involved solving unanswered questions, driven by my curiosity to explore new realms. However, during my PhD journey, I've come to realize that research transcends mere problem-solving. It encompasses a comprehensive range of activities, extending beyond the technical aspects of investigation. While I cannot yet provide a definitive conclusion, I recognize that this endeavour is not limited to research projects alone.it is a reflection of my own growth and development. The PhD experience has broadened my perspective, allowing me to observe and learn from the world in a more systematic manner, leading to more reliable and accurate conclusions.

So, thanks to this interesting and colourful world, thanks to all the people who want to know more truth, and thanks to my colleagues who are always supporting me, especially my supervisor Panagiotis Papadopoulos, who gives me the most direct help and advice when I need it most.

By the way, hope the work in this thesis can benefit the world.

Journal Paper Publications

H. Tian, D. Tzelepis, and P. N. Papadopoulos, "Electric Vehicle Charger Static and Dynamic Modelling for Power System Studies," *Energies*, vol. 14, no. 7, p. 1801, 2021. doi: 10.3390/en14071801

H. Tian, E. Kontis, G. Barzegkar-Ntovom, T. A. Papadopoulos, and P. N. Papadopoulos, "Dynamic modeling of distribution networks hosting electric vehicles interconnected via fast and slow chargers," *International Journal of Electrical Power & Energy Systems*, vol. 157, 2024. doi: 10.1016/j.ijepes.2024.109811.

Conference Poster

Hengqing Tian, Investigate the feature of EV penetrations into the distribution network on the dynamic load model aspect, Poster presented at the Manchester Energy and Electrical Power Systems Symposium (MEEPS 2022), University of Manchester, Manchester, UK.

Contents

List of Figures

List of Tables

Glossary of Terms

AC/DC converter: Alternating Current to Direct Current Converter

AI: Artificial Intelligence

CCT: Critical Clearing Time

CO2: Carbon Dioxide

DC/DC converter: Direct Current to Direct Current Converter

DNs: Distribution Networks

DSL: DIgISLENT Simulation Language

dq: Direct-Quadrature

EMT: Electromagnetic Transients

ERLM: Exponential Recovery Load Model

EV: Electric Vehicle

FMU: Function Mock-up Unit

GIS: Geographical Information Systems

G2V: Grid-to-Vehicle

ICEVs: Internal Combustion Engine Vehicles.

IEA: International Energy Agency

MPC: Model Predictive Control

NTS: National Travel Survey

PEC: Power Electronic Converter

PFC: Power Factor Control

PI Control: Proportional and Integral Control

P: Active Power

Q: Reactive Power

R^2: coefficient of determination

RMS: Root Mean Square

RoCoF: Rate of Change of Frequency

SG: Synchronous Generation

SoC: State-of-Charge

TD: Time Domain

V2G: Vehicle-to-Grid

V2H: Vehicle-to-Home

V2L: Vehicle-to-Load

V2M: Vehicle-to-Microgrid

VPPs: Virtual Power Plants

Chapter 1
Introduction

1.1 Background

The impact of climate change on global temperatures is a topic of increasing concern, with excessive emissions of greenhouse gases being the primary cause of accelerated warming [1]. During the last decades, CO_2 emissions from the transport sector have been continuously increasing. In particular, they rose from 5.8 gigatons (GT) in 2000, and CO_2 emissions caused by transportation rose to 8.2 GT in 2018 [2]. As the energy sector is a major contributor to greenhouse gas emissions, it is critical to develop strategies to reduce emissions and mitigate the impact of climate change. It is important to explore the use of advanced statistical methods for load forecasting in the energy sector, to improve accuracy and reduce the need for fossil fuel-based power generation. Moreover, transportation is one of the most important carbon emission channels, which makes transportation decarbonization becoming a key part of supporting climate mitigation goals. Road vehicles are responsible for approximately 75% of carbon emissions [3]. Currently, ICEVs (Internal Combustion Engine Vehicle) are still the most popular type of vehicle in the market. These vehicles use petrol or diesel as fuel and these fuels will emit CO2 after releasing energy. Of course, in some situations, other harmful gases such as Sulfur dioxide (SO2) will also be released due to oil quality, this issue will not be discussed in this thesis. Compared with ICEVs, EVs (Electric Vehicles) require electricity to charge and do not directly emit any greenhouse gases during operation. This feature makes EVs become an alternative transportation method to face the climate change problem, following the successful decarbonisation of electricity networks. In summary, transitioning to zero-carbon electricity sources is crucial for mitigating climate change and achieving a sustainable energy future. To decarbonize the transport sector, several countries across the globe have implemented bans on the sale of new internal combustion engines [2][4], and have also promoted the purchase of EVs via incentive schemes [5][6].

Despite the considerable time that has passed since the inception of EVs, their widespread adoption as a mainstream transportation solution for the general population remains elusive. The market share of EVs remains relatively small compared to traditional fuel-powered vehicles. One of the primary reasons for this is the limitations of EV technology. When compared to ICEVs, EVs have longer charging times and shorter travel ranges.

As technology has advanced and human needs have evolved, EVs have gradually made inroads into various sectors, including logistics, public transport, and private use, over the past few years. This trend has been further encouraged by policymakers who recognize the potential of EVs to help address climate change [7]. For example, the European Union has announced plans to ban the sale of fuel-powered vehicle, thereby promoting the shift towards EVs [4]. Such policy initiatives signal a significant shift towards sustainable mobility, and EVs are expected to play a crucial role in achieving the necessary reductions in carbon emissions in the transportation sector. As a result, it is essential to examine the opportunities and challenges associated with the transition to electric mobility and identify strategies that can accelerate the adoption of EVs [8]. Influenced by these radical policies, an increasing number of vehicle manufacturers have begun to actively develop and sell EVs. Furthermore, due to beneficial policies and enhanced environmental awareness, more consumers are considering purchasing EVs instead of ICEVs. The International Energy Agency (IEA) published an outlook showing that there were more than 5.1 million EVs worldwide in 2018. Consequently, the global EV fleet is increasing at a fast pace. For instance, EV sales in Europe present an increase of two-thirds on a year-on-year level. In China and the United States, EV sales in 2021 tripled and doubled, respectively, compared to 2020 [9][10][11]. This trend is anticipated to intensify further in the near future. If the market share continues to increase by 2 million annually, the global stock of total EV ownership will exceed 130 million by 2030 [12][13]. The adoption rates of EVs across different countries, their impact on the automotive industry, and associated environmental benefits have been analysed in [14].

The global push towards transport decarbonization has seen significant policy developments across various regions. The UK plans to achieve net zero emissions across the entire transport sector by 2050 [15]. The European Union aims to reduce CO_2 emissions from new cars by 55% by 2030 and achieve a 100% reduction by 2035 compared to 2021 levels, as part of its fit for 55 packages [16]. China has set a target for 20% of all new vehicle sales to be new EVs by 2025, with a broader goal of achieving carbon neutrality by 2060 [17]. Japan plans for 100% of new car sales to be electric or hybrid by the mid-2030s, aligning with its objective of reaching carbon neutrality by 2050 [18]. These aggressive goals are a big opportunity for EVs, but also a challenge for EV impacts on power system dynamics.

As the adoption of EVs increases, it is important to recognize that there may be potential problems associated with the shift towards electric mobility. One such issue arises from the fundamental difference between EVs and ICEVs in terms of energy conversion. Both types of vehicles convert stored energy into kinetic energy to facilitate transportation. However, the key difference is that ICEVs convert the chemical energy stored in fossil fuels into kinetic energy, whereas EVs utilize electricity stored in batteries, which is typically generated through chemical processes. As a result, the energy streams of ICEVs and EVs differ significantly, with fossil fuels being sourced from pipelines or tanker trucks and the electricity for EVs being supplied through power networks. The reference [19] compares the life cycle impact of ICEVs and EVs. This difference has implications for the infrastructure and supply chain required to support the shift towards electric mobility and highlights the need to consider the broader impacts of transitioning to EVs, particularly in terms of electricity generation and distribution. Nevertheless, as the number of EVs on the road increases, it becomes increasingly important to recognize that transportation energy will be more reliant on the power system. This poses a new challenge for the operation of the power grid, and it is essential to understand the impact of EV charging from the perspective of the power system. These challenges are mainly related to voltage regulation and power quality issues, increased network losses, and congestion problems created due to the simultaneous charging of several EVs [20][21]. Furthermore, centralized charging of EVs in a region can create a power demand comparable to that of large-scale power electronics charging load, such as those used for aircraft. According to the existing study [22] implies that this substantial charging demand could impact the system frequency stability, which can provide effective primary and secondary frequency responses to improve the frequency nadir by 0.2 - 0.3 Hz under grid disturbance. This will be especially the case for urban regions and during certain times of the day. Specifically, it is important to identify any specific characteristics associated with EV charging and how these compare to existing loads on the grid [23]. Understanding the differences between EV charging and other loads can help to identify the infrastructure and grid-management requirements necessary to support the transition towards electric mobility. By assessing the potential impacts of EV charging on the power system, stakeholders can develop strategies to optimize the utilization of renewable energy sources and minimize the transportation sector carbon footprint.

The frequency response in DNs is crucial for maintaining grid stability, especially with the increasing integration of renewable energy sources and EVs [24]. It is essential to consider the variability of EV load response to meet system requirements and maintain frequency stability by optimizing the daily EV charging profile [25]. EVs can also help stabilize electrical grids by providing voltage support. This involves maintaining stable voltage levels to ensure a reliable power supply. EVs can do this through Vehicle-to-Grid (V2G), Vehicle-to-Home (V2H), Vehicle-to-Load (V2L), and Vehicle-to-Microgrid (V2M) applications [26][27]. Inverter control is crucial for this process, allowing EVs to adjust voltage and frequency dynamically. This helps balance supply and demand, especially during peak times. EV voltage support enhances grid stability, facilitates renewable energy integration, and offers economic benefits to EV owners.

Moreover, as renewable energy becomes increasingly integrated into the electric power network, combining fast charging with renewable energy at central charging stations presents a viable option to harness the benefits of both. The proximity between the power generation source and the consumption point significantly reduces transmission losses. However, this setup introduces new challenges, such as more complex power dispatch requirements. Consequently, the network faces difficulties in accurately determining the timing and duration of charging and generation operations.

Another unavoidable question is how the pandemic has affected the EV market. The COVID-19 pandemic has significantly transformed various aspects of our lives, including our daily routines, work patterns, and transportation choices. With more flexible work arrangements, the need for long-distance commuting decreased. As a result, potential EV buyers reconsidered their transportation preferences [28]. In this context, the EV market has experienced notable shifts. The unprecedented drop in global car sales and the contrasting performance of EVs have been expressed in [29], despite this, the demand for EVs has remained robust [30]. However, the market is influenced not only by demand itself but also by manufacturing processes and supply chains. Amidst the pandemic, disruptions to supply chains, particularly those related to chips and other essential elements, have also had an impact on EV sales [31].

In alignment with the zero-emission objectives for the transportation system and prevailing market trends, EVs have become an increasingly significant load with specific characteristics that cannot be ignored in the electric power network. Consequently, a systematic study of EV penetration into power networks from the perspective of dynamic stability is imperative. The motivation behind this thesis is to address the dynamic characteristics of distribution systems hosting EV penetration. Understanding the dynamic characteristics of DNs is crucial for ensuring stability. By providing a comprehensive summary of the two primary EV charging approaches - slow and fast charging. It further simplifies the converter-based model into a dynamic load model suitable for system-level simulations. Additionally, investigating the influence of varying EV penetration levels by quantifying the dynamic response to transformer tap change events will help in developing robust solutions for future power systems.

1.2 Dynamic modelling for EV charging

1.2.1 EV Charging standards and status

EV is a form of transportation, but from the perspective of the power system, it is considered as a specific type of load when it is charging. To express this load, the first step is to calculate its load demand, which is defined by the EV charging speed. As mentioned in the previous section, EVs have existed in the market for many years, but they have only occupied a small market share for a long time.

The normal charging speed can be defined by the EV charging standards IEC62196 [32], which focuses on physical connectors, and IEC61851 [33][34], which focuses on charging modes and requirements. The Electric Power Research Institute (EPRI) and the Society of Automotive Engineers (SAE) have methodically categorized EV charging levels as AC level-1, AC level-2, and DC fast charging [35]. These diverse charging standards encompass a spectrum of EV charging speeds, ranging from gradual to rapid and ultra-fast charging.

Table 1.1 Charging archetypes as defined by charging locations, charging methods, and charging power.

<table>
<tr><td>Power type</td><td colspan="2">AC</td><td colspan="3">DC</td></tr>
<tr><td rowspan="2">Scenarios</td><td colspan="2">Residential</td><td></td><td colspan="2" rowspan="2">Charging station</td></tr>
<tr><td></td><td colspan="2">On street / public</td></tr>
<tr><td>Speed level</td><td>Level 1</td><td>level 2</td><td>level 3</td><td>Super charge</td><td>Ultra-fast</td></tr>
<tr><td>Charge condition</td><td>120 Volt</td><td>240 Volt</td><td>CHAdeMO/CCS</td><td>Tesla 480 V</td><td>Experimental</td></tr>
</table>

Charge speed	3.7 kW	7.4 kW	11 kW ~ 60 kW	Up to 140 kW	Up to 400 kW
Normal speed			>11 kW	>60 kW	

Table 1.1 combines the information on different charging scenarios. These charging strategies are defined by the network and location conditions. For example, the network in the United States is 110 V, which results in a relatively slow speed of charging. Moreover, some smaller electric transportation vehicles such as electric scooters have even lower charging speeds [34]. Nowadays, 7.4 kW (32A single phase) can be installed in residential areas [36][37]. This is also the main choice for installing chargers in European homes (240V AC supply). Not only can EVs be charged at home, but they can also be charged in public places such as workplaces, streets, and highway service stations. These scenarios can also provide faster charging methods such as CHAdeMO [38] and CCS (SAE Combined Charging System) [39]. These charging methods are supplied by DC power, the actual charging rate is adjusted by the charging piles, normally 11 kW ~ 60 kW.

Not all vehicle manufacturers are following these standards. Some small charge speeds can be about 1.4 kW (110V AC voltage network), but some fast chargers can exceed 60 kW (DC fast charge). For example, the Nissan Leaf has a charging speed of 3.6 kW or 6.6 kW, while the BMW i3 is 7.4 kW, and some new manufacturers have new technologies like the Tesla supercharger that can provide even 250 kW charging speed.

Note that, these DC charging approaches are still developing rapidly, for example, the CHAdeMO 2.0 can provide an “ultra-fast” charging speed of 400 kW. The Tesla charging station is one of the types of “ultra-fast” charge approaches. More and faster charging stations might be added in the future. On the other hand, integrating fast charging with renewable energy at central charging stations presents a promising approach. The proximity between the power generation source and the consumption point significantly reduces transmission losses. However, this setup introduces new challenges, such as more complex power dispatch requirements. Consequently, the network faces difficulties in determining the optimal timing and duration of charging and generation operations. Furthermore, Due to the high power consumption of fast charging, placing the charging station close to the on-site generation source and grid connection points is advisable to minimize transmission losses. However, it is important to note that chargers, being switch-based converters, can introduce harmonics. Conversely, V2G and reactive power control during charging can be beneficial in this setup. It is crucial to consider the differences between chargers, as more commercial and consumer-oriented chargers can complicate the understanding of their operational details by network companies, particularly in response to short-circuit events. However, these experimental products, which have not yet to be a solid standard, are temporarily out of the scope of this thesis.

In 2024, the typical battery capacity for electric vehicles ranges from approximately 60 kWh to 70 kWh [40], Companies like Tesla offer various battery capacity options to customers, with the Model 3 having an approximate capacity of 60 kWh [62], and the Model Y reaching up to 90 kWh [41]. With the anticipated increase in fast charging stations, the duration required for charging is expected to decrease.

1.2.2 Converter-based EV charger modelling

Although EVs primarily serve as a mode of transportation, it is crucial to elucidate their impact from the standpoint of the power system since they can be seen as charging/discharging elements from the sight of the network. There are two main control modes when EVs connect to the power network G2V (Grid-to-Vehicle) and V2G (Vehicle-to-grid). In both modes voltage and current are regulated, ensuring that the power system variables remain within normal operating conditions. This regulation is achieved through a converter-based control loop model.

A converter-based control loop model represents the dynamic behaviour of power converters and their associated control mechanisms within a power system. This model typically encompasses multiple control loops, including voltage and current regulation loops, as well as power control loops, all of which are designed to preserve system stability and optimize performance [42]. Moreover, it possesses the capability to sustain system stability and efficiency maintain the balance between variable power demands and supplies. The model influences system stability by delivering a responsive action to disturbances. The converter-based control loop modelling for EV chargers has been studied in the literature. Some articles focus on its reliability [43] - [46], and some articles focus on optimizing the design of converter-based charging control loops for fast charging [47] - [50], Several scholarly articles have investigated the intricate interaction between the electric system and fuel system in hybrid EVs [51]. In Chapter 3, this thesis will compare and discuss the similarities and differences of these models, and build the two most typical charging approaches (AC slow charge – level 1 and 2; DC fast charge – level 3). Furthermore, the influence of the PI control parameter will also be illustrated. The charger is not the only crucial component of EV charging, but the battery also plays a significant role [52]. This thesis will also investigate the battery features and how they impact EV charging in Chapter 5.

1.2.3 Dynamic load modelling in the presence of EVs

The load characteristics of EVs can have a crucial influence on system stability as EVs exhibit dynamic behaviour in response to disturbances, which is markedly different from traditional load types and the load models that were previously utilized in power systems. This results in more complex dynamic responses that cannot be adequately represented by traditional load model structures. Consequently, there is a necessity for higher-order models and a comprehensive understanding of parameter sensitivities. As demonstrated in the preceding section, a plethora of power electronic charger designs for EV charging already exist. However, despite encapsulating intricate details of EV charging, the converter-based model remains cumbersome for dynamic power system studies involving EVs, since it requires to build the full control loop for each EV charger, with millions of such devices potentially connected. the converter-based model must undergo simplification to be suitable for system-level studies. Therefore, the EV chargers shall be simplified through a dynamic load model, which does not compromise the characteristics that impact system dynamics.

Dynamic load modelling in power systems is a method utilized to simplify the analysis of large-scale power networks by reducing the complexity of the system without compromising the essential dynamics characteristics of the loads. This process involves creating a model that represents the aggregate behaviour of various individual loads which are integrated within the network. The objective is to accurately represent the static and dynamic influence of the original load on the system [53].

In addition, the transfer function is an important part of the dynamic load model which provides the oscillatory behaviour of the dynamic responses [54]. On the other hand, the orders of the transfer function, which refers to the highest exponential parameter of (s) in the denominator, can affect the characteristics of the dynamic responses, such as the first/second or higher type of responses.

V2G is an innovative technology that allows EVs to not only draw power from the grid but also send power back to it. This bi-directional charging capability helps stabilize the power grid by balancing supply and demand, particularly during peak usage times [55]. Although some studies model V2G as a PQ unit [56], V2G is being investigated in various types of studies, such as frequency response [57] and power quality and stability [58]. To accurately represent the characteristics of V2G during EV charge-back to the network, the V2G model must include relevant characteristics of these studies, such as frequency response and the Rate of Change of Frequency (RoCoF).

This thesis aims to utilize a simplified model for EVs to enable system-level simulations within a single software environment, specifically using a dynamic load model. However, the generic dynamic load model [59] does not include characteristics. Note that, essentially, the dynamic load modelling for EVs simplifies the EV charging characteristics to suit the target simulation aspect. This simulation is focusing on the dynamic responses of DNs during a voltage step change event, such as transformer tap changes. Consequently, the resulting EV dynamic load model may be insufficient for other types of studies, such as frequency response, rotor angle stability studies, and V2G. Additionally, this thesis does not contribute to these directions.

Therefore, in this thesis, the EV dynamic equivalent load model will be developed to facilitate static and dynamic analysis of power systems [59][60] by considering different order level based transfer functions.

1.3 System-level studies on the impact of EV penetration

In the context of EV charging in the network, a fundamental question is concerning to schedule the start time and duration of charging, which are strongly related to human behaviour. For instance, some people choose to charge their EVs when returning home in the afternoon, while others prefer a nearby DC fast charger, either on the street or at their workplace. The duration of charging discussions encompasses considerations related to battery capacity and desired SoC thresholds. Notably, modern EVs mostly employ lithium-ion batteries (such as the widely recognized '18650 battery' manufactured by Panasonic), featuring energy capacities spanning 10 kWh to 100 kWh [61][62]. Several studies have extensively analysed EV charging behaviour and human preferences using Monte-Carlo simulation techniques[63][64][65]. However, these articles limit their research to temporal (when the charging starts and ends) and spatial (charge location, home, or workplace) aspects. This thesis contributes to the field of EV charging research from the perspective of power system stability.

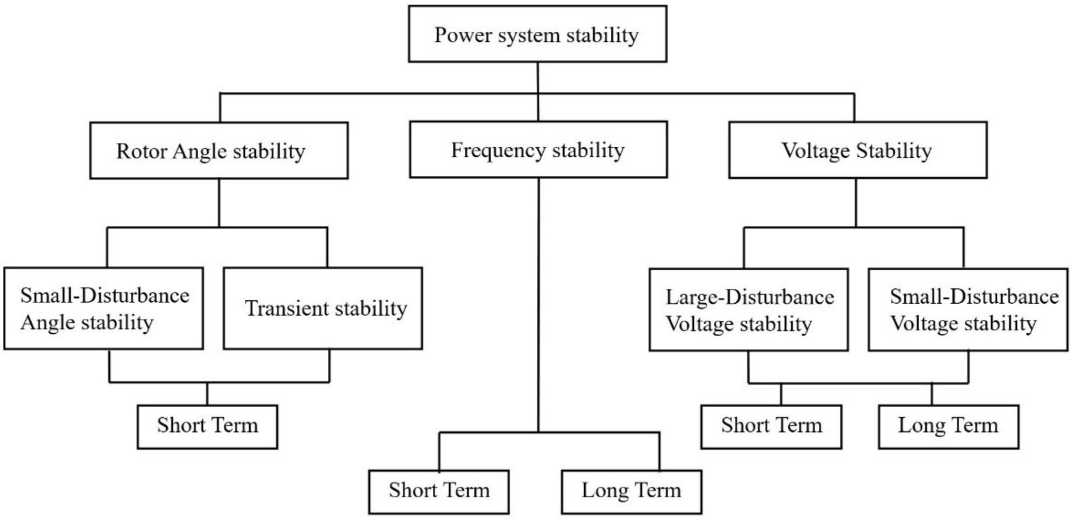

Figure 1.1 Classification of power system stability [60].

Power system dynamic studies analyse the behaviour of electrical power systems over time, focusing on how they respond to disturbances like faults, load changes, and switching operations. These studies examine variables such as voltage, frequency, rotor angles, and power flows. Power system stability studies are a subset of dynamic studies that specifically look at the system's ability to return to a stable state after disturbances. They include transient stability (response to large disturbances), voltage stability (maintaining acceptable voltage levels), and frequency stability (maintaining steady frequency)[66]. This thesis considers the EVs charging in the DNs, and focuses on maintaining acceptable voltage levels under various operating conditions and disturbances, ensuring that the voltage remains within safe limits. In this study, the event selected is a voltage step change, and the output is the dynamic change of power consumption. By the classification of power system stability which is shown in Figure 1.1, this study belongs to the small-disturbance voltage stability.

Based on this small disturbance, this study investigates the impact of various load characteristics, specifically those associated with the EVs dynamic load model. In this thesis, the EV charging static aspect will be represented by using two distinct approaches: the exponential model, which is based on exponential functions, and the ZIP model, which presents the relationship between voltage and power consumption in a steady-state scenario.

In this section, the significance of the EV dynamic load model is underscored, alongside the critical importance of the methodology for integrating it into power system simulations. This methodology ensures an accurate representation of EV charging behaviour, taking into account factors such as load impact and dynamic behaviour. Therefore, the power network, which is integrated with EVs dynamic load model, is capable of conducting system studies, including steady-state and dynamic analysis. The detailed process of this study is expressed in Chapter 3, and these results will also be quantified through indicators.

1.4 Quantifying the differences in dynamic responses

The system dynamics will be affected when the dynamic load model of EVs is integrated into the simulation network. And this influence is strong related to the different EV penetration levels. As more EVs penetrate the DNs as dynamic load models, the DN's equivalent model will exhibit more dynamic characteristics. These dynamic characteristics can be applied to investigate voltage support and network constraint management with high EV penetration scenarios.

The aim of this study is to examine the impact of the system's time-domain response under various EV penetration scenarios. The differences, which scenarios are compared between no-EV and various levels of EV penetration, will be quantified through indicators.

The difference in EVs penetrating the distribution network can be quantified through indicators, such as $RMSE$ (Root Mean Square Error), R^2 (Coefficient of determination), SSE (Steady-State Error), OE (Overshoot Error), which will be utilized to quantify the differences between the network with/without EV penetration. As will be explained in Chapter 4, the control parameter settings of PI (Proportional-Integral control) can significantly impact the EV dynamic load model parameters, which consequently affect its dynamic response. This dynamic recovery may exhibit varying degrees of oscillatory behaviour, and these subtle differences are not adequately captured by existing metrics of differential magnitudes, such as $RMSE$ and R^2.

An additional potential challenge arises from the fact that EV manufacturers do not provide the settings of the control parameters within the EVs. Consequently, all conducted studies are based on case studies, implying that EVs produced by different manufacturers may exhibit varying control parameter settings. From the perspective of the system, the diverse EV dynamic load models with distinct dynamic recoveries can add complexity to the overall system dynamic response. This complex dynamic response necessitates illustration and quantification through appropriate methodologies. This investigation will be presented in Chapter 5.

The distribution network can be analysed as an aggregated dynamic load model, effectively illustrating the dynamic characteristics of the entire distribution system. The methodology is the same as that utilized in EV dynamic load modelling. However, the difference is the more complicated dynamic response may necessitate higher order transfer function during the fitting process. Chapter 5 also delves into the selection of different orders of transfer functions and discusses their applicability under varying conditions.

Additionally, focusing on the dynamic recovery process, this thesis employs the Pole-Zero analysis which is commonly used in control loop stability analysis, to quantitatively assess the detailed dynamic characteristics across different EV penetration levels and control parameter settings.

1.5 Research questions

Definition and Modelling of EVs:

- What are the essential components and behaviours of EVs within the context of power systems?
- What kind of EV model is sufficiently simplified for system-level dynamic simulations while retaining necessary characteristics? During developing this type of model, what method can be utilized to define the model parameters accurately?

Integration into Network Models and Simulations:

- What are the dynamic characteristics of DNs that are affected by varying levels of EV various charging times and penetration?
- How do EVs impact the system-level dynamics of DNs under various operating conditions?
- A significant number of results are expected to be presented as dynamic response curves. What approaches can be utilized to manage and analyse the large volume of dynamic responses while maintaining the integrity of the recovery process details to derive reasonable conclusions?

1.6 Main objectives

Definition and modelling of EVs - The EVs incorporated into the simulation are modelled to represent the existing real-life counterparts. It is crucial to identify the necessary elements for the simulation and determine the level of detail required when modelling the EVs. The objective is to model EVs based on existing literatures, focusing on aspects relevant to power systems, such as the charging process, charging converters, and batteries. This task includes:

- Evaluating the ability of existing static and dynamic equivalent models for the representation of EVs.
- Proposing a modelling approach based on parameter fitting and dynamic equivalent load models to represent the dynamics of EVs.
- Investigating the impact of different control parameters on the dynamic equivalent load model structure.

The objectives of integrating the EV model into system-level simulations. The power consumption of EVs depends not only on the EV model but also on human behaviour, such as the timing of charging based on electricity pricing policies. The objectives include:

- Developing daily charging profiles based on existing literature and integrating these profiles into the CIGRE benchmark MV DNs to simulate.
- Investigating the impact of high EV penetration on DNs, considering different control parameters and operating conditions. The dynamic response

of the network to these scenarios is investigated through typical charging scenarios, such as maximum EV penetration and peak charging times.

- Conducting systematic simulations and statistical analysis, which involves systematically simulating scenarios across various EV penetration levels and system operation conditions. Statistical analysis of error metrics is utilized to identify the impact of EV charging on DNs.
- Obtaining dynamic equivalent models to represent DNs hosting EVs and identifying the optimal order of the transfer function, which aims to represent the detailed dynamic recovery process accurately.
- Analysing the characteristics of the obtained dynamic equivalent models using Pole-Zero analysis, and highlighting significant observed features.

An additional objective examines the impact of reduced charging speeds as EV batteries approach full charge on EV load modelling. It is necessary to investigate the effects of the characteristic on converter-based models and evaluate whether the EV model needs adjustment to represent this state accurately, which involves:

- Investigating the role of the battery model within the overall converter-based EV charge model.
- Identifying changes during high SoC scenarios and their impact on EV dynamic response.
- Integrating the battery model into the converter-based EV charge model and simulating high SoC scenarios to determine whether adjustments are needed.

1.7 Method scope

Methods:

For the modelling method, make the EV model capable of system-level studies with dynamic characteristics. The study analyses the converter-based control model for EV charging, including single/three-phase power supply, IGBT switches, control loop, and PWM modulation. A circuit-based model for the battery will also be considered.

Static and dynamic load modelling methods are applied to develop a dynamic EV charge model suitable for system-level studies. It includes the testing, which is the EV charging converter-based model operating during the dynamic events in DNs. This part of the work shall be implemented by Simulink software. Afterwards, the measurements shall be recorded by the MATLAB Simulink, and the corresponding algorithm, which is expressed in detail, and be applied to implement the EV dynamic load modelling. Furthermore, this task also includes the fitting technique, which is utilized to obtain the transfer function to represent the recovery process of the dynamic load model, the method of assessment is used to quantify the difference between the measured data and the obtained dynamic load model. This process is implemented on MATLAB coding.

For investigating the impact of EV charging in DNs, this study integrates the accomplished EV dynamic load model into DNs and simulates various scenarios. For the method of integrating the EV model into DNs, this study starts with the existing EV charging start/end data from the literature, which has already considered human behaviour and other conditions, and converted it into an EV charging profile. This EV charging profile shall be adjusted by assuming different EV ownership levels, which is utilized to avoid predicting the EV market share in the future. Also, the residential & industrial demand shall be considered and integrated as other components into the DNs. Finally, the daily demand profiles of the DNs, which include different components and EV ownership levels, are prepared for the dynamic stability studies. This process is implemented using MATLAB coding, and the EV dynamic load model will be developed in DIgSILENT PowerFactory through DSL modelling.

Equivalent dynamic load modelling methods are used to analyse the entire DNs' dynamic responses. The dynamic equivalent load modelling and the fitting technique, which have been utilized in EV dynamic modelling, are utilized to achieve this equivalent model. The assessment methodologies, such as $RMSE$ and R^2, are applied. Statistical analysis of error metrics is conducted, and Pole-Zero analysis is utilized to examine dynamic recovery curves. This process is implemented on MATLAB coding.

In order to analyse the dynamic recovery in more detail, the method of Pole-Zero analysis is applied. This method represents the dynamic recovery curve by poles and zero that can analyse a large number of results together to find the underlying laws of various EV penetrations

Conditions:

EV modelling perspective - The study considers different charging approaches (slow & fast) and various control parameters (e.g., PI parameters). And tests under different levels of voltage disturbances.

System-level dynamic studies - The study examines EV penetration, including ownership levels, demand locations, charging times, and the daily load profile of all network loads, considering different types of EVs charging simultaneously.

Assumptions:

Converter based models - The study adapts the existing converter-based control EV charging model into a dynamic load model. The process begins by the selected converter-based EV model from the literature. Any modifications to this model could introduce variables, potentially compromising its accuracy for EV charging. To ensure the final model accurately represents EV charging, no changes are made to the selected converter-based model. Furthermore, this study does not aim to optimize the design of the converter-based EV charging model. The influence of each control component on the dynamic characteristics is analysed in Section 3.2.

Technique for parameters estimation - In the static and dynamic load modelling process, this study employs the parameter estimation technique to derive the parameters for the dynamic equivalent model, which involves determining all the corresponding static and dynamic parameters that affect the dynamic characteristics. Furthermore, assessment metrics are utilized to quantify the discrepancies between the measured and estimated data using specific indicators. Each step of the fitting process is expressed in detail by the algorithm. However, this study focuses solely on the similarity between the measured and estimated data, rather than the parameter estimation technique itself. It does not delve into the development or optimization of the fitting techniques themselves. The detailed process for parameter estimation is described in Section 3.4.

Frequency and Rotor Angle Characteristics – The model must include relevant characteristics to accurately represent EVs (both G2V and V2G) in frequency response and rotor angle stability studies. However, the generic dynamic load model used in this study to simplify the EV charging model for system-level simulations does not include these characteristics. The accomplished EV dynamic load model lacks the detailed frequency and rotor angle characteristics as well. However, these characteristics are essential for V2G studies. Therefore, the EV dynamic model developed in this study is inadequate for V2G studies. The capability and characteristics of the dynamic load model is expressed in Section 3.3.

Dynamic Studies Focus - In system-level studies, there are numerous variables that affect EV penetration levels, such as charge time scheduling and EV market share predictions. In simulations, these variables collectively determine the EV penetration level settings, hence the dynamic characteristics of the dynamic equivalent models. To avoid injecting more independent variables, the EV daily demand profile is derived from existing EV charging start/end simulation data by literature to avoid discussing the differences caused by EV charge time schedule. The ownership level considers different EV ownership levels and includes the scenario where all vehicles are replaced by EVs as the worst case, without predicting EV market penetration. The details of this process are expressed in Section 4.4.2. In summary, this study does not contribute to providing a new EV charge time scheduling or EV market share predictions.

1.8 Thesis contributions

The first main contribution of this thesis is the representation of the dynamic behaviour of EVs through equivalent dynamic load models, along with the investigation of the applicability of typical dynamic equivalent load models in systems with high penetration of EVs. This work employs a typical load modelling methodology, including the exponential recovery and ZIP model, to represent EVs in terms of dynamic behaviour. This research investigates the extent to which these models can accurately represent EVs. The dynamic equivalent load models are developed through rigorous testing of EV charger models, which are derived from detailed converter-based models This contribution also proposes typical parameters for dynamic load model structures that can accurately represent EVs, thereby filling the technical gap of having recommendations for using typical dynamic equivalent load models and associated parameters to represent the dynamic behaviour of EVs. Furthermore, this thesis examines the impact of varying control parameters and generates corresponding sets, which demonstrate that different EV dynamic load models can be influenced by these parameters. Additionally, this thesis contributes to the field by proposing transfer function based dynamic models to represent the EV dynamic recovery process and the particularities of dynamic responses (e.g. the appearance of oscillatory behaviour) across various scenarios.

The second principal contribution of this thesis involves the comparison and quantification of the impact of EVs on dynamic characteristics of the benchmark medium voltage (MV) grid of CIGRE with EV penetration. The study addresses a critical gap concerning the impact of EVs on the DN. By utilizing the existing EV charging scheduling algorithm, this research examines the dynamic response of power networks during voltage disturbance events, considering varying EV penetration levels within a single day across diverse EV ownership scenarios. Building on these accomplished methodologies, this study integrates the implemented EV dynamic load model into the network considering the dynamic equivalent load modelling aspects specifically representing EV charger dynamics. These results are quantified by indicators and combined to provide a comprehensive view of the impact of EVs integrated into the power system.

The third contribution of this thesis involves the introduction of a methodology to quantify the subtle differences that emerge from a complex dynamic recovery process. This process can be decoupled from dynamic responses, by employing Pole-Zero based analysis. To implement the dynamic equivalent model in system level studies, this study constructed the complex dynamic load modelling by DIgISLENT Simulation Language (DSL) in DIgSILENT PowerFactory.

A parametric analysis is performed to validate the suitability of the proposed equivalent model for dynamic analysis of DNs under specific EV penetration levels. Additionally, this thesis presents guidelines for deriving generic parameters for the proposed equivalent model.

Last but not least, one of the significant contributions of this thesis is the exploration of the influence of the battery's SoC (State-of-Charge). The SoC reflect the charging level related to the battery capacity and impact the coefficient such as the battery excitation voltage E_{batt}. This study integrates the conventional electric circuit-based battery model into the control model of the EV charging converter. This research helps in understanding how the SoC during battery charging impacts EV load modelling and whether this influence necessitates adjustments to the implemented EV load modelling.

1.9 Thesis Outline

The remainder of this thesis is organised as follows:

Chapter 2 – This literature review Chapter, begins with an overview of the fundamental concepts and technical aspects of EVs, followed by an exploration of various modelling techniques used in simulating EV behaviour within power networks. Subsequent sections address the methodologies employed in integrating EV models into system-level simulations and analyse the impacts of different EV penetration levels on the dynamic stability of power systems. This review highlights the challenges and future directions in EV-related research, laying the groundwork for the ensuing chapters of this thesis.

Chapter 3 – The aim of this chapter is to develop an accurate dynamic load model for EVs. To achieve this objective, this chapter first reviews and generalizes existing power electronic models for EV charging. Then, this study replicates two typical EV charging converter-based control models from selected literature using MATLAB Simulink. After simulating a voltage step change disturbance event, this study utilizes the dynamic response of the detailed models to implement the EV dynamic load model using a parameter estimation algorithm. Then this study compares the results obtained from the two converter-based control models and analyses their similarities and differences. Furthermore, it investigates the impact of different EV control parameter settings and transfer function parameter estimation on the dynamic load model results. Consequently, this study quantifies their differences using appropriate indicators.

Chapter 4 – The impact of EVs on system dynamic responses at the distribution level is the target of this chapter. To achieve this, the load demand profile of the EVs is determined using a Monte-Carlo based methodology. Subsequently, the dynamic load model of the EVs, derived in Chapter 3, is incorporated into the benchmark CIGRE MV distribution network to assess its capacity to accommodate EV charging.

This study also takes into account the variability in EV ownership per household. Under different predictions of EV ownership per household, extensive simulations are conducted to investigate the dynamic response of the power network at various times throughout the day. These results encompass various penetrations of EVs and other loads. These findings are then compared with scenarios that have the same settings but exclude EVs, and all results are quantified using indicators. Ultimately, this study presents results comprehensively, visualized using boxplots, to provide a clear understanding of the impact of EV charging on the power system dynamic behaviour.

Chapter 5 – This chapter focuses on the complex dynamic response of DNs with increasing penetration of EVs.

Comparative analysis of the results between single and composite type EV penetration, this study identified that the existing quantification indicators are inadequate for discerning detailed differences. This thesis applied Pole-Zero analysis to power system voltage stability analysis to quantify the impact of different conditions on the DNs' dynamic response.

Moreover, this study conducts a parametric analysis to verify the applicability of the proposed equivalent model for the dynamic analysis of DNs under discrete EV penetration levels and quantify the influence of the penetration of dynamic EV models. Overall, this study presents a valuable contribution to the understanding of the complex dynamic response of DNs with high EV penetration levels and provides a tool to support the planning and management of future power systems.

Chapter 6 – This chapter enhances the existing research on EV charging static load modelling by investigating the influence of battery charging at various SoC. It reviews and analyses the features of the battery, and discusses the influence of different battery SoC on EV charging. Subsequently, this study incorporates an electronic circuit-based battery model from the literature. This battery model has also been utilized to extend the existing EV power electronics model. Through this enhanced model, this study examines the impact on EV load modelling using simulation results.

Chapter 7 – This chapter draws a number of conclusions and provides a list of areas of ongoing and future activity that can build upon the findings and outcomes of the research work reported in the thesis.

Chapter 2
Literature Review

2.1 Modelling and parameter settings of converter-based EV chargers

Converter-based EV charging involves complex interactions between power electronic converters, such as rectifiers, inverters, and DC-DC converters, and the power grid [67][68]. The dynamics of these systems can be categorized into static and dynamic characteristics.

In steady-state operation, the converter balances input and output power, stabilizing voltage and current waveforms [69]. It maintains constant charging parameters using feedback loops and aims for a unity power factor to minimize losses [70]. The converter should provide a steady DC output for the EV battery and a sinusoidal AC input from the grid. Efficiency is measured as the ratio of output power to input power under these steady-state conditions.

Dynamic characteristics of converter-based EV charging involve system behaviour during disturbances or transients. Electromagnetic transients (EMT) include fast changes in voltage and current due to switching events or grid faults, often modelled using circuit-based simulations[71][72]. Electromechanical dynamics, though less relevant for EV chargers, can impact grid stability and power quality during large charging events. The converter's dynamic response affects voltage stability, power quality, and frequency regulation. Dynamic control of charging current or voltage is crucial for responding to voltage fluctuations, load changes, or grid disturbances [73].

To summarize the mathematical modelling differences between static and dynamic models for EV charging: Static models use steady-state equations, ignoring time derivatives of voltages and currents. For example, an AC-DC converter in steady-state is modelled as a constant power source with linear input-output relations. Dynamic models handle transients with differential equations for time-varying currents and voltages. These include State-Space models for control dynamics, Switching models for converter behaviour, and impedance models for grid interaction analysis [71].

On the perspective of timescales, steady-state conditions are reached over seconds to minutes, depending on the charging rate and control system. EMT occur in microseconds to milliseconds due to high-frequency switching. Electromechanical dynamics occur in tens to hundreds of milliseconds to a few seconds, especially during grid disturbances or large load changes. Static timescales are longer, while dynamic timescales are shorter. These differences are crucial for understanding the behaviour of converter-based EV charging systems [59].

The simulation of EVs charging in DNs is a comprehensive task, which contains several simulators. Each simulator has its own solver and works simultaneously and independently on its own model [74]. In this simulation strategy, the different part of the simulator relies on the communications and Function Mock-up Unit (FMU) to connect the different simulation interfaces with different simulation software [74]. On the other hand, lots of new challenges arise with the co-simulation. The different simulation tools run in a synchronized manner is difficult to reach and keep reliable [75], the data exchange among different simulation tools is difficult to be efficient and accurate [76]. This thesis focuses exclusively on EV charging in the context of dynamic voltage stability at the distribution grid level. By removing unnecessary simulation components, a simplified methodology is employed, enabling all simulations to be conducted within a single software environment.

When EVs connect to the power grid, they operate in two primary modes: V2G and G2V. In these modes, EVs charge and discharge respectively. Precise control of voltage and current is essential in both modes to maintain the stability and efficiency of the power system. This control is implemented through a converter-based control loop model.

To understand this control, it is necessary to understand the EV charging structure on the power electronic aspect to explore the EV's dynamic characteristics that can be utilized in dynamic load modelling. In [77], a model for EV fast charging stations is developed in the dq (Direct-Quadrature) frame. A multi-timescale modelling approach for fast charging stations is proposed in [78][77]. Moreover, in [79] a dynamic EV model for power system oscillatory stability analysis is developed. Nevertheless, in the abovementioned approaches, detailed EV modelling at the converter level is required. With respect to the dynamic response of EVs, detailed modelling approaches were introduced in [80][81][82], these approaches can represent in detail the dynamic features of EV chargers, such as G2V [83], V2G [84][85] and residential charging [86]. The battery dynamic modelling for EVs has also been implemented in [87]. However, such models are not suitable for large-scale power system stability and dynamics studies due to the increased complexity and required computational effort. Consequently, these intricate power electronic charging models cannot be directly employed in power system-level simulations, necessitating the development and utilization of dynamic load models.

On the perspective of control parameter settings, a Proportional-Integral (PI) controller is a type of feedback controller widely used in referred EV converter-based modelling. It can be seen as a Proportional-Integral-Derivative (PID) controller with a derivative part deactivated [88]. It combines two control actions: proportional and integral, to provide a balanced and effective control strategy.

The proportional component of the PI controller produces an output that is directly proportional to the current error value. The error is the difference between the desired setpoint and the actual process variable. The proportional term helps to reduce the overall error by applying a correction that is proportional to the magnitude of the error. The integral component of the PI controller addresses the cumulative sum of past errors. This term is crucial for eliminating steady-state errors that persist over time. By integrating the error over time, the integral action ensures that any residual discrepancies are corrected, leading to zero steady-state error.

It is important to note that PI control is not the sole method applicable to EV charging. With the installation of additional EV charging converters in parallel, droop control, primary control and secondary control become necessary within the network. Droop control is utilized in microgrids and parallel converter systems, enabling decentralized control. This allows each converter to operate independently without the need for communication links [89][90]. Primary control in a small network with multiple EVs focuses on immediate, local management tasks. It ensures voltage and frequency stability during charging and balances the load among chargers to prevent overloading. This control reacts quickly to changes in demand, such as when multiple EVs start charging at once. By managing these aspects, primary control helps maintain a stable and efficient charging process. Secondary control, on the other hand, functions as a higher-level control mechanism, managing the restoration of system frequency and balancing power supply and demand among various converter-based EV chargers [91]. The secondary control is a crucial element of smart charging system, which coordinating multiple charging stations to balance the network load [92].

In summary, the selection of a control architecture for multiple EV charging within a small network is contingent upon the specific requirements and constraints of the system.

PI control is favoured for its simplicity and robustness, whereas droop control offers advantages in decentralized operation and load sharing. Secondary control provides enhanced performance but introduces increased complexity.

2.2 Dynamic load modelling of EV chargers

Although the converter-based model includes the necessary characteristics for dynamic stability studies, it is excessively complex for integration into system-level simulations. Consequently, a simplified model that retains all essential features is required for effective EV charging system-level analysis. Additionally, there is a notable gap in the study of EV load modelling [47]. This section presents the corresponding studies implemented to establish a dynamic load model for EVs.

In the context of power system dynamic load modelling, this type of model needs to include both static and dynamic characteristics of the load, which account for time-dependent changes, capturing transient behaviours and interactions with the power system through complex differential equations. A precise and appropriate model which both includes the static and dynamic characteristics [93][94][95] has already been established and utilized for power system dynamic load model studies. One of the goals of this chapter is to represent EV charging through these dynamic load models. To achieve this, this study needs to build some typical existing EV charging converter-based control models and test them in voltage step change events, and then, record their dynamic response. Obviously, this dynamic response is affected by the controller of the chargers, such as the PI (proportional and integral) control parameters. These differences affect the dynamic characteristics of the EV [96], which will also be discussed in this study.

On the other hand, artificial intelligence (AI) techniques are increasingly utilized to model the dynamic response in power system stability studies. AI-based methods for creating dynamic equivalent models of power systems significantly enhance the accuracy and efficiency of these models [97][98]. Potentially, these methods can be utilized in EV dynamic load modelling.

2.3 Parameters from the dynamic responses

To accurately represent the dynamic response using target dynamic load model functions, which include the relationship between the voltage supply and power consumption, such as the power and voltage before and after the dynamic events occur and the detailed recovery process. It is essential to quantify the dynamic recovery curve and translate it into a transfer function with well-defined parameters, hence the curve fitting techniques. Not only the vector fitting technique can be utilized to implement the target estimation [100], but also the established toolbox can provide a variety of target fitting function selections [101]. Furthermore, the fitting technique has already been widely utilized in high-order dynamic load modelling [102][103]. This methodology will be utilized in this study to represent EV charging dynamic behaviours by the dynamic load model. The fitting quality which includes results from various fitting transfer functions is quantified through indicators which will also be compared in this chapter. Moreover, curve fitting can also be applied in a measurement-based manner using data from a real EV charger, which could be explored as future work from this study.

Beyond traditional fitting techniques, several advanced methods are employed to model the dynamic response. These include primary frequency response, which models the immediate system response to frequency deviations [99], caused by EV charging or discharging in this study. Secondary frequency response involves the analysis of slower, controlled responses that restore system frequency following a disturbance [100]. High-frequency response modelling captures rapid dynamics through detailed EMT simulations [105]. Additionally, for the system dynamics, virtual inertia provided by EVs addresses the impacts of reduced system inertia, while contingency analysis and dynamic security assessment help model the effects of a sudden loss of generation or load [106]. Loss of infeed in power systems refers to the sudden disconnection of generation units or external imports, causing significant frequency deviations and stability issues. To prevent cascading failures and maintain stability, the system must effectively manage these deviations [107]. Impedance-based oscillation analysis, which examines the impedance characteristics of systems with high power electronics penetration, helps identify and mitigate oscillations, ensuring stable operation and understanding small-signal dynamics [108].

It is important to note that, this study focuses on dynamic voltage stability and does not address frequency or rotor angle stability only necessitates attention to dynamic voltage response.

Although the parameters of the dynamic recovery curve can be derived from detailed modelling of power electronics, only assuming the control loop and parameters are known. In practical scenarios, it is often challenging to obtain all parameters for EV charger converter design due to intellectual property constraints. Furthermore, in system-level simulations, the large number of devices makes it impractical to model each one individually. Therefore, this study aims to achieve precise parameter estimation through measurement-based equivalent models, which facilitate the aggregation of responses in the DNs. Consequently, this thesis utilizes fitted results as the parameters for dynamic recovery curves.

2.4 EV charge time scheduling

Prior to investigating EV charging in the context of power system dynamic stability, it is essential to clarify the power demands associated with EV charging. Furthermore, these charging requirements are influenced by random variables, such as travel distance and charging preference [109][110][111].

Standard charging - This charging plan implies a lack of formal scheduling; it presumes that customers will plug in and charge whenever a charging point is available after completing their last trip. Commonly, this daily charging occurs in the evening when people return home. Consequently, there may be variations in traffic patterns between weekdays and weekends. Moreover, peak charging times often coincide with evening hours. If the EV penetration rate is sufficiently high, it becomes feasible to establish a new daily system that peaks during the evening, corresponding with people's return home.

Multiple tariff charging - This charging plan is based on a market-driven approach to managing energy demand. By offering electricity supply at relatively cheaper rates during specific hours, customers are incentivized to charge their EVs during these off-peak timeframes [110]. For instance, some suppliers provide reduced electricity prices at midnight. Consequently, some customers prefer to charge their EVs late at night rather than immediately upon arriving home. This strategic shift helps mitigate stress on the electricity grid during peak demand hours.

Smart charging - Smart charging is a strategy designed to mitigate peak-time stress on the power grid by shifting energy demand to off-peak hours. In contrast to multiple tariff charging, smart charging depends on control systems to determine charging start and end times, rather than relying solely on economic incentives to influence customer behaviour. Typically, EV mobility during off-peak hours is limited, facilitating efficient charging management.

Note that multiple scheduling strategies can be applied simultaneously, such as coordinate charging, which refers to the strategic management of EV charging to optimize energy use and grid stability by utilizing both multiple tariffs and smart charges [112]. Furthermore, Virtual Power Plants (VPPs) can also be considered, which provide grid services such as balancing supply and demand, reducing peak loads, and enhancing grid stability which requires the smart charging infrastructure [113]. Hierarchical control of EV aggregation involves multiple levels of control strategies to manage large-scale EV charging and ensure that both local and global objectives are met [114].

In the realm of optimization methods, both non-linear and linear techniques have been extensively reviewed. The paper [115] provides a comprehensive overview of various optimization techniques, including non-linear methods, specifically for scheduling EV charging. Additionally, the study [116] explores optimization-based approaches for EV routing and smart-charging. In terms of distribution network-charging demand coordination and co-optimisation, the paper [117] proposes a control strategy aimed at enhancing regional consumption levels. Similarly, the research [118] investigates a coordinated planning method for distribution networks that incorporates demand response. Within the context of model predictive control (MPC), the paper [119] presents an MPC-based optimization for the real-time optimal charging of EV aggregators. Furthermore, the study [120] discusses an MPC strategy that employs mixed integer linear programming for optimal charge scheduling.

Moreover, the V2G technique is also included in the smart charge category, which can be considered as an extension. In this strategy, the power flow between the EV and the power network becomes bi-directional [86][114]. This allows EVs to charge back to the power grid during peak hours to reduce the electricity demand during those periods. In this context, EVs act as a source of energy rather than a load.

Several studies focused the EV charging on the power network, these studies focus on two aspects - Time of start/end and the Place of home/work/station of charging [121] [122].

Regarding the temporal perspective, some studies such as [123][124] assume all the EVs arrive at a specific time with a single fixed energy requirement. For instance, these studies estimated all EVs arrive home and start charging at 6 pm for a set duration. In contrast, some research, such as [125][126], defined that EVs are plugged into the network at different times. Regarding simulation modelling, the time-varying EV load model located at different busbars was performed in [127][128]. A management algorithm for the EV charge in real-time has been developed in [129][130], which also considered the operation conditions of the distribution system. Although these works provided the assumption of all EVs arriving at a given time, there are also some studies based on real-world datasets pertaining to EV charging in a given area. Numerous studies have evaluated the impact of electric vehicles on power demand, including extensive investigations into the EV power demand curve within smart grid environments [131]. Furthermore, certain charging scenarios such as charging in the retail building have been studied in [132]. The research on the spatial and temporal analysis of EV charging demand has also been discussed in [133][134][135]. The algorithm of anticipating the EV load demand in a real distribution power network in the residential-dominated Southside area of Glasgow in the UK, has been implemented by [63][64]. This predicted EV charging demand data from the algorithm has been implemented in this study to present residential area charging demand. Further, some studies also present the optimized methodology to reduce the load pressure on the power system [136]

Regarding the spatial aspect, this encompasses the location, distance, and duration of trips which can be utilized to simulate the arrival time and energy demand of a fleet of EVs. Because the EVs are the replacement for ICEV, the individual trip behaviours are assumed not to change. The US-based travel survey [137] and the UK travel survey [138] have been employed to derive probability distributions of the arrival time of the vehicle in daily drive simulation [139][138]. Additional articles take into account the probabilistic aspect or generate different driving behaviours to analyse the arrival time and charging location [140][141].

2.5 Algorithm of EV charging events

Various EV charging scheduling management methods can be applied to networks and simulations, necessitating efficient and reliable techniques to predict and manage charging events. Two prominent approaches in this domain are the Monte Carlo method and the Markov Chain model [142][143].

The Monte Carlo method utilizes random sampling to simulate diverse scenarios of EV charging events. This technique is particularly effective in addressing the uncertainty and variability inherent in EV charging patterns [63][64]. By generating numerous potential charging scenarios based on probabilistic distributions of driving patterns, charging needs, and station availability, the Monte Carlo method can predict the load on the power grid [142].

Markov Chain models, on the other hand, employ a sequence of possible events where the probability of each event depends solely on the state attained in the previous event [143]. This method is adept at modelling the sequential nature of EV charging events. However, it requires accurate transition probabilities, which can be complex to implement.

Combining Monte Carlo simulations with Markov Chain models, known as Markov Chain Monte Carlo (MCMC) [144][145], leverages the strengths of both methods. MCMC can generate more accurate and realistic simulations of EV charging events by incorporating the sequential dependencies and variability in charging behaviours [146][147].

In addition to Monte Carlo and Markov Chain methods, machine learning methodologies offer powerful tools to address these challenges by predicting charging demand, optimizing charging schedules, and ensuring efficient energy distribution [148][149].

2.6 The Distribution system under study

Subsequently, the impact of EV penetration level on the DN is investigated. Note that in this thesis, EV penetration is defined as the ratio of EV load to the total system load. For this purpose, the benchmark MV grid of CIGRE [150][151] is simulated in DIgSILENT. Several scenarios are considered assuming different EV penetration levels and time-varying consumption profiles. Simulations are performed using typical residential and industrial load profiles. Further, both residential and industrial loads will be defined as ZIP loads with the parameter provided in [152] to ensure they reflect real-world conditions.

2.7 Circuit-based modelling of EV batteries

Despite revolutionary advancements in EV technology, such as DC fast charging, V2G, and plug-in hybrid charging, the battery remains a critical component that dominates the charging speed limitations of EVs, as it is the source of all required energy [109]. These technologies are heavily dependent on battery packs. Consequently, it is imperative to elucidate the role of the battery in EV charging within power system studies and to identify the characteristics of the battery that warrant attention.

The representation of a battery in power system studies is crucial. The literature primarily illustrates three types of battery models: experimental, electrochemical, and electric circuit-based models. Among these, the experimental and electrochemical models are not suitable for modelling in power networks. The electric circuit-based model offers the advantage of representing the electrical characteristics of batteries. This model, in its simplest form, comprises a voltage source in series with internal resistance [109][153]. Therefore, this chapter will employ the electric circuit-based battery model for the study.

In the context of the electric circuit-based battery model, it is essential not only to include the voltage source and internal resistance but also a parameter to signify the stored electrical charge within the battery, commonly referred to as the SoC.

Unlike the batteries used in other electronic devices such as mobile phones and laptops, batteries for EVs require the capacity to manage high power and energy within a cost-effective and spatially efficient framework [109]. From the material perspective, EVs were initially designed to utilize rechargeable lead-acid batteries for short trips. Presently, two primary battery technologies employed in EVs are the Nickel Metal Hydride (NiMH) battery, used in vehicles such as the Honda Civic and Nissan Altima, and the Lithium-Ion (Li-ion) battery, used in vehicles such as Tesla and GM Chevyvolt [154]. Among these, the electric circuit-based modelling of lead-acid batteries has been implemented [153]. The modelling of NiMH batteries can be found in [155], the reference [156] discusses the advancements in NiMH battery technology, covering aspects such as design flexibility, energy, power, environmental acceptability, and cost. The modelling of the Li-ion battery has been presented in [87], and the reference [157] provides a detailed review of the state of the art and future perspectives of Li-ion batteries, emphasizing their immense potential in various contexts.

This study necessitates not only the electronic circuit-based battery model but also the consideration of the upstream AC/DC structure, given its integral role in EVs. The AC/DC component can be composed of a diode and a PFC controller, as depicted in the literature [159][160][161]. Alternatively, this AC/DC component can be implemented via a full-bridge converter, encompassing outer voltage and inner current control [47]. The specifics of this component have been illustrated in Chapter 3. This chapter will concentrate on the variations induced by the battery model when connected under diverse SoC scenarios.

Concerning the distinctions that need to be observed in this study from the perspective of power system load modelling, the modelling will follow the methodologies introduced in references [61][94][95]. Additionally, a precise dynamic load model for EV charging has been implemented in Chapter 3. The work presented in this chapter can be viewed as an extension of this model, considering the charging characteristics under various SoC settings.

Chapter 3
Electric Vehicle Dynamic Load Modelling

3.1 Introduction

3.1.1 Motivation

While EVs are commonly associated with transportation, power system studies recognize them as multifaceted entities. In addition to serving as loads, EVs also function as inverter-based energy sources, particularly in V2G systems. To represent EVs as loads in power system studies, it is essential to comprehend their charging structures and control loops. This understanding enables the identification of specific EV charging characteristics relevant to power system stability simulations. The subsequent step involves selecting an appropriate dynamic load model to represent EVs, considering both their charging behaviour and the requirements of power system dynamic stability simulations. This study investigates the impact of varying PI control parameters on dynamic load modelling in the context of charging control. The primary objective of this chapter is to develop an accurate dynamic load model specifically tailored for EVs, facilitating its utilization in power system dynamic stability analyses.

3.1.2 Contributions

This chapter investigates the extent to which standard static and dynamic load models used in power system studies could represent typical slow and fast EV chargers, as well as their sensitivity to changes in control parameters. Complex detailed models (including the detailed behaviour of power electronics) are initially used to extract parameters for typical load models used in power system studies, following a fitting approach. In more detail, the key contributions of this chapter are the following:

- Detailed models are used to test the capability of a standard dynamic load model commonly used in power system dynamic studies namely, the adopted dynamic load model to represent EV charging dynamic behaviour. Curve fitting is used to define appropriate model parameters for both the static and dynamic load models.
- Different control settings (PI parameters) for two charging approaches (a fast and slow charger) are investigated, showcasing the impact they have on the ability of the exponential recovery dynamic load model to accurately represent the response of EV charging.

- Ultimately, the thesis presents a set of parameters that can be utilised to represent EV charging behaviour for certain control settings and for both static and dynamic responses. Thus, this thesis offers insight into the potential limitations of standard models in representing EV charger dynamic behaviour.

3.2 Charging approaches for EV

EV charging is the process that transfers the electricity from the power network into the battery. These two electrical energy transmission approaches have some detailed differences, which is the placement of AC/DC converter installations as illustrated in Figure 3. 1.

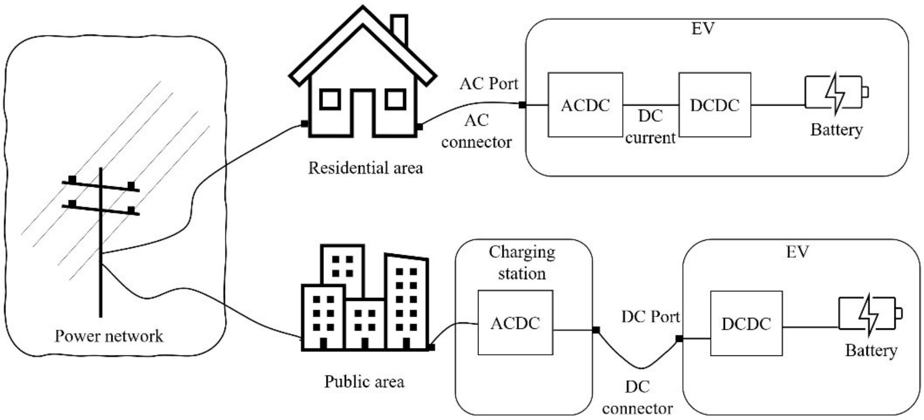

Figure 3. 1. Two typical charging scenarios [109].

Here are two typical charging scenarios, one is charging at home or residential area, and another is in charging stations. Both receive electricity from the power network. The difference is the charging in the residential areas connects the EV to the residential supply voltage which is 230V in the UK. In this scenario, the EV charging cable will be plugged into the AC port, and this approach can be classified as the AC charge. On the other hand, if the EV charges from the charging station, the inbuild AC/DC converter will provide DC current to the DC charge port. In this scenario, the EV will receive DC and convert it into a battery with an acceptable voltage level [109]. This approach can be classified as the DC charge. One thing that needs to be emphasized is that some of the modern manufactured EVs have both AC and DC ports on the build, but only one will be activated in the charging process. Therefore, this study treats them as separate charging approaches. By the end of the charging process is the battery part, Chapter 6 will discuss whether the different battery State-of-Charge will impact the EV charging load modelling in detail.

In this section, two typical models are adopted and utilized to represent a relatively slow (7.4 kW, level-2 charge) and fast charge (~50 kW DC fast charge). The relatively slower charge approach (named "Approach A" in this study) is based on a diode rectifier and a DC/DC converter [159][160][161]. On the other hand, the fast charge approach (named "Approach B" in this study) uses a 3-phase full-bridge converter and a DC/DC converter [47][162]. Approach A is characterised by a simplified control structure, which is popular for residential chargers e.g., level-2, ~7.4 kW). Despite this, approach A has functional limitations (i.e., unidirectional power flow), and it is also inappropriate for smart charging applications. Approach B is characterised by the possibility of bidirectional power flows and fast charging features. For DC fast charging, 50 kW chargers are popular (e.g., ABB Terra 53 [38] and CHAdeMO DC 50 kW quick charger [163]); therefore, the 50 kW charging level was chosen for approach B in the modelling of this section.

From these two charge approaches, both AC/DC and DC/DC exhibit similar dynamic responses. However, the slow charge model is suitable for single-phase charging in residential installations, and the fast charge for three-phase power supply in charging stations. Sections 3.2.1 and 3.2.2 provide a detailed discussion of these two charging approaches. The results, including dynamic response curves and the dynamic load model with parameters, are presented in sections 3.5.2 and 3.5.3.

These approaches are modelled using detailed power converter models in MATLAB/Simulink, in order to obtain the detailed response of EVs charging for small voltage disturbances. These detailed dynamic responses are utilized to establish the static and dynamic EV dynamic load models for power system studies.

3.2.1 Approach A - Typical EV slow charge model (~7.4 kW level-2)

This charging approach is generally used in slow charging and relatively low-power designs, such as electric scooters, which can be charged through the household power supply. The charging approach A consisted of two main parts, one is a diode rectifier [164][165] and PFC (Power Factor Correction) controller [166][167] in order to transfer AC to DC, and another is a DC/DC converter [159][160][161], as depicted in Figure 3. 2.

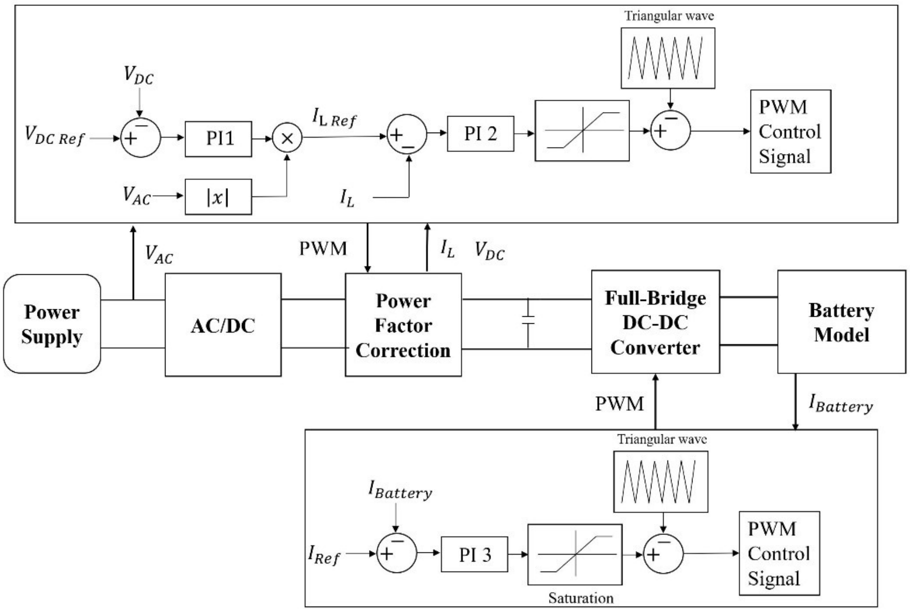

Figure 3. 2. Topology for charging approach A (~7.4 kW, level-2 charge)

Despite, the AC/DC has already provided the DC power supply that can charge the battery, two-stage power conversion (i.e., AC/DC and DC/DC) provides inherent low-frequency ripple rejection and has been used in modern battery charger topology [159][168].

As the structure illustrated in Figure 3. 2, several technologies can be utilized for each part. For example, a diode rectifier can be used on the AC/DC converter [81][169][170]. The purpose of PFC control is to keep the power factor close to 1, which can also be implemented in charger structures. This can be done by appropriately controlling the boost converter between the diode rectifier and the full bridge DC/DC converter as defined in [159][160][171]. The DC/DC part can be implemented by a series-loaded resonant DC/DC converter [160], or even a buck converter [47].

There are three PI (Proportional-Integral) controllers; PI1 and PI2 are located in the AC/DC and PFC components, respectively, and PI3 is located in the DC/DC converter. PI1 compares and integrates the difference between $V_{DC\,ref}$ and V_{DC} . PI2 compares and integrates the difference between $I_{L\,ref}$ and I_L , primarily impacting the power factor by adjusting the phase angle.

In this study, the EV charging approach A is based on the architecture described in [171], which utilised a diode rectifier, a boost converter (including PFC) and a full bridge DC/DC converter.

3.2.2 Approach B – Typical DC fast charge model (~50 kW)

The DC fast chargers are usually not installed in private homes, on the contrary, they focus on public charge stations as shown in Figure 3. 3. Therefore, they can be powered by three-phase power. The Approach B represents the DC fast charge which can physically consist of a full-bridge 3-phase converter and a DC/DC converter [172] as shown in Figure 3. 3 below [47].

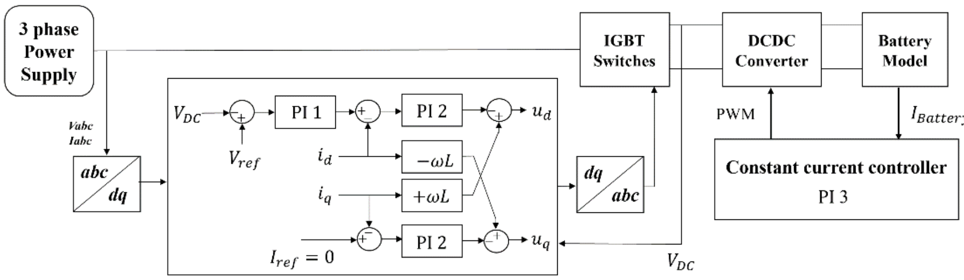

Figure 3. 3. Topology for charging approach B (Level-3, DC fast charge)

Unlike the slow charging approach, which involves placing the AC/DC component within the EV, DC fast charging incorporates a high-power full bridge AC/DC converter in the charging station. This full-bridge converter consists of both outer voltage and inner current control [47][79][162]. The inner current control loop drives the converter based on dq (Direct-Quadrature) currents which are generated by the associated references of the outer control loops. To meet power quality requirements and control the battery charging, a DC/DC converter is also used. Additionally, the DC/DC converter can be part of a battery management unit that regulates battery charging in CC (constant current) and CV (constant voltage) modes [161][173].

The fast charging approach also utilizes three PI controllers, with PI1 and PI2 located in the full-bridge AC/DC converter and PI3 located in the DC/DC converter in front of the battery. PI1 is placed in the voltage outer loop control and adjusts the voltage dynamic response by comparing and integrating the difference between V_{DC} and V_{ref} . This signal will pass to the current inner loop control and adjust the phase angle and power factor by comparing with I_d on the Direct axis and comparing I_q and I_{ref} on the Quadrature axis.

For the purpose of this study, the impact of the built-in DC/DC converters in both Approach A and B on dynamic load modelling is considered negligible. Nevertheless, these structures are retained in the models utilized in this chapter, as the comprehensive development of detailed models fell beyond the scope of this research. Consequently, state-of-the-art models reported in the existing literature were implemented.

In summary, the difference between charging approaches A and B (slow and fast) strongly related to their charging speeds. Slow charging typically uses lower power levels (e.g., Level 1 and Level 2 chargers), which are suitable for overnight charging at home by single-phase. Fast charging, on the other hand, uses higher power levels (e.g., Level 3 chargers or DC fast chargers), usually provided by charging stations by 3-phase, which can charge an EV much more quickly, often in less than an hour.

Indeed, the electrical architecture of approaches A and B is similar, as shown in Figure 3. 1 Both utilize the basic electrical architecture (AC – AC/DC – DC/DC – EV battery), ensuring compatibility and efficiency in converting AC power from the grid to DC power for the EV battery. However, there are detailed differences: for slow charging, the AC/DC converter is installed in the EV and uses a single-phase power supply, whereas for fast charging, it is located in the charging station and uses a three-phase supply. Additionally, as illustrated in Figure 3. 2 and Figure 3. 3, slow charging includes power factor correction, while fast charging employs the abc/dq framework

3.3 Power system dynamic load modelling

The characteristic of the power system load has an important influence on system stability. This characteristic can be divided into two aspects - Static and Dynamic, characterising the responses of active and reactive power to certain power system conditions [54].

The static load model illustrates load characteristics by algebraic functions at any instant of time [174], since it does not contain any dynamic information. The dynamic load model is important to analyse power system dynamic behaviour both in small and large disturbances. It focuses on the response in a period of time, which does not contain steady-state information. Both static and dynamic parts of the load model for both EV charging approaches are analysed in this section.

3.3.1 Structure of the static load model

The static load model expresses load characteristics at any instant of time, the P (Active power) and Q (Reactive power) are considered separately. The relationship between voltage supply and power consumption is fundamental in load modelling. As voltage (V) deviates from its nominal value (V_0), the power consumed by the load changes according to the equations. Traditionally, the voltage dependency of load characteristics is represented by the exponential model:

$$P = P_0(\frac{V}{V_0})^a \tag{3.1}$$

$$Q = Q_0(\frac{V}{V_0})^b \tag{3.2}$$

The P_0, Q_0, are the active power, and reactive power when the supply voltage corresponds to 1 p.u. When the $\frac{V}{V_0}$ is equal to 1 means the active power and reactive power are operating at the nominal voltage. The exponential parameters a and b as shown in equations (3.1) and (3.2) describe the relationship of active and reactive power with respect to voltage [102][175][176]. These exponents determine how sensitive the load is to voltage changes. For instance, if a is greater than 1, the active power increases more than proportionally with voltage. With the exponents a and b equal to 2, 1 or 0, the model represents constant impedance, constant current, and constant power characteristics, respectively.

Not only the exponential equations can be utilized in static load model description, but also a polynomial load model can represent the static features, which can also be named as the ZIP model (Z for impedance, I for current, P for Power).

$$P = P_0 \cdot [p_1(\frac{V}{V_0})^2 + p_2\frac{V}{V_0} + p_3] \tag{3.3}$$

$$Q = Q_0 \cdot [q_1(\frac{V}{V_0})^2 + q_2\frac{V}{V_0} + q_3] \tag{3.4}$$

Both the Exponential function and ZIP function represent the same thing, which is the relationship between the voltage supply and power consumption. The exponential fitted curve to an exponential equation, while the ZIP model follows a polynomial equation, each maintaining their respective mathematical properties. These two methods can be transformed into each other. However, they offer distinct ways to represent the underlying relationships between coefficients. In equations (3.1) - (3.4) , for a constant impedance load, the parameter a in the exponential model should be approximately 2, and p_1 in the ZIP model should be close to 1. For a constant current load, the parameter a in the exponential model should be approximately 1, and p_2 in the ZIP model should be close to 1. For a constant power load, the parameter a in the exponential model should be approximately 0, and q_3 in the ZIP model should be close to 1 [54][102]. The independent parameter in both Exponential functions and ZIP functions is $\frac{V}{V_0}$, which means the per-unit supply voltage.

3.3.2 Structure of the dynamic load model

Static load models in power systems represent loads that remain constant over time, utilizing simple mathematical relationships for steady-state analysis. Conversely, dynamic load models account for time-dependent variations, capturing transient behaviours and interactions within the power system through complex differential equations. One thing that needs to be emphasised is that, the dynamic load model is also called the Exponential Recovery Load Model (ERLM) in the literature [61][94], because its recovery process can be represented by an exponential function in the time domain. It is different from the exponential static load model illustrated in the previous paragraph. The ERLM is concerned with the relationship between time and power consumption, on the other hand, the exponential static load model is related to the voltage supply and power consumption at any instant in time.

The ERLM typically encompasses the instantaneous change at the moment the disturbance occurs and the recovery process in the following seconds. It is expressed as the change of Active/Reactive power over time. On the other hand, the ERLM only supports the exponential function in its recovery process, rendering it inadequate to represent some complicated dynamic characteristics in the recovery process. Given that EVs exhibit dynamic behaviours that significantly differ from traditional types of loads and load modelling in the current power system, the use of exponential recovery may prove inadequate for representing this process. As a result, it may be necessary to employ higher-order dynamic responses to augment the capability of the dynamic load equivalent model.

As shown in Figure 3. 4, the adopted dynamic equivalent model can be seen as a block diagram interconnection of a linear transfer function, described by $G(s)$, and two nonlinear functions, described by f_1 and f_2. The equivalent model receives as input the grid voltage (V_L) and provides as output the real/reactive power response (y_d). The lower branch of the block diagram representation is determined by f_1, which is a nonlinear function that is used to describe the transient part of the real/reactive power response [93]. The upper branch consists of f_2 and $G(s)$. f_2 is a second nonlinear function used to describe the new steady-state of the power, i.e., the new steady-state after the voltage disturbance. $G(s)$ is a linear transfer function used to simulate the recovery response of the real/reactive power.

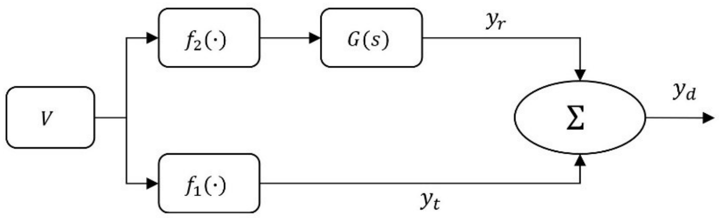

Figure 3. 4. General structure of adopted dynamic load model.

The whole response is divided into two parts as shown in Figure 3. 4, the mathematical expression of the adopted dynamic model is defined as in [103]:

$$y_s(t) = y_0 \left[\frac{V_L(t)}{V_0}\right]^{N_s} \qquad y_t(t) = y_0 \left[\frac{V_L(t)}{V_0}\right]^{N_t} \tag{3.5}$$

$$y_d(t) = y_r(t) + f_1\big(V_L(t)\big) \tag{3.6}$$

$$T_y \dot{y}_r + y_r(t) = f_2\big(V_L(t)\big) \tag{3.7}$$

$$f_1\big(V_L(t)\big) = y_t(t) \qquad f_2\big(V_L(t)\big) = y_s(t) - y_t(t) \tag{3.8}$$

The N_t and N_s are the transient and steady-state voltage exponential parameter that corresponds to the exponential parameter a to equation (2.1) shown above. The output y_d is the time domain real/reactive power response. y_r is the time domain recovery response of the power. y_t and y_s are two exponential functions used to simulate the transient and the steady-state behaviour of the power response, respectively. V_L is the load voltage, that corresponds to V from equations (3.1) ~ (3.4). The V_0 and y_0 are the voltage magnitude and the total power consumption prior to the disturbance.

As shown in Figure 3. 4, a transfer function has been utilized to represent the recovery process, it makes the dynamic load model better capable of representing a more complicated recovery process. The implemented dynamic load model consists of a transfer function and two nonlinear functions [61]. The input time-varying voltage $V_L(t)$ is shown in (3.6) and (3.7).

On the other hand, the ERLM only contains an exponential function to represent the dynamic recovery process, which can be seen as a 1st order transfer function in the Laplace domain. In order to represent the higher order transfer function based oscillatory response, in this study, the exponential function in ERLM will be replaced by transfer function $G(s)$, which is capable of having the same order level as the oscillatory recovery, to make the model become the adopted load model [102].

$$G(s) = \frac{\beta_\nu s^\nu + \beta_{\nu-1} s^{\nu-1} + \cdots + \beta_0}{s^\mu + \alpha_{\mu-1} s^{\mu-1} + \cdots + \alpha_0} \tag{3.9}$$

The component in upper branch $G(s)$ is a transfer function used to approximate the recovery response of power. One thing that needs to be emphasised is that, the parameters $\nu < \mu$, to ensure that the load recovery is continuous. Set of parameters $\theta = [N_s, N_t, \beta_\nu, \beta_{\nu-1}, \dots \beta_0, \alpha_{\mu-1}, \dots \alpha_0]$ will be specified using measurements.

Here is an example to illustrate the adopted dynamic load model response in the following Figure 3. 5.

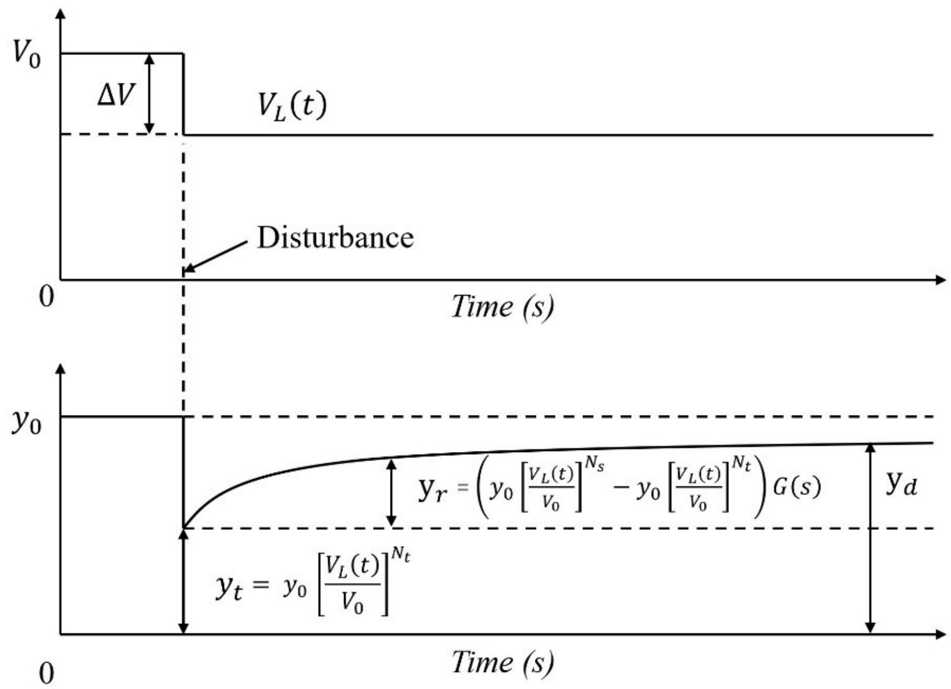

Figure 3. 5 The adopted dynamic load model

The voltage supply $V_L(t)$ has a step change in the disturbance that occurs. Corresponding to the dynamic power consumption y_d also has the instantaneous step change at the same time, and the transient power consumption is y_t. Regarding to the dynamic characteristics of the load model, there is a recovery after that instantaneous change, the amplitude of this recovery can be calculated by y_t, which has also been expressed in equation (3.7). The static load model in power systems represent loads in the steady state, which means the steady state component $y_0\left[\frac{V_L(t)}{V_0}\right]^{N_s}$ is the static load model in Figure 3. 5.

The dynamic model can be utilized in representing different loads such as EV by adjusting the parameters among these equations. The method to access the parameters from measurement data is expressed in Section 3.4.

3.4 Technique for parameter estimation

The required set of parameters, i.e., $\theta = \left[N_s, N_t, \beta_\nu, \beta_{\nu-1}, \dots \beta_0, \alpha_{\mu-1}, \dots \alpha_0\right]$, is estimated using the iterative procedure of Algorithm-1, presented in Table 3. 1, A detailed analysis of all required steps is provided in the next paragraphs.

Table 3. 1. Algorithm for parameter estimation.

Algorithm-1: Pseudocode for the parameter estimation
Step-1: Record voltage $V_L(t)$ and power $y_d(t)$ responses. Determine the desired tolerance, i.e., tol
Step-2: Filter the recorded responses using an LPF
Step-3: Determine the optimal window length
Step-4: Compute N_t and N_s exponents using (3.10) and (3.11), respectively
Step-5: Calculate f_1 and f_2 in TD using (3.8)

Step-6: Calculate $y_r(t)$ using (3.6)

Step-7: Set $\mu = 0$ and $R_0^2 = 0$

Step-8: Set $\mu = \mu + 1$ and **Repeat** Steps 9 to 11

Step-9: Compute a μ order approximation for the $G(s)$

Step-10: Compute $\mu = \mu - 1$ in TD, using (3.14)

Step-11: Compute R_μ^2 and $\varDelta R^2$

Step-12: **Until** $\varDelta R^2 < tol$

Step-13: Finalize model with order equal to $\mu - 1$

The main steps of the proposed Algorithm are explained below:

Step-1: When a disturbance occurs, the resulting voltage and power dynamic responses are recorded. In this study, data is recorded from simulation from MATLAB Simulink. The user also defines the desired tolerance (tol). tol is a predefined tolerance threshold used to determine the desired order μ. Further information about tol is provided in **Step-12.** The voltage $V_L(t)$ and power $y_d(t)$ can be obtained by the detected dynamic response directly.

Step-2: The recorded responses are filtered using a low pass filter (LPF).

Step-3: Prior to the parameter estimation, the optimal length of the window analysis is determined using the method of [103].

Step-4: Exponents N_t and N_s are determined using (3.10) and (3.11), respectively.

$$N_t = \frac{log\left(\frac{y_+}{y_0}\right)}{log\left(\frac{V_+}{V_0}\right)} \tag{3.10}$$

$$N_s = \frac{log\left(\frac{y_{ss}}{y_0}\right)}{log\left(\frac{V_{ss}}{V_0}\right)} \tag{3.11}$$

Here, V_+ and y_+ denote the voltage magnitude and power consumption immediately after the disturbance, respectively; V_{ss} and y_{ss} express the voltage magnitude and power consumption at the new steady-state. The (3.10) and (3.11) can derived using formula (3.5).

Step-5: f_1 and f_2 are computed in the time domain (TD), using (3.8).

Step-6: The recovery response of the power (y_r) is calculated using (3.6).

Step-7: Set $R_0^2 = 0$.

Step-8: Set the estimated order μ for the transfer function and execute Steps 9 to 11.

Step-9: Compute a μ order the approximation for the characteristic function $G(s)$ and determine the corresponding parameters, i.e., $[\beta_v, \beta_{v-1}, \dots \beta_0, \alpha_{\mu-1}, \dots \alpha_0]$. Parameters are estimated using $tfest$ function in MATLAB.

Step-10: The estimated power response, i.e., $y_{est}(t)$, is computed. For this purpose, the estimated recovery response, i.e., y_{est} is initially calculated via the $lsim$ function in MATLAB, using as inputs the identified transfer function $G(s)$ and f_2. Afterwards, y_{est} is calculated via (3.12).

$$y_{est}(t) = y_{r,est}(t) + y_t(t) \tag{3.12}$$

Step-11: The coefficient of determination for the μ -th iteration, i.e., R_μ^2, is computed via (3.13)

$$R_\mu^2 = \left(1 - \frac{\sum_{n=1}^{N}(y_d[n] - y_{est}[n|\boldsymbol{\theta}])^2}{\sum_{n=1}^{N}(y_d[n] - \overline{y}_d)^2}\right) \tag{3.13}$$

$$\Delta R^2 = R_\mu^2 - R_{\mu-1}^2 \tag{3.14}$$

In the above notation, *N* is the total number of TD samples. $\overline{y}_d$ is the mean value of y_d. For the first iteration of Algorithm-1, R_0^2 is set to zero. A R^2 value equal to 100% denotes a perfect estimate.

Step-12: If ΔR^2 is lower than the user defined tolerance, i.e., tol, then the Algorithm moves to **Step-13**. Otherwise, the Algorithm moves back to **Step-8** and a higher order approximation for the $G(s)$ function is computed.

Step-13: The fulfilment of the ΔR^2 criterion implies that the accuracy of the model is not increased between the last two iterations. Therefore, to ensure that the developed models will have the lowest possible complexity, the Algorithm terminates by setting the model order to $\mu = \mu - 1$.

3.5 Dynamic load modelling and parameterization of EVs

In this section, both static and dynamic parameters will be identified. The process is divided into two steps, the first step is clarifying the static load model parameters such as N_s and N_t by exponential static load model, Subsequently, the parameter for this study determines the parameters for the ZIP model as well.

The second step focuses on the modelling of the dynamic recovery process. A parameter estimation algorithm is used to implement the fitted model based on different order levels of transfer functions. The recovery curve will be affected by the choice of PI control parameters. This study will also analyse how these selections vary and determine the most appropriate fitting method for different scenarios. The quantification indicator R^2 value will identify which is better to be utilized in the EV load model.

In the context of EV charging, reactive power consumption is typically negligible. This is primarily due to the inherent characteristics of the charging process. The AC supplied by the grid is converted into DC within the charging system to facilitate the charging of the EV's battery. Reactive power, quantified in VAr (Volt-Amps Reactive), is essentially provided by the phase differential between the voltage and current. Given that the EV charging process does not actively generate this phase differential, the EV can be seen as a load that only consumes active power. However, depending on the design of the charging system and the characteristics of the electrical grid, it cannot guarantee that reactive power consumption will always be zero [177]. Therefore, only the active power aspect will be considered in this study.

3.5.1 Static load model parameters for charging Approaches A & B

As illustrated from equations (3.1) and (3.3), the static load model characterises the relationship between the supply voltage and active power exchange for EV chargers. The active power output at each voltage level is obtained from detailed simulations after they reach steady-state values. The curve fitting analysis was performed to determine the static load model parameters for the active power, as expressed in equations (3.1) and (3.3). Both exponential function and polynomial function fitting can be easily obtained by the CFTOOL [101] in MATLAB. The results of the fittings of the exponential and ZIP static models, respectively, are shown in Figure 3. 6.

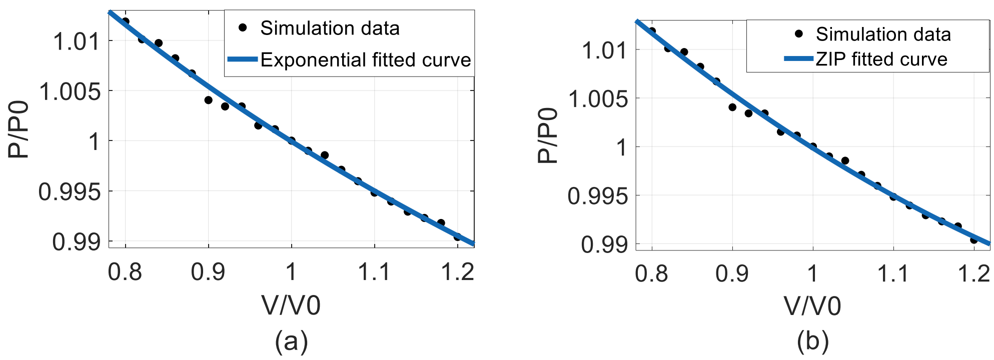

Figure 3. 6. Simulation & curve fitting results for active power and charging approach A: (a) exponential model, (b) ZIP model.

The range of voltage in this study is 0.8 p.u. to 1.2 p.u., the active power does not show a significant change within this range, indicating that the EV charger exhibited behaviour close to a constant active power load. This is observed for the exponential and ZIP models.

In particular, the curve fitting exercise produced numerical results, as presented in Table 3. 2. For the exponential model, the corresponding parameter is very close to 0; for the ZIP model, the P parameter is close to 1. Such numerical results indicated that an EV could be treated as a constant power load when operating in charging Approach A.

In a similar manner, the static model parameter under Approach B is also obtained. Which is presented in Figure 3. 7. The produced numerical results for the static load parameters for the exponential and ZIP models are presented in Table 3. 2.

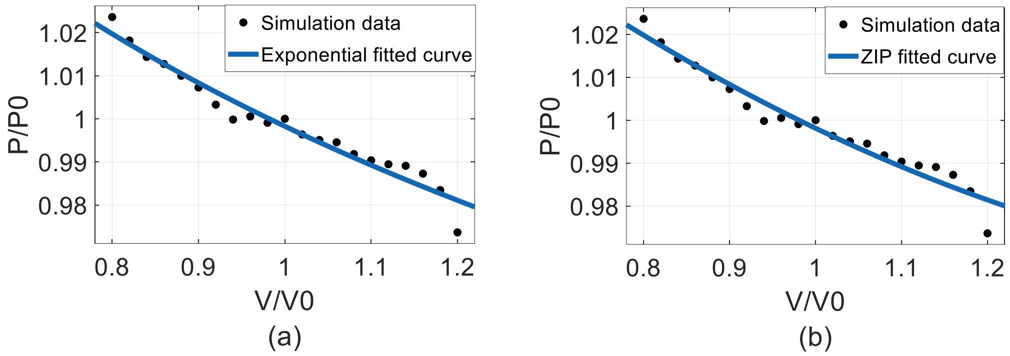

Figure 3. 7 simulation & curve fitting results for active power and charging approach B: (a) exponential model, (b) ZIP model.

Overall, the trends of active power consumption are the same as Approach A, albeit with a slightly larger deviation. Consequently, the EV charging characteristic, in this case, is also close to a constant power load. this result can also be verified from Table 3. 2 - the active power exponential load model parameter was close to 0 while the P parameter from the ZIP model was close to 1. To summarize: the exponential and ZIP models can both represent EV charger static behaviour.

Table 3. 2 Static load model parameters for EV charging

EV Charge Static Load Model Parameters				
Charging type	**Exponential parameter**	**Parameter Z**	**Parameter I**	**Parameter P**
Approach A	-0.052	00034	-0.1199	1.086
Approach B	-0.092	0.0620	-0.2199	1.156

3.5.2 EV dynamic load model for AC voltage single phase charging

As the detailed EV converter-based control model presented in Figure 3. 2, the dynamic response can be measured by voltage step changes for various sets of parameters under the different PI controllers. Then, the measured responses were used to fit the parameters of the typical dynamic load model structure.

It needs to be emphasised that, both charging Approaches A & B have three controllers, PI1, PI2, and PI3, in this study. The PI1 controller corresponds to the voltage outer loop, the PI2 controller to the current inner loop, and the PI3 controller to the DC/DC battery charge loop (depicted in Figure 3. 2 and Figure 3. 3). It is important to understand the distinctions among these PI controllers influence the dynamic response curve., hence, influence the EV dynamic load modelling. It is necessary to figure out whether and how these PI controllers affect the dynamic response, and how the P and I parameters affect the dynamic response respectively.

This study utilized Simulink to connect the voltage source directly to the EV model. Consequently, the 5% voltage step change in the simulation reflects an actual voltage change. This voltage variation is implemented by controlling the voltage source. To investigate the proportional parameter influence, Figure 3. 8 presents the effect of the proportional gain of PI1. Decreasing the proportional gain caused the behaviour of the model to become less oscillatory and to deviate from 1st order responses. In this situation, the $G(s)$ in (3.9) needs to become a higher-order transfer function that can represent the dynamic response precisely.

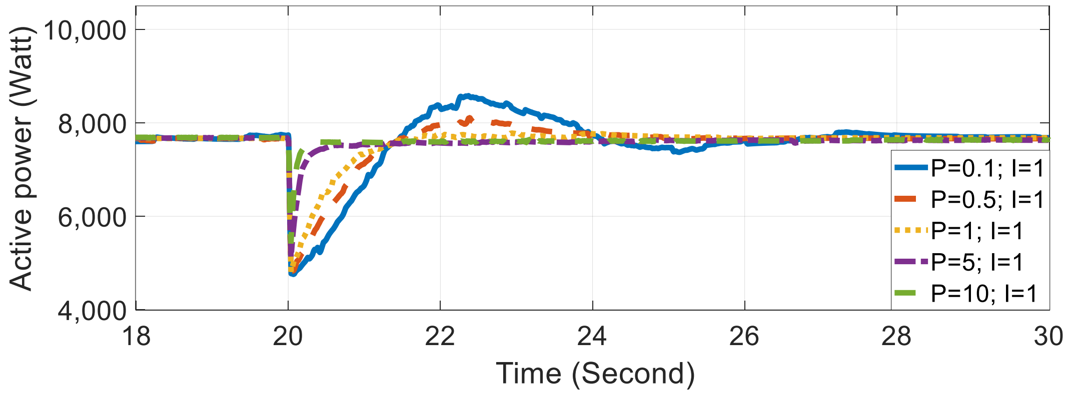

Figure 3. 8. Dynamic response for different proportional gain values of PI1 for a −20% voltage

In the charging approach A, PI1 had a significant influence on the dynamic response of the model when a disturbance was caused on the AC side. On the other hand, PI3, which is placed on the DC/DC converter, does not affect the overall response of the model as Figure 3. 9 shows below.

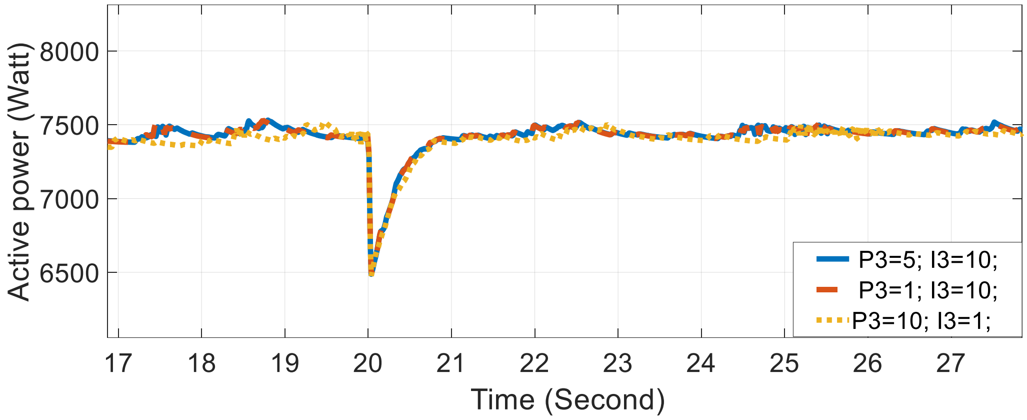

Figure 3. 9. Comparison of dynamic response by different DC/DC PI parameter settings for −5% voltage disturbance (P1 = 1; I1 = 0.1; P2 = 10; I2 = 5).

The amplitude of the voltage step disturbance can impact the dynamic response. For additional clarity, Figure 3. 10 presents the response of the EV model for P1 = 1 and I1 = 10 for different voltage step disturbances (both increased and decreased) ranging from 5 - 20%. These data further highlight that the response was closer to a 2nd order system which can effectively present oscillatory behaviour.

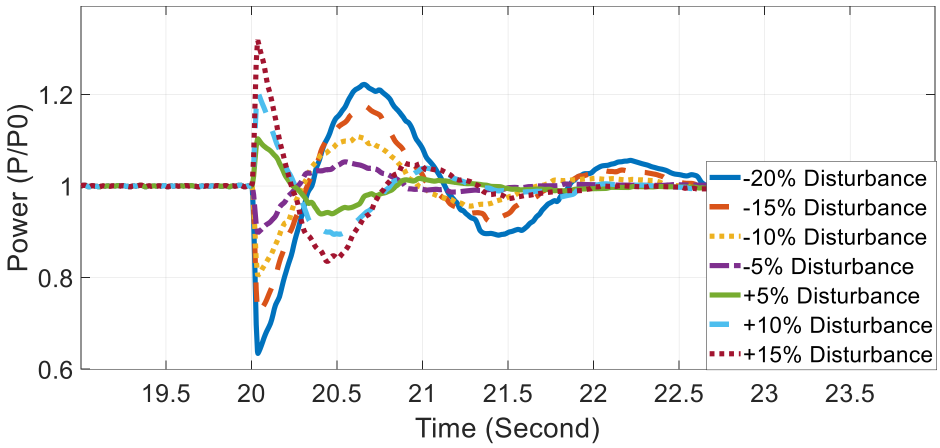

Figure 3. 10. Dynamic response for control approach A, considering different voltage disturbances (PI settings: P1 = 1; I1 = 10; P2 = 10; I2 = 5; P3 = 5; I3 = 10.

To investigate the impact of integral parameters on dynamic response is also important. Initially, the impact of PI settings of the EV chargers on the resulting active power dynamic responses is demonstrated via a simple example. For this purpose, a -15% voltage disturbance is simulated and six cases for the PI values are considered. In particular, for Case#1, Case#2, and Case#3 the value of the proportional term is set to 1, i.e., P=1, while the value of the integral term (I) is set to 0.1, 1, and 30, respectively. For Case#4 and Case#5 Case#6, it is assumed that I = 0.1 I = 1 and I = 30, respectively. For

Case#4 Case#5 and Case#6 the proportional term is set to 10. The resulting active power dynamic responses for each of the examined cases are summarized in Figure 3. 11.

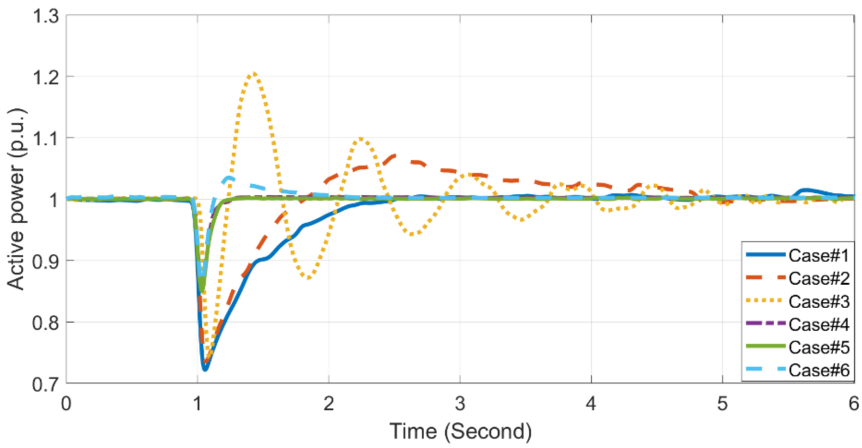

Figure 3. 11. Dynamic response for the different values of integral gain of PI1 for a −20% voltage disturbance occurring at the 20th second; P2 = 10; I2 = 5; P3 = 5; I3 = 10

The results demonstrate that the proportional parameter significantly influences the power recovery time. Specifically, a higher value of the proportional term leads to faster recovery. Additionally, the integral term significantly impacts the dynamic behaviour of power during the recovery phase. As the value of the integral term increases, the recovery phase becomes more oscillatory. The presented results verify that based on the PI settings different order equivalent models are required to accurately capture the dynamic behaviour of the power. This is further exemplified in Figure 3. 12 where equivalent models are developed for Cases#1, #2 and #3.

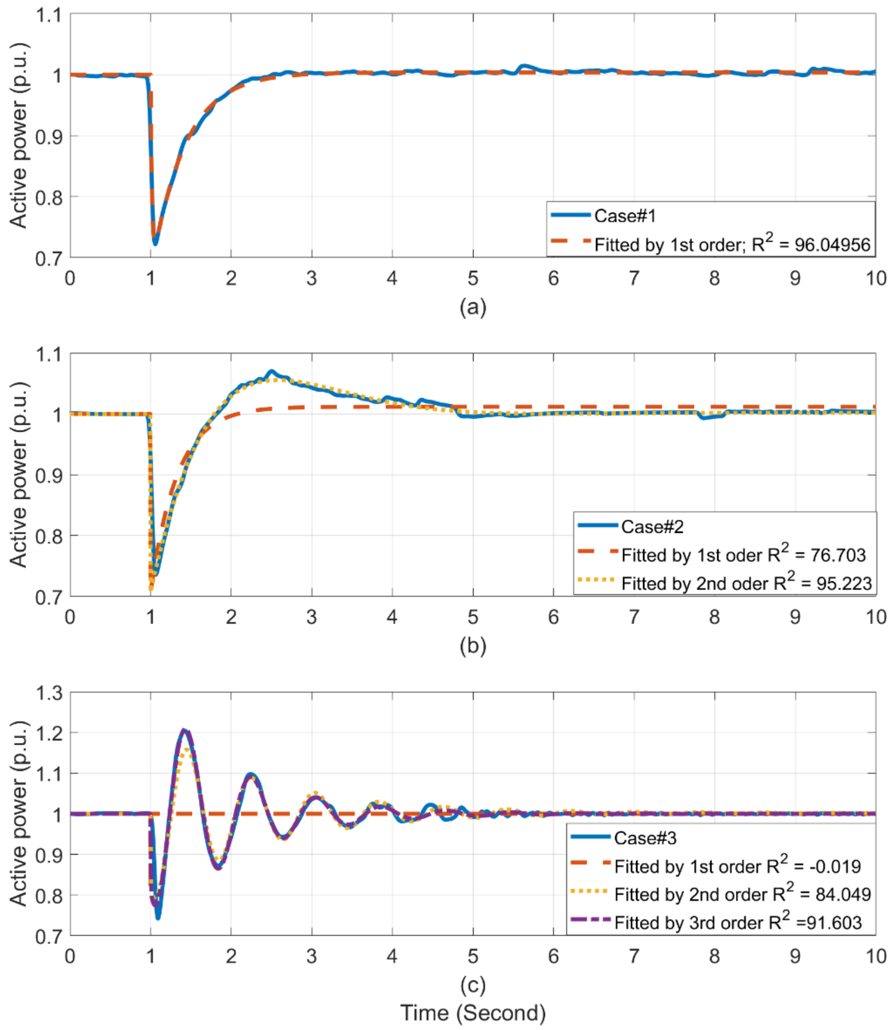

Figure 3. 12. Representative curve fitting results for slow charging. Comparison of the fitted curve and original response data from charging slow charge, considering -15% voltage disturbance. (a) measured data from EV charge power electronics model controlled by P = 1; I = 0.1; (b) controller setting as P = 1; I = 1; (c) controller setting as P = 1; I = 10.

As the fitting result in Figure 3. 12, a 1st order dynamic equivalent model is inadequate to analyse the dynamic behaviour of the EVs for all possible PI settings. Indeed, a 1st order model cannot capture the oscillatory behaviour that may be exhibited due to high integral gains. This is clearly demonstrated in Figure 3. 12(b) and Figure 3. 12(c). Under these conditions, higher order equivalent models are required. In the presented example, a 1st order equivalent is not adequate for the modelling of Case#2 and Case#3. For these cases, a 2nd order equivalent model is required. It shall be noted that using the proposed approach, this study has recorded the fitting results obtained from the 1st 2nd and 3rd transfer functions. These results serve as a basis for comparing their respective fitting qualities and details. In addition, in a high integral setting scenario, such as Figure 3. 12(c), the 2nd order equivalent is also not adequate for the modelling. In this case, the 3rd order equivalent is necessary to be utilized.

Further, the higher order transfer function does not mean better fitting quality such as some inappropriate fitting results illustrated in Figure 3. 12, and the corresponding R^2 value shown in Table 3. 3.

Table 3. 3 Dynamic load model parameters for slow charge Approach A

Model	Order	N_s	N_t	R^2	β_2	β_1	β_0	α_3	α_2	α_1	α_0
P=1; I=0.1	1	-0.052	2.257	96.049			2.23			1.00	2.26
P=1; I=0.1	2	-0.052	2.257	96.214		2.04	4.32		1.00	3.94	4.39
P=1; I=0.1	3	-0.052	2.257	98.863	3.41E+04	2.85E+04	4.97E+06	1.00	4.74E+04	2.19E+06	5.05E+06
P=1; I=0.5	1	-0.052	2.137	88.162			2.60			1.00	2.59
P=1; I=0.5	2	-0.052	2.137	96.089		2.00	1.02		1.00	2.15	1.05
P=1; I=0.5	3	-0.052	2.137	91.902	1.73E+03	-4.68E+03	2.10E+05	1.00	2.82E+03	7.61E+04	2.09E+05
P=1; I=1	1	-0.052	2.131	76.703			3.04			1.00	3.01
P=1; I=1	2	-0.052	2.131	95.224		2.01	1.94		1.00	2.11	1.98
P=1; I=1	3	-0.052	2.131	94.812	1.79	7.94	5.77	1.00	5.08	8.50	5.90
P=1; I=10	1	-0.052	2.107	33.938			7.19			1.00	7.21
P=1; I=10	2	-0.052	2.107	96.179		1.76	19.99		1.00	2.00	20.35
P=1; I=10	3	-0.052	2.107	96.183	1.67	25.42	58.19	1.00	4.94	26.23	59.31
P=1; I=30	1	-0.052	2.236	-0.019			6.17E+04			1.00	6.35E+04
P=1; I=30	2	-0.052	2.236	84.049		-0.82	58.00		1.00	1.89	59.69
P=1; I=30	3	-0.052	2.236	84.095	-0.86	58.10	81.33	1.00	3.34	62.48	83.74

P=10; I=0.1	1	-0.052	1.756	86.664			10.12			1.00	10.53
P=10; I=0.1	2	-0.052	1.756	91.651		-3.52	419.37		1.00	35.49	4.37E+02
P=10; I=0.1	3	-0.052	1.756	95.542	9.73E+03	-2.76E+05	1.35E+07	1.00	1.65E+04	9.17E+05	1.40E+07
P=10; I=0.5	1	-0.052	1.807	86.620			10.07			1.00	10.56
P=10; I=0.5	2	-0.052	1.807	92.275		-2.88	3.72E+02		1.00	31.66	390.83
P=10; I=0.5	3	-0.052	1.807	95.495	1.31E+04	-3.93E+05	1.88E+07	1.00	2.39E+04	1.30E+06	1.98E+07
P=10; I=1	1	-0.052	1.849	85.938			9.80			1.00	10.31
P=10; I=1	2	-0.052	1.849	91.809		-3.38	364.58		1.00	31.48	3.84E+02
P=10; I=1	3	-0.052	1.849	94.840	1.37E+04	-4.22E+05	1.92E+07	1.00	2.56E+04	1.36E+06	2.02E+07
P=10; I=10	1	-0.052	1.774	78.651			11.91			1.00	12.36
P=10; I=10	2	-0.052	1.774	87.549		-1.49	3.43E+02		1.00	25.30	3.56E+02
P=10; I=10	3	-0.052	1.774	90.862	2.02E+04	-5.95E+05	2.88E+07	1.00	3.86E+04	1.62E+06	2.99E+07
P=10; I=30	1	-0.052	1.711	65.093			14.65			1.00	15.11
P=10; I=30	2	-0.052	1.711	86.764		10.25	43.39		1.00	10.48	45.07
P=10; I=30	3	-0.052	1.711	91.468	-0.03	3.50E+02	6.70E+02	1.00	27.17	3.53E+02	6.97E+02

Table 3. 3 presents the fitting results of the PFC slow charging approach. “PI” is the Proportional-Integral controller utilized inside of EV charging approaches which are indicated in the preceding sections. The coefficients N_s and N_t are illustrated in Section 3.3.1, Notably, these coefficients remain unaffected by independent parameters, including PI control or the order level of transfer function settings. The $\beta_2 - \beta_0$ and $\alpha_3 - \alpha_0$ are expressed in section 3.3.2. The fitting quality between the measured curve and the estimated curve is represented by the R^2 value, illustrated in equation (3.13). To summarize, the 2nd order transfer function has the best overall fitting quality for charging approach A, only in a few scenarios, the 3rd order fitting results have a slight advantage.

There are also some characteristics that can be observed from Table 3. 3, The steady-state values N_s are the same. Further, the different orders of the transfer function will not impact the transient power change, that is because the transfer function only represents the recovery process. Therefore the N_t is the same in the same control parameter settings. From the point of view of integral parameter setting, for the fitting quality of the 1st order transfer function, the higher the integral parameter can result in the smaller the fitting quality coefficient R^2. Due to the influence of a higher integral parameter, the recovery process exhibits increased oscillations, and 1st order transfer function cannot represent it well. On the contrary, higher-order transfer functions exhibit improved R^2 when subjected to higher integral parameter settings. However, upon careful observation and comparison of the fitted and original curves, these advantages are not that apparent.

3.5.3 EV dynamic load model for DC fast charging

Instead of charging approach A which has a relatively slower charging speed (~7.4 kW, Level-2 charging), charging approach B is built for fast charging (Level-3, DC fast charge). In this section, the results of dynamic load modelling of EV charging approach B are presented in detail. In the same setting as the slow charging approaches studies, for Case#1, Case#2, and Case#3 the value of the proportional term (PI1) is set to 1, i.e., P=1, while the value of the integral term (I) is set to 0.1, 1, and 30, respectively. For Case#4 and Case#5 Case#6, it is assumed that I = 0.1 I = 1 and I = 30, respectively. For Case#4 Case#5 and Case#6 the proportional term is set to 10.

Although, Section 3.2 provides an illustration of the distinct power electronic structures of Approach A and Approach B, it is noteworthy that they exhibit relatively similar dynamic response characteristics during voltage step change disturbances. Figure 3. 13. which is shown below, presents the response of the charge approach B for different values of the outer voltage loop control parameters (PI1). Compared with Figure 3. 8 and Figure 3. 11, which represent the same scenario by using approach A, it becomes evident that increasing the integral gain leads to the onset of oscillatory behaviour.

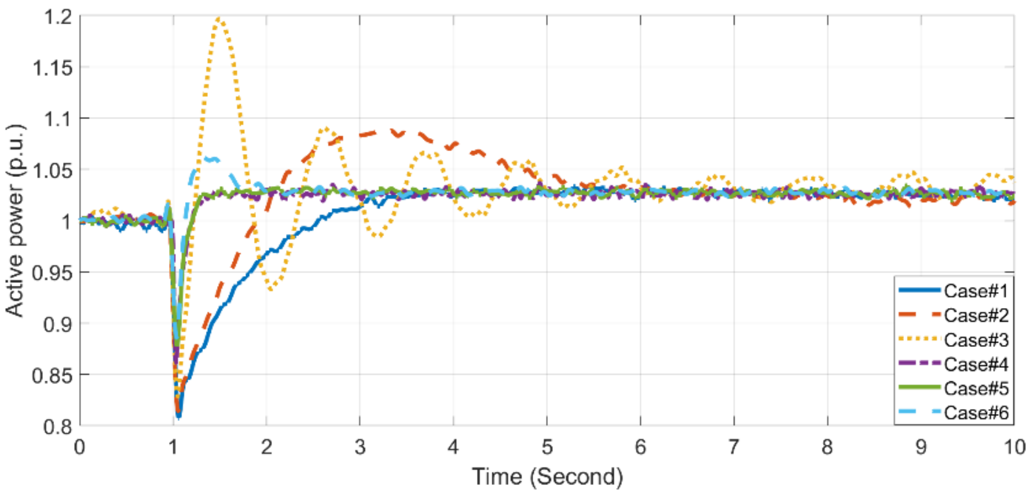

Figure 3. 13. Fast charger approach. Active power dynamic responses, derived using the detailed model, assuming different values for the PI control parameters. All responses are recorded during a -15% voltage disturbance, occurred at t=1 s.

The fitting results for such cases by different transfer functions are presented in Figure 3. 14, highlighting instances for the higher integral parameter set in which the 1st order transfer function is unable to offer a proper fitting or accurately represent the dynamic behaviour of an EV charging dynamic response for approach B.

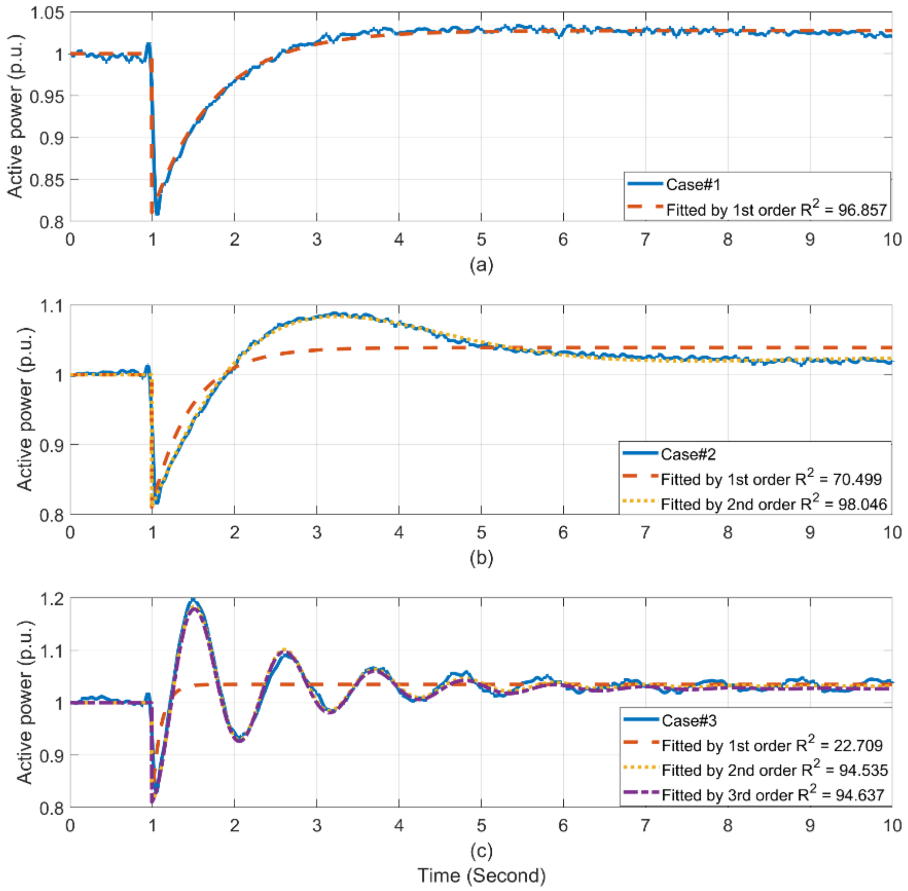

Figure 3. 14. Representative curve fitting results for the fast charger. (a) Case#1, (b) Case#2, and (c) Case#3

Figure 3. 14 illustrates representative curve fitting outcomes for fast charging, specifically comparing the fitted curve with the original response data obtained from DC fast charge while considering a -15% voltage disturbance. Figure 3. 14(a) showcases the measured data from the EV charge power electronics model controlled by P = 1 and I = 0.1. On the other hand, Figure 3. 14(b) exhibits the controller settings with P = 1 and I = 1, while Figure 3. 14(c) depicts the controller settings with P = 1 and I = 10.

It is evident that the dynamic response can be accurately represented by a 1st order transfer function, particularly when the integral parameter (I1) is set to 0.1. However, as the value of the integral gain increases (e.g., I1 = 1), the model starts exhibiting oscillations. Under such circumstances, the 2nd and 3rd transfer functions offer improved fitting results by higher R^2. Nevertheless, the R^2 for these fitting results exhibits only minimal variation, as indicated in Table 3. 4.

Table 3. 4. Dynamic load model parameters for fast charge Approach B

Model	Order	N_s	N_t	R^2	β_2	β_1	β_0	α_3	α_2	α_1	α_0
P=1; I=0.1	1	-0.092	1.294	96.857			1.37			1.00	1.29
P=1; I=0.1	2	-0.092	1.294	97.379		1.25	0.50		1.00	1.49	0.48
P=1; I=0.1	3	-0.092	1.294	98.907	5.89E+04	-7.01E+04	4.54E+06	1.00	6.93E+04	3.20E+06	4.29E+06
P=1; I=0.5	1	-0.092	1.256	84.593			1.84			1.00	1.64
P=1; I=0.5	2	-0.092	1.256	98.214		1.20	0.66		1.00	1.18	0.63
P=1; I=0.5	3	-0.092	1.256	98.195	1.34	22.40	12.01	1.00	19.49	22.01	11.41
P=1; I=1	1	-0.092	1.238	70.449			2.30			1.00	2.06
P=1; I=1	2	-0.092	1.238	98.046		1.40	0.94		1.00	1.21	0.90
P=1; I=1	3	-0.092	1.238	98.163	1.14	2.49	0.62	1.00	1.98	2.15	0.61
P=1; I=10	1	-0.092	1.274	36.296			5.34			1.00	5.06
P=1; I=10	2	-0.092	1.274	95.795		1.78	10.18		1.00	1.49	9.61
P=1; I=10	3	-0.092	1.274	97.668	0.13	22.44	47.01	1.00	6.35	19.10	45.11
P=1; I=30	1	-0.092	1.241	22.709			9.81			1.00	8.91
P=1; I=30	2	-0.092	1.241	94.535		0.94	36.43		1.00	1.38	33.56

P=1; I=30	3	-0.092	1.241	94.637	0.85	37.50	21.76	1.00	2.03	34.42	20.12
P=10; I=0.1	1	-0.092	1.274	72.981			10.14			1.00	9.60
P=10; I=0.1	2	-0.092	1.274	73.095		9.42	70.03		1.00	15.57	66.33
P=10; I=0.1	3	-0.092	1.274	90.768	5.54E+02	2.00E+03	3.53E+05	1.00	3.67E+02	3.25E+04	3.35E+05
P=10; I=0.5	1	-0.092	1.101	88.550			10.57			1.00	9.53
P=10; I=0.5	2	-0.092	1.101	88.938		8.90	104.84		1.00	17.48	94.69
P=10; I=0.5	3	-0.092	1.101	94.135	6.06E+04	1.68E+05	4.76E+07	1.00	8.49E+04	4.19E+06	4.29E+07
P=10; I=1	1	-0.092	1.106	88.471			9.50			1.00	8.89
P=10; I=1	2	-0.092	1.106	88.940		7.62	102.50		1.00	17.37	96.04
P=10; I=1	3	-0.092	1.106	96.288	5.79E+04	3.55E+04	3.50E+07	1.00	7.07E+04	3.29E+06	3.28E+07
P=10; I=10	1	-0.092	1.127	84.128			12.19			1.00	11.17
P=10; I=10	2	-0.092	1.127	90.621		10.19	13.22		1.00	9.53	12.24
P=10; I=10	3	-0.092	1.127	91.028	9.09E+04	-1.24E+05	7.42E+07	1.00	1.33E+05	5.35E+06	6.81E+07
P=10; I=30	1	-0.092	1.128	73.691			14.31			1.00	13.25
P=10; I=30	2	-0.092	1.128	90.312		9.28	40.49		1.00	9.06	37.75
P=10; I=30	3	-0.092	1.128	90.473	8.58	132.55	320.49	1.00	17.61	124.68	299.25

Table 3. 4 presents the dynamic load model parameters for different integral parameters and fitting transfer function settings in the same disturbance. As the integral parameter increased, the value of N_t decreased, implying that the active power transient response amplitude (caused by the transient voltage change) was smaller. Compared between Table 3. 3 and Table 3. 4, the model under charging approach B had a smaller value of N_t, indicating a smaller instantaneous change in the transient active power response. The DC fast charging approach has different control structures but has similar characteristics in the dynamic response curve. The 1st order transfer function is suited for smaller integral parameter settings, but it proves inadequate for higher integral parameter settings. Regarding the result of R^2 from both Table 3. 3 and Table 3. 4, the higher order transfer functions significantly fit better. However, the excessively high-order transfer function does not always lead to improved fitting, they may not be necessary due to their tendency to increase complexity without necessarily enhancing accuracy.

3.6 Summaries

This chapter meticulously investigates the performance of a widely used dynamic load model within the power system, specifically, it assesses its capability to accurately represent the dynamic characteristics of EVs in response to voltage disturbance. Further, this chapter implements two detailed EV models using MATLAB/Simulink software, representing two distinct charging approaches: relatively slower charging (as Approach A) and DC fast charging (as Approach B).

Initially, the analysis of the static behaviour of the detailed model revealed that the behaviour of both charging approaches closely approximates constant power. It is identified that, this study identifies the EV charging load model as effectively representing a constant power load in the static aspect. By applying curve fitting by exponential and polynomial functions, the static behaviours of both models are fitted to the exponential and ZIP static load models. The results show that their static characteristics can be precisely represented by the standard load model which is commonly utilized in power system stability studies.

The main contribution of this chapter is the investigation of the performance of the typically adopted equivalent model (based on ERLM) utilized in dynamic power system research to represent the dynamic characteristics of two detailed EV models. The parameter estimation algorithm is utilized to fit the dynamic load model to the measured response data from these detailed EV models. The results show that the specific value of control parameters can affect the shape of the dynamic response of the EV chargers. The 1^{st} order transfer function based dynamic load model is insufficient to represent the dynamic behaviours under some control parameters (PI control parameters) settings. For both models, the fitting quality by the different order of transfer functions has been quantified and compared. In the context of different PI settings in EV chargers, the oscillatory behaviour of dynamic load models might be different from the 1^{st} order recovery transfer function. In this scenario, it becomes necessary to consider 2^{nd} and 3^{rd} order recovery transfer functions for more accurate curve fitting.

Such information may be useful to system operators considering how to model the dynamic behaviour of EVs when performing stability studies, as their numbers are increasing. Investigating the magnitude of the potential impact of such differences is also a future research direction.

Chapter 4
Dynamic Modelling Considerations for Distribution Networks with EVs

4.1 Introduction

4.1.1 Motivation

In recent years, the market penetration of EVs has seen a steady increase, elevating their significance as a critical load type within the power network. In studies at the power system level, several fundamental questions related to EV charging have been investigated, including the start/end times of charging, charging duration, battery capacity, and charging event locations. In these studies, EVs have been treated as loads under specific conditions - such as direct current (DC) loads driven by human behaviour analysis and probabilistic studies. However, existing models used to represent EVs lack essential dynamic characteristics, leading to a scarcity of research on EV charging in the context of power system dynamics. As concluded, the preceding chapter established that EV charging can be effectively represented using a dynamic load model for power system stability studies.

This chapter aims to investigate the dynamic behaviour of EV charging within the power system and address existing research gaps. These gaps include methods for systematically integrating EVs into DNs to represent various EV penetration levels, determining the typical time points for simulation, and understanding the dynamic characteristics of DNs under these conditions. Additionally, it includes appropriate approaches for managing and analysing the large volume of dynamic responses to derive reasonable conclusions.

To fill these gaps, this study integrates the EV dynamic load model into the CIGRE benchmark MV network, considering various levels of EV ownership and daily operation times. The study defines typical time points, such as maximum EV penetration times and peak times of the day, to run simulations and present the dynamic responses of the DNs. Furthermore, systematic simulations and statistical analyses are applied to identify the impact of EV charging on DNs.

This Chapter integrates the EV as a dynamic load model, previously implemented in Chapter 3, into the network simulation. This dynamic load model has been defined following the ERLM (Exponential Recovery Load Model) from [61][94][95], and the parameters for the dynamic load model definition have been provided in the preceding chapter. To facilitate simulation at the distribution power system level, this EV dynamic model will be re-built through DIgSIlENT PowerFactory DSL (DIgSILENT Simulation Language) model to fit the simulation platform.

The dynamic response of the entire DN will be recorded. This study constructs a dynamic equivalent model for the entire DN, incorporating EVs with the aim of observing the difference in dynamic responses under various EV penetration rates at different times and EV ownership levels, the results will be quantified by specific indicators.

4.1.2 Contributions

This chapter investigates the dynamic behaviour of the power system during transformer tap change events under varying levels of EV penetration. To accomplish this, this study employs an EV dynamic load model derived from a parameter estimation algorithm. Subsequently, the EV dynamic load model will be implemented into the CIGRE benchmark MV network as a new independent variable. The difference in dynamic response under various EV penetration rates is observed and quantified by specific indicators. The specific contributions are as follows:

- This research integrates the developed EV dynamic load model into the CIGRE benchmark MV network to investigate the impact with respect to dynamic equivalent modelling. Furthermore, this study draws conclusions from the simulation results by comparing the effects of single and composite types of EV penetration.
- The comprehensive influence of EV charging on system dynamic responses is quantified for different EV ownership levels and daily operating times through the indicators of $RMSE$, R^2, SSE, and OE.
- The extensive simulation results are statistically analysed, providing a more generalized understanding of how EV charging impacts the dynamic behaviour of the DN.
- Since the simulation software - DIgSILENT PowerFactory does not include the 2nd order transfer function based dynamic load model defined, a custom DSL model has been constructed and integrated into the software platform. This model is based on the proposed dynamic load model structure.

Additionally, a method for parameter conversion has been implemented to accommodate complex DSL modelling.

4.3 EV load demand profile definition

Since the usual EV charging scenarios have been depicted in the preceding section, the method used to derive a set of the specific EV load model profile will be expressed in detail in this section, and this data will be utilized in the dynamic stability analysis. It should be noted that, the EV daily load profile implemented in this section will be utilized simply as an input with the focus on modelling the dynamic behaviour of EVs for power system dynamic studies.

In the referenced study [63] the management of EV charging events was addressed by considering the anticipated energy requirements for car-based transportation of residents served by an existing power network. To implement this, geographical information systems (GIS) data of a real distribution network and GIS data from the UK Census are considered. This method can be divided into two main aspects: the power system perspective and Algorithm modelling of EV charging events. The code for the data generation is available in [178].

4.3.1 Introduction of charging database

A real distribution network in the residential-dominated Southside area of Glasgow is utilized as a practical example for EV charging. This network includes a secondary (11 kV / 0.4 kV) substation and three 0.4 kV distribution feeders and serves 157 households by 47 endpoints. The image is available from Google Maps [179].

The UK National Travel Survey (NTS) is conducted annually for around 15.000 residents. Their 7-day period trips have been recorded [180]. This data includes the driving Origin (e.g. home/shop/work), Destination, Time for Start/End, and Distance. In this study, travel was categorized based on the type of employment an individual had and the way they travelled to work. According to UK census data from the same field, this is utilized to assign travel diaries to fleets of electric vehicles instantiated in a network that may represent the travel habits of individuals served by the network.

4.3.2 Obtain the EV charging daily profile

In the study a Monte-Carlo generated data for individual EV charging, as provided by the literature [63], is utilized to estimate the EVs' daily charging profile. The code for the data generation is available in [178]. Network data and Census data are combined to create a fleet of EVs, as described in the algorithm [63].

In summary, this Monte-Carlo based approach is utilized to model uncertainties associated with the charging habits of customers who owned EVs per household. The results will be utilized in the following sections, which include events for 24 hours (12 pm to 12 pm), and 10,000 individual vehicles. This routine method assumes drivers will always plug their charger into the system when they arrive home, without considering the remaining electricity in the battery. This corresponds to the standard charging illustrated in the preceding section. The data includes the information of the time EV plug in/out (the times t_{in} and t_{out} are in 10 timesteps, 0-142 covering 24 hours), the electricity amount E_{start} and E_{end} in the battery (united by kWh) at start/end of the charging event. The way to integrate them together is shown below:

EV	t_{in}	t_{out}	E_{start}	E_{end}
1	36	120	38.35847	40
2	2	114	68.82013	75
3	25	28	38.35847	39.56662
...	...	...	...	...

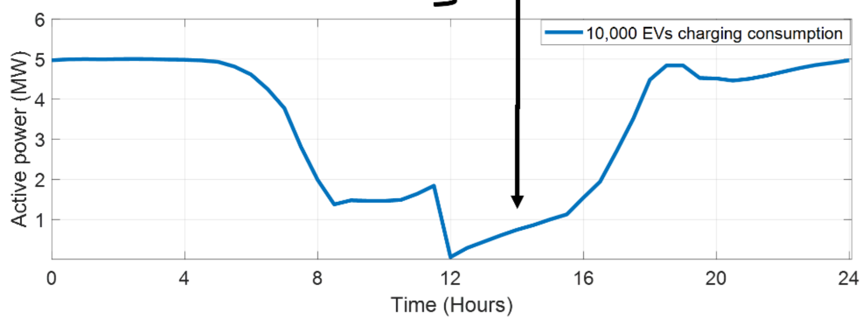

Figure 4. 1. EV prediction model into daily load profile.

As depicted in Figure 4. 1, the predicted EV charge plug-in/out data are integrated into a daily demand profile, comprising total dynamic charge power and time. This profile can be considered as an average comprehensive load model for EV charging in residential areas. In this study, the EV is added to the power network as one type of load. On the other hand, other variables such as the EV ownership per household are also important for the EV penetration rate in the area. The process of incorporating this averaged EV charging demand daily profile data into the power network will be expressed in Section 4.4 in detail.

4.3.3 DSL modelling in DIgSILENT PowerFactory for EV charging

The simulation of the DNs was conducted using the software – DIgSILENT PowerFactory. Notably, this software only supports the definition of a 1st order dynamic load model within its "Generic load model definition" feature. Therefore, to accommodate higher order transfer functions, a novel model structure was developed in DIgSILENT, which is a significant contribution to this thesis. Based on the results obtained from the preceding chapter, it is suggested that the EV dynamic load model could potentially be based on 2nd or even higher order transfer functions. Consequently, it is necessary to accomplish the manually defined dynamic load model that incorporates a high order transfer function. The detailed structure for both the "Composite model" and "Common model" definitions are illustrated in Figure 4. 2 below.

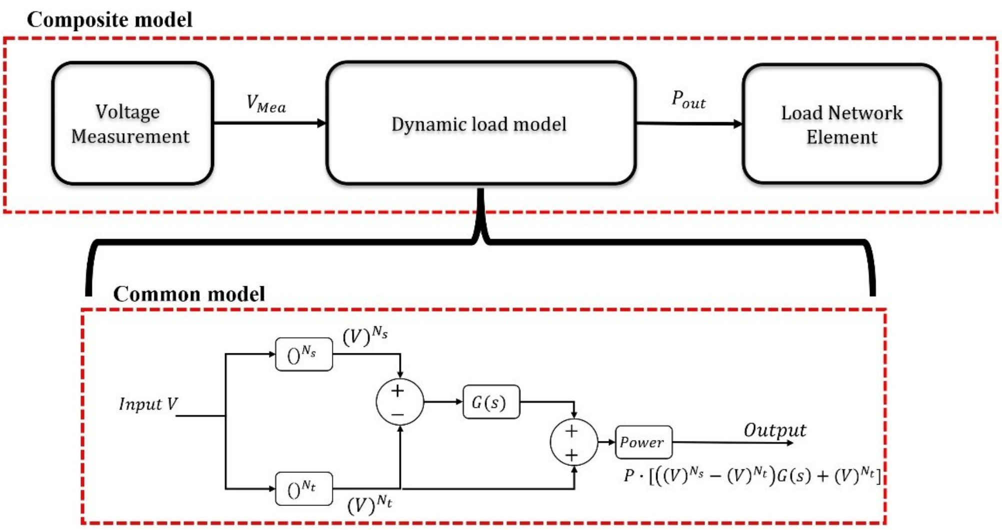

Figure 4. 2. The manual defined model structure in DIgSILENT PowerFactory

The DIgSILENT PowerFactory allows for the manual definition of the dynamic load model, which encompasses contains two types of model definitions, the "Composite model", and the "Common model". The "Composite Model" is constructed to replace the generic load model which is limited to providing a 1st order dynamic response. Within the composite model, the "Voltage Measurement" is connected to the busbar where the EV loads are connected, and it measures the voltage, denoted as V_{mea} from the busbar, afterwards, converts to the "Dynamic load model". The "Dynamic load model" is the most important part that can be included by the "Common model". The "Common model" serves as the fundamental unit for manual model definition in DIgSILENT, which determines the mathematical relationship between various parameters. In this study, the "Common model" is constructed following the dynamic load model structure depicted in the preceding chapter. The N_s is the steady state power voltage exponent, N_t is the transient power voltage exponent refer to Equation (3.5), as expressed in section 3.3.2. The power recovery P_{out} can be obtained from the "Common model", and then passed to the "Load Network Element" to act on the target element, which is the "Load" in the power system model.

Note that, the "Composite model" and "Common model" must be constructed individually in DIgSILENT. Subsequently, both models should be imported into the project. The EV model in this study will be defined based on the "Generic load model" [181]. The transition from the "Generic load model" to the defined "Composite model" is achieved by connecting the "measurement point" to the busbar and associating the "Load Network Element" to the load itself. Following this, the "Dynamic load model" within the "Composite model" is set to become the defined "Common model". The interrelationship among the power network, "Composite model" and "Common model" is depicted in Figure 4. 2. After this definition, all parameters of the dynamic load model can be set in the "Common model" which can make the defined "Generic load model" represent the EV dynamic model.

This manually defined model is more capable and can represent the model with more complicated dynamic characteristics through the incorporation of higher order transfer functions.

4.3.4 Parameter conversion for complex DSL models

The existing dynamic load model which has been implemented in the preceding section may not possess the requisite capability for the aggregated dynamic load modelling. Which may encompass extremely complicated dynamic characteristics. This section strives to implement the high order transfer function based dynamic load model from DIgSILENT PowerFactory. As mentioned above, the default dynamic load model (generic dynamic load) in DIgSILENT PowerFactory only includes 1st order recovery.

Section 4.3.3 has built the user-defined "Common model" in DIgSILENT, which is only capable support the 2nd order transfer function. That model is sufficient for to representing a single EV, but it lacks the capability to accurately represent the dynamic characteristics of the entire DNs. Notably, there is no support for a transfer function higher than the 2nd order within the "Common model" definition options. a series connection for more than 2 2nd order transfer functions can make a "Variable over defined" error.

To solve this question, this study integrated several 2nd order transfer functions "Common model" in the "Composite model" level to implement the high order transfer function based dynamic load model at the system level. For example, the 5th order based transfer function dynamic load model, which is shown in the figure below:

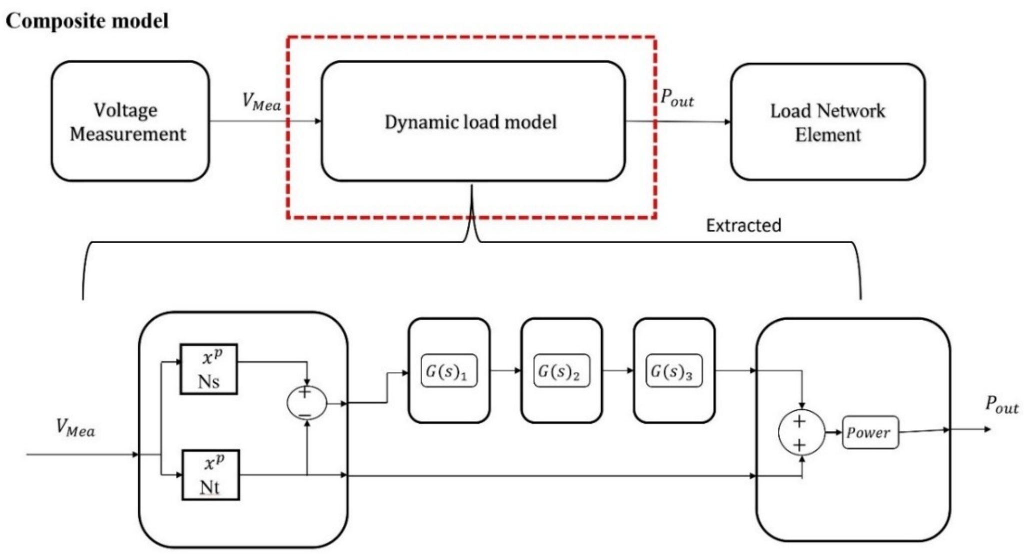

Figure 4. 3. Structure of implemented 5th order transfer function based dynamic load model

Comparing the structure between the dynamic model shown in Figure 4. 2 and Figure 4. 3, the only difference is the transfer function $G(s)$ has been separated into $G(s)_1$ $G(s)_2$ and $G(s)_3$. Essentially, it is separating the 5th order transfer function into the multiple multiplications of 3 lower order transfer functions, such as the 1st and 2nd order transfer functions, which can be expressed through the equations shown below.

$$G(s)_{5-order} = \frac{\alpha_5 s^5 + \alpha_4 s^4 + \alpha_3 s^3 + \alpha_2 s^2 + \alpha_1 s + \alpha_0}{\beta_5 s^5 + \beta_4 s^4 + \beta_3 s^3 + \beta_2 s^2 + \beta_1 s + \beta_0} \tag{4.1}$$

$$G(s)_1 = \frac{A_{11}s + A_{10}}{B_{11}s + B_{10}} \tag{4.2}$$

$$G(s)_2 = \frac{A_{22}s^2 + A_{21}s + A_{20}}{B_{22}s^2 + B_{21}s + B_{20}} \tag{4.3}$$

$$G(s)_3 = \frac{A_{32}s^2 + A_{31}s + A_{30}}{B_{32}s^2 + B_{31}s + B_{30}} \tag{4.4}$$

$$G(s)_{high-order} = G(s)_1 \cdot G(s)_2 \cdot G(s)_3 \tag{4.5}$$

From the software this method is feasible, but another challenge is also coming, more variables need to be defined. For example. Only $\alpha_5 - \alpha_0$ and $\beta_5 - \beta_0$ need to be defined in (4.1), but when this 5th order transfer function is separated into the multiplications of (4.2), (4.3) and (4.4), the variable $A_{10} - A_{32}$ and $B_{10} - B_{32}$ also need to be defined.

In this study, the transfer function is conceptualized as a polynomial equation. Notably, there is no general solution in radicals to polynomial equations of the 5th or higher [182][183]. Fortunately, the coefficient of the 5th order in (4.1) can be defined as 1 since it is a transfer function, this renders the subsequent derivation feasible. Consequently, the primary task in this section is to meaningfully simplify the extended transfer functions.

It is obvious that the equation (4.5) can be simplified, Specifically, the 5th order transfer function can be represented by only 2 2nd order and 1 1st order transfer functions. This simplification is based on the implemented dynamic load model with parameter settings, the 5th order transfer function can be simplified as the equation shown in equation (4.6).

$$G(s)_{5-order} = \frac{(s^2 + A_{21}s + A_{20})(A_{32}s^2 + A_{31}s + A_{30})}{(s + B_{10})(B_{22}s^2 + B_{21}s + 1)(B_{32}s^2 + B_{31}s + B_{30})} \tag{4.6}$$

This equation strives to remove irrelevant variables, the variable A_{11} is set to 0, and the variables A_{10}, A_{22} B_{20} and B_{11} are set to 1. It needs to be emphasised that, this is not the only approach for this simplification, this study just provides an inspiration to solve this question.

Afterwards, derivate the equation (4.6) and compare it to equation (4.1), the corresponding components can be summarized through the equations below:

$$\begin{cases} \alpha_5 = 0 \\ \alpha_4 = A_{32} \\ \alpha_3 = A_{21} + A_{31} \\ \alpha_2 = A_{30} + A_{21}A_{31} + A_{20}A_{32} \\ \alpha_1 = A_{21}A_{30} + A_{20}A_{31} \\ \alpha_0 = A_{20}A_{30} \end{cases} \tag{4.7}$$

$$\begin{cases} \beta_5 = B_{22}B_{32} \\ \beta_4 = B_{22}B_{31} + B_{21}B_{32} + B_{10}B_{22}B_{32} \\ \beta_3 = B_{22}B_{30} + B_{21}B_{31} + B_{32} + B_{10}B_{22}B_{31} + B_{10}B_{21}B_{32} \\ \beta_2 = B_{21}B_{30} + B_{31} + B_{10}B_{22}B_{30} + B_{10}B_{21}B_{31} + B_{10}B_{32} \\ \beta_1 = B_{30} + B_{10}B_{21}B_{30} + B_{10}B_{31} \\ \beta_0 = B_{10}B_{30} \end{cases} \tag{4.8}$$

A multitude of methods can be employed to solve the equation sets presented in Equation (4.7) and (4.8), including programming solutions in MATLAB and Maple. However, the specifics of these methods are not beyond the scope of the thesis. Essentially, this process converts the parameter from high order transfer function $G(s)$, which is obtained by the fitting process illustrated in Section 3. 4, to the lower order transfer function that can be defined in DIgSILENT software.

The procedure for parameter definition within DIgSILENT parallels the process expressed in Section 4.4.3 but becomes more complicated. Figure 4. 4 lists the parameters that need to be set in DIgSILENT in each slot.

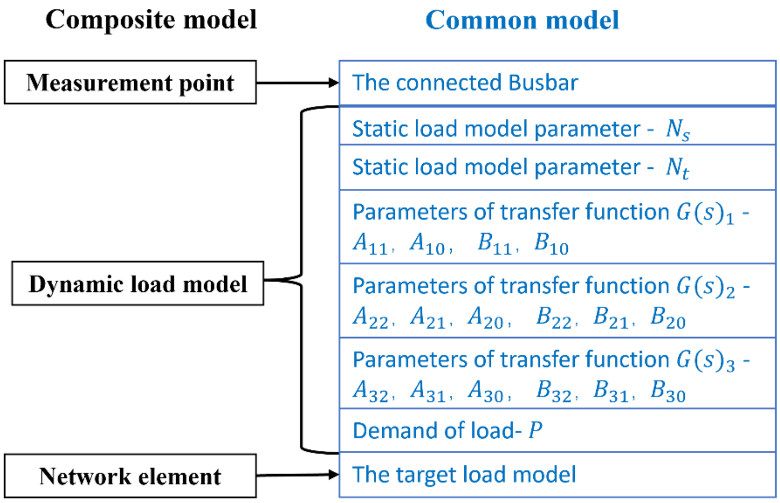

Figure 4. 4. The process of defining the parameters in DIgSILENT PowerFactory model

.

Note that, this implemented high order transfer function based dynamic load model can also be feasible to represent low order model. For example, set the parameters A_{12}, A_{11}, B_{12}, B_{11} to be 0, and A_{10}, B_{10} to be 1, the transfer function $G(s)_1$ can be seen as inactivated.

This study also attempted to employ the Pole-Zero representation of the polynomial equation which can be readily obtained via MATLAB commands, rather than the solution. However, due to the Fundamental Theorem of Algebra, Poles and Zeros could be complex numbers in high order polynomial equations [184][185]. Regrettably, DIgSILENT PowerFactory does not accommodate the use of complex numbers within DSL modelling. Consequently, this approach is not feasible.

4.4 Power network simulation benchmark

In this Section, the impact of EV penetration on DN dynamics is investigated using a set of error metrics. Towards this objective, a model of an extended DN is created and several loading conditions are examined. The rest of this Section is organized as follows: In Section 4.4.1 the system under study is described. In Section 4.4.2 daily consumption profiles, used to create realistic loading conditions, are presented. The modelling of EVs and DN loads is discussed in Section 4.4.3. A summary of the examined cases is presented in Section 4.4.4. The assessment methodology is explained in Section 4.4.5. Indicative results are summarized in Section 4.5.

4.4.1 System under study

The examined DN is depicted in Figure 4. 5, and it is based on the European MV grid of CIGRE [150] The nominal voltage and frequency of the system are 20 kV and 50 Hz, respectively. The DN hosts both residential and industrial customers. The nominal power of industrial and residential loads is summarized in Table 4. 1. For each load, the connection node is also reported. Variables $S_{residential}$ and $S_{industrial}$ in Table 4. 1 denote the nominal apparent power (in MVA) of residential and industrial loads, respectively, while PF is the corresponding power factor [150]. For the analysis, it is assumed that nodes with residential customers host also EVs. The number of EVs, connected at each node, is defined as follows: initially, the total number of households connected at each node of the examined DN is determined. The load model parameters settings of residential and industrial load models are following the reference [152]. The residential loads are presented by ZIP model, the active power Z_p=0.827; I_p=-0.049; P_p=0.827, its reactive power Z_q=14.14; I_q=-24.838; P_q=11.696. The industrial loads are presented by exponential model, the active power exponent k_p=0.772; Reactive power exponent k_q=4.522. In particular, it is assumed that a typical household has a peak consumption of 3.5 kW [186]. Based on this value and the total power of residential loads, provided in Table 4. 1, the number of households is defined.

Concerning the number of households that have EVs, six scenarios (N_S=6) are generated. In each scenario, the EV ownership level is assumed to be different. For the analysis, in the first scenario (S1), the EV ownership is set to 0.2. This practically implies that only 2 out of 10 households per system node have an EV. In S2, S3, S4, and S5 the EV ownership is set to 0.4, 0.6, 0.8, and 1, respectively. Therefore, in S5 all households are equipped with an EV. Finally, in S6 EV ownership is set to 1.2. This implies that there are 12 EVs per 10 households, i.e., 1.2 vehicles per household. During 2020 every household in the UK owned 1.2 vehicles [138]. Therefore, S6 corresponds to the case where all traditional vehicles with internal combustion engines are replaced by EVs. The nominal power of EVs for the six examined scenarios is provided in Table 4. 1. Connection nodes of all EVs are also reported.

Table 4. 1 The nominal power of residential industrial and six examined EVs load settings.

Node	$S_{residential}$	PF	$S_{industrial}$	PF	S1	S2	S3	S4	S5	S6
1	0.4466	0.98	0.4435	0.98	0.1633	0.3265	0.4898	0.6531	0.8163	0.9796
2										
3	8.22E-03	0.97	0.0199	0.85	4.40E-03	8.80E-03	0.0132	0.0176	0.0220	0.0264
4	0.0129	0.97			3.56E-03	7.12E-03	0.0107	0.0142	0.0178	0.0214
5	0.0216	0.97			6.00E-03	0.0120	0.0180	0.0240	0.0300	0.0360
6	0.0164	0.97			4.52E-03	9.04E-03	0.0136	0.0181	0.0226	0.0271
7			6.83E-03	0.85	7.20E-04	1.44E-03	2.16E-03	2.88E-03	3.60E-03	4.32E-03
8	0.0175	0.97			4.84E-03	9.68E-03	0.0145	0.0194	0.0242	0.0291
9			0.0509	0.85	5.40E-03	0.0108	0.0162	0.0216	0.0270	0.0324
10	0.0142	0.97	6.03E-03	0.85	4.56E-03	9.12E-03	0.0137	0.0182	0.0228	0.0274
11	9.86E-03	0.97			2.72E-03	5.44E-03	8.16E-03	0.0109	0.0136	0.0163

Note that for each one of the examined scenarios, a power flow analysis is conducted using the rated powers of Table 4. 1 to determine the currents flowing in the lines of the DN. The computed currents are then compared to the corresponding thermal limits in order to identify potential congestion issues. In all scenarios no thermal constraints were reached, thus justifying the applicability of the selected scenarios.

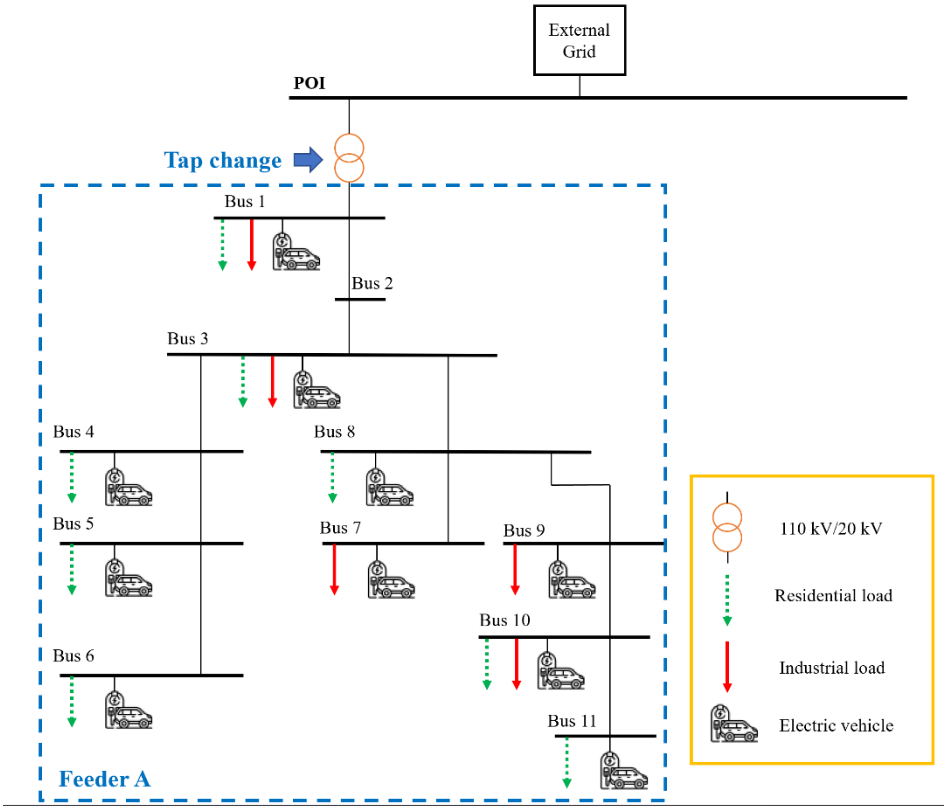

Figure 4. 5. Utilized Medium-Voltage network model.

4.4.2 Daily consumption profiles

To replicate realistic loading conditions, typical consumption profiles are used. Residential and industrial profiles in per unit, along with peak-time energy consumption in MW, are extracted from [150] and [151]. respectively, to establish detailed real and reactive power consumption profiles for each busbar. The impact of policy adjustments, such as price mechanisms, as well as temporal and spatial aspects on charging profiles of EVs are indirectly taken into account in this study by employing the method of [64]. In particular, [64] is based on the UK national travel survey and uses real data from 10.000 individual EVs. By exploiting the individual data, an aggregated EV profile is created. The code for data generation is available in [178], and incorporated into the network using the methodology delineated in Section 3.3.2.

All considered consumption profiles, i.e., residential, industrial, and EV profiles, are normalized based on the corresponding maximum consumed power. The derived normalized profiles are depicted in Figure 4. 6.

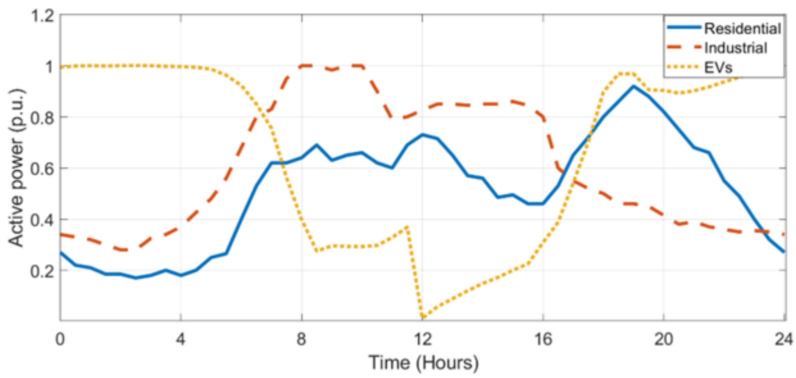

Figure 4. 6. Normalized daily profiles for residential, industrial loads and EVs.

4.4.3 Modelling of EVs dynamic loads

In order to represent various types of EV penetration, this study investigates two scenarios. The first scenario considers a single type of EV penetration. The second scenario involves a composite model, which includes different types of EVs, to encapsulate the most complex scenario and illustrate different aspects. By comparing the results of these scenarios, this study aims to provide a comprehensive understanding of how differentiated EVs impact the system's dynamic behaviour. Note that the EVs penetrate in this system level studies only as dynamic load, this means that this study does not include any V2G or grid intelligent dispatching analysis.

For the scenario involving charging of a single type of EV, this study employs the DC fast charging approach with parameter settings of P = 1 and I = 1.

In the scenario of composite EV penetration, to establish a realistic test case, EV chargers with varying characteristics, such as different types and discrete PI control parameters, are taken into account. Consequently, three types of chargers with distinct dynamic characteristics are assumed for analysis. The first type corresponds to a slow charger with P = 1 and I = 0.1. The second type corresponds to a fast charger with P = 10, I = 10. Finally, the third type is a slow charger with P = 1, I = 30.

To demonstrate the different dynamic characteristics of the composite type of EV load penetration, their active power responses during a -15% voltage step disturbance are illustrated in Figure 4. 7.

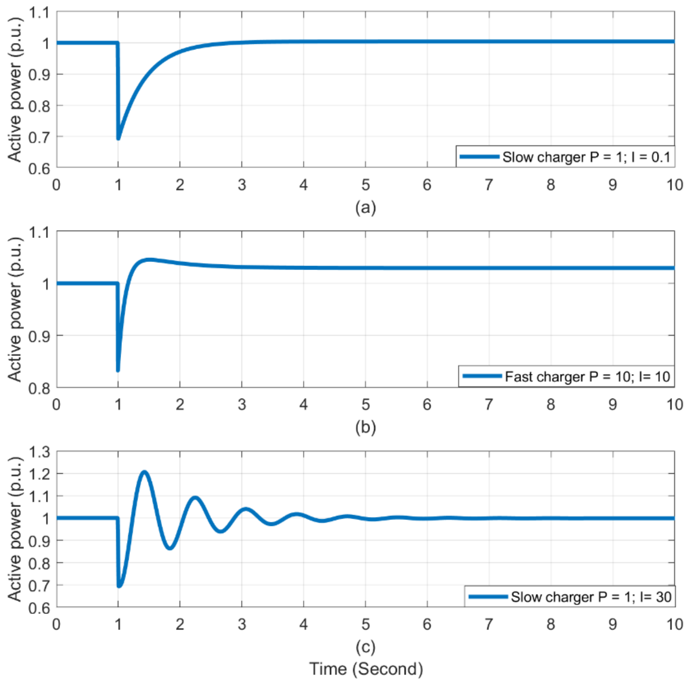

Figure 4. 7. The dynamic characteristics of the selected EV dynamic load model. (a) Slow charge P = 1, I = 0.1; (b) Fast charge P = 10; I = 10; (c) Slow charge P = 1; I = 30.

As shown in Figure 4. 7(a), the active power of the first charger exhibits a smooth recovery without any overshoots or oscillations. The second charger has the fastest recovery, with an overshoot observed during the recovery phase. The third charger presents oscillatory behaviour during recovery.

To simulate the considered EVs and to integrate them into the DN model, the parameters of Figure 4. 1 are used. More specifically, in this Table, the optimal order for the proposed equivalent and the corresponding parameters are summarized for each one of the examined EVs. Note that for each node host EVs, equal participation of all models is considered.

Table 4. 1. Parameters of selected dynamic load models

Model		Order	N_s	N_t	α_2	α_1	α_0	β_3	β_2	β_1	β_0
Fast charge	P=1; I=1	2	-0.092	1.238	0	1.40	0.94	0	1	1.21	0.90

Slow charge	P=1; I=0.1	1	-0.052	2.257	0	0	2.227	0	0	1.000	2.260
Fast charge	P=10; I=10	2	-0.092	1.127	0	10.194	13.218	0	1.000	9.527	12.237
Slow charge	P=1; I=30	3	-0.052	2.236	-0.857	58.103	81.331	1.000	3.340	62.475	83.744

Since the simulation software, DIgSILENT PowerFactory, does not support transfer functions higher than 2nd order within a single DSL, a conversion method is required to implement the complex dynamic load model integration. The methodology for this conversion is detailed in Section 4.3.4. Following this, the parameters should be converted using equations (4.7) and (4.8).

The converted parameters are shown in Table 4. 2 below.

Table 4. 2 Converted dynamic load model parameters for DIgSILENT PowerFactory parameters settings.

Charging approach	Fast	slow	fast	slow
Parameters	P=1; I=1	P=1; I=0.1	P=10; I=10	P=1; I=30
N_s	-0.092	-0.052	-0.092	-0.052
N_t	1.238	2.257	1.127	2.236
B_{10}	1.000	1.000	1.000	1.000
B_{11}	0.000	0.000	0.000	0.000
A_{10}	1.000	1.000	1.000	1.000
A_{11}	0.000	0.000	0.000	0.000
B_{20}	1.000	1.000	1.000	1.401
B_{21}	0.000	0.000	0.000	1.000
B_{22}	0.000	0.000	0.000	0.000
A_{20}	1.000	1.000	1.000	1.000

A_{21}	0.000	0.000	0.000	0.000
A_{22}	0.000	0.000	0.000	0.000
B_{30}	0.900	2.260	12.237	59.755
B_{31}	1.210	1.000	9.527	1.937
B_{32}	1.000	0.000	1.000	1.000
A_{30}	0.940	2.227	13.218	81.331
A_{31}	1.400	0.000	10.194	58.103
A_{32}	0.000	0.000	0.000	-0.857

The parameters $A_{10} - A_{32}$ and $B_{10} - B_{32}$ as defined in Equations (4.2) – (4.4), are utilized to define the DSL model depicted in Figure 4. 3. Once these EV dynamic load models are connected to the DNs, the network exhibits complex dynamic characteristics in response to a -2.17% voltage disturbance. An illustrative example of this composite EV model dynamic recovery process is provided in Figure 4. 8. It is estimated that each household owns 1 EV, and the simulation time is 2 am.

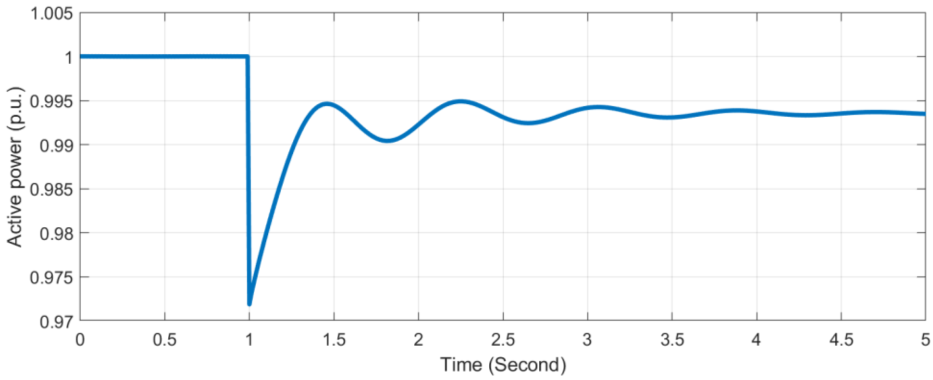

Figure 4. 8. The dynamic recovery of the DNs with 1 EV ownership per household at 2 am in the morning.

4.4.4 Examined Cases

To thoroughly evaluate the impact of EV penetration level on DN dynamics, several test cases are considered. For this purpose, realistic loading conditions are created for the examined DN as well as discrete scenarios regarding the EV penetration level are examined. Towards this objective, Daily consumption profiles are constructed for each node of the examined DN by multiplying the nominal power of each load, depicted in Table 4. 1, with the corresponding normalized profile of Figure 4. 6. For all profiles a one-hour resolution is considered (N_h=24). Note that for each EV ownership level, i.e., for scenarios S1, S2, S3, S4, S4, and S6, dedicated EV consumption profiles are used, i.e., profiles that correspond to the examined EV ownership level. Using this approach, a set of $N = N_h \times N_s = 24 \times 6 = 144$ cases, corresponding to different loading conditions and EV penetration levels are constructed.

An indicative example of the examined loading conditions is presented in Figure 4. 9. In this figure, the total load demand for scenario S5, which means 1 EV owned per household, throughout the day is presented. The total power consumed per load type, such as EVs, residential, and industrial loads, is also illustrated. Additionally, the load composition for four specific hours of the day, namely 02:00, 12:00, 14:00, and 19:00, is reported. Similar profiles are created for all examined scenarios.

Household leading	12:00	
Residential	71.96%	1.9116 MW
Industrial	27.41%	0.7280 MW
EV	0.63%	0.0168 MW
Total	100%	2.6565 MW

Peak time	19:00	
Residential	58.09%	2.401 MW
Industrial	9.78%	0.2054 MW
EV	32.14%	1.3328 MW
Total	100%	4.1474 MW

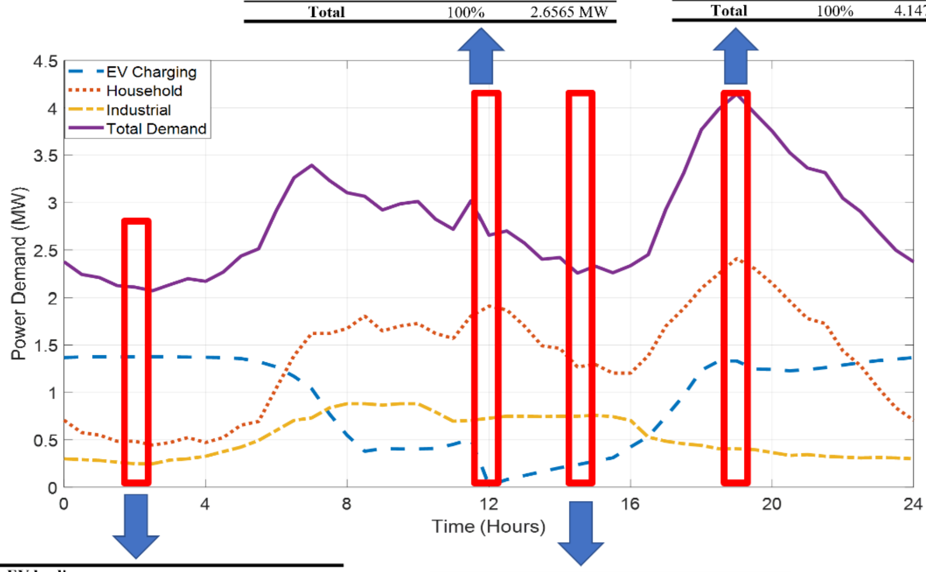

EV leading	2:00	
Residential	21.51%	0.4452 MW
Industrial	11.93%	0.2468 MW
EV	66.56%	1.3775 MW
Total	100%	2.0694 MW

Industrial leading	14:00	
Residential	56.30%	1.4664 MW
Industrial	33.21%	0.7492 MW
EV	10.50%	0.2367 MW
Total	100%	2.2560 MW

Figure 4. 9 Considerable 4 scenarios from daily load profile

4.4.5 Assessment methodology

To quantify the impact of EVs on the dynamic performance of DNs, the following procedure is adopted: for each one of the 144 cases reported in Section 4.4.2, a -2.17% voltage disturbance is analysed by changing the tap position of the interconnection transformer (see Figure 4. 5) For this purpose, RMS simulations are performed using the corresponding DIgSILENT module.

For all examined cases, the resulting dynamic response of active power (P_{EV}) at the point of interconnection (POI) is recorded and normalized. The basis for normalization is the maximum value of active power. Subsequently, for each one of the 144 cases, the EVs are disconnected from the DN, and the same voltage disturbance is examined. The resulting real power response ($P_{No,EV}$) is recorded and normalized using as a base its maximum value. Afterwards, $P_{No,EV}$ is compared with the corresponding P_{EV} response. For the comparisons, the following metrics are used [187].

$$RMSE = \sqrt{\frac{1}{N}\sum_{n=1}^{N}(P_{EV}[n] - P_{NO,EV}[n])^2} \tag{4.9}$$

$$R^2 = 1 - \frac{\sum_{n=1}^{N}(P_{EV}[n] - P_{NO,EV}[n])^2}{\sum_{n=1}^{N}(P_{EV}[n] - \overline{P_{EV}})^2} \tag{4.10}$$

$$SSE(\%) = \left|\frac{P_{EV,ss} - P_{NO,EV,ss}}{P_{EV,ss}}\right| \cdot 100\% \tag{4.11}$$

$$OE(\%) = \left|\frac{P_{EV,+} - P_{NO,EV,+}}{P_{EV,+}}\right| \cdot 100\% \tag{4.12}$$

In the above equations, $\overline{P_{EV}}$ is the mean value of the DN response when EVs are connected. $P_{EV,ss}$ and $P_{NO,EV,ss}$ are the new steady-state values of active power after the voltage disturbance, assuming EVs are connected or not, respectively. $P_{EV,+}$ and $P_{NO,EV,+}$ are the active power immediately after the voltage disturbance for the cases where EVs are connected or not, respectively.

The $RMSE$ measures the average difference between the predicted values $P_{EV}[n]$ and actual values $P_{NO,EV}[n]$. It provides an indication of the model's prediction accuracy, with lower values indicating better performance. R^2 measures how well the model's prediction explains the variance in the actual data. R^2 value of 1 indicates perfect prediction, while R^2 equal to 0 indicates no predictive power. $SSE(\%)$ quantifies the error between the steady-state predicted value and the actual steady-state value. $OE(\%)$ measures the error between the peak predicted value and the actual peak value.

In this study, the $RMSE$ and R^2 are used to assess the similarity of P_{EV} and $P_{NO,EV}$ responses. Additionally, the steady-state error (SSE) and the overshoot error (OE) are used to quantify the differences between P_{EV} and $P_{NO,EV}$ in terms of the new-steady state and the power immediately after the voltage disturbance, respectively.

4.5 Dynamic voltage characteristics of DNs with EV penetration

4.5.1 Indicative results

Initially, indicative results are presented for four representative time instances of S5. These time instances are those reported in Figure 4. 9, the i.e., T_1=02:00, T_2=12:00, T_3=14:00, and T_4=19:00. T_1=02:00 corresponds to the time instance with the maximum EV penetration level. Indeed, for T_1, EV penetration is equal to 66.5%. Note, that EV penetration is defined in this study as the ratio between the power consumed by all EVs and the total load consumption. T_2 is the time instant with the minimum EV penetration level (only 0.6% of the total load is consumed by EVs); T_3 and T_4 correspond to two instances with moderate EV penetration levels.

For each one of the above-mentioned time instances P_{EV} and $P_{No,EV}$ are compared assuming a -2.17% voltage disturbance. For the single type of EV penetration scenario, the corresponding responses are illustrated in Figure 4. 10. As shown, the DN presents different dynamic characteristics during the day. In fact, the higher the EV penetration level is, the more oscillatory the response of the DN is. Moreover, as the EV penetration increases, the DN tends to behave as a constant power load after the voltage disturbance, i.e., the post-disturbance steady-state power is closer to the corresponding pre-disturbance value. EV penetration also increases the magnitude of power undershoots.

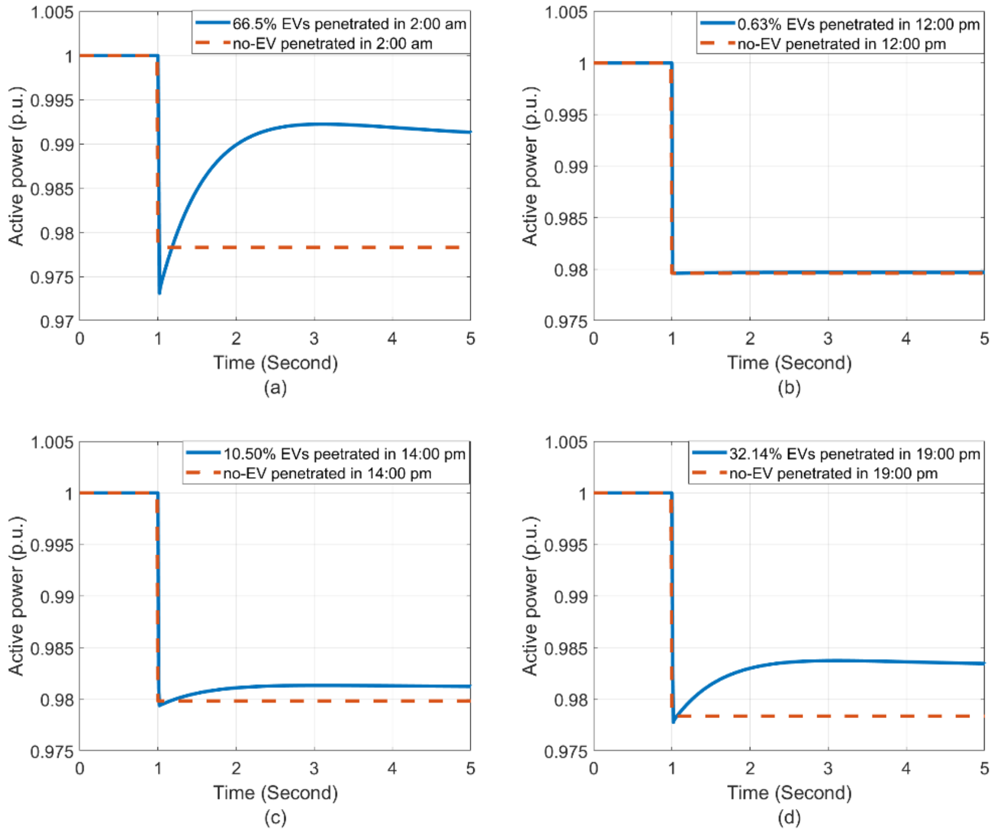

Figure 4. 10. Comparison of single type of EV penetration P_{EV} and $P_{No,EV}$ responses for S5 scenario during a -2.17% voltage disturbance. Time instance (a) T_1 (b) T_2 (c) T_3 (d) T_4.

To facilitate a more intuitive observation of the differences introduced by the single type of EV penetration into the system, the indicators quantify the difference between the grid without EV penetration and the four scenarios of EV penetration. The results are shown in Table 4. 3 below.

Table 4. 3. Quantifying the difference among four scenarios with single type EV model

Time	EV penetration	$RMSE$	R^2	SSE	OE
2:00	66.56%	0.0119	0.4999	0.1421	0.0052
12:00	0.63%	7.60E-05	0.9863	5.79E-06	1.80E-06
14:30	10.50%	0.001	0.5721	0.0011	3.56E-04
19:00	32.14%	0.0048	0.5028	0.0235	6.27E-04

As delineated in Table 4. 3, the time of the highest EV penetration, which is at 2:00, exhibits the most significant deviation from the no-EV penetrated scenario. This is because the most of residential and industrial loads are in-operated during the midnight, at the same time, the EV is still charging, so the EV dynamic load is dominant. This is also reflected in the largest $RMSE$ value and the smallest R^2 value. Because these two indicators represent the fitting quality by comparing the estimated value and obtained value between with/without EV penetration, implied by the equations (4.1) and (4.2). The higher $RMSE$ means the larger differences between the with/without EV, conversely, the higher R^2 means the with/without EV penetration data is more similar.

Furthermore, considering the largest recovery process observable in Figure 4. 10, this recovery contributes to a larger difference compared to the data with lower EV penetration. Consequently, the data at 2:00 has a larger SSE as shown in Table 4. 3. Additionally, more EV penetration results in more dynamic characteristics in the response, leading to a heavier OE that can be detected at the instantaneous of the disturbance. The data at 2:00 also exhibits the largest OE value.

Another obvious rule can be found in Table 4. 3 is that the scenario with higher EV penetration consistently has larger $RMSE$, SSE and OE values, and smaller R^2 values. The strength of this relationship is also investigated in this study.

Comparing the dynamic responses at (a) T_1 (midnight) and (d) T_4 (peak time), the EV charging load demands are very similar, at 1.3775 MW and 1.3228 MW, respectively, as shown in Figure 4. 9. However, the dynamic response in DN is significantly different. This indicates that the dynamic response is influenced not only by the EV load demand but also by the EV penetration level, which shares the demand with other loads.

By the sight of R^2 values, the R^2 at (a) T_1 (c) T_3 (d) T_4. are relatively small and around 0.5 as shown in Table 4. 3. Despite this, their dynamic response appears not that similar in Figure 4. 10.

For the composite EV penetration scenario, the results are shown in Figure 4. 11.

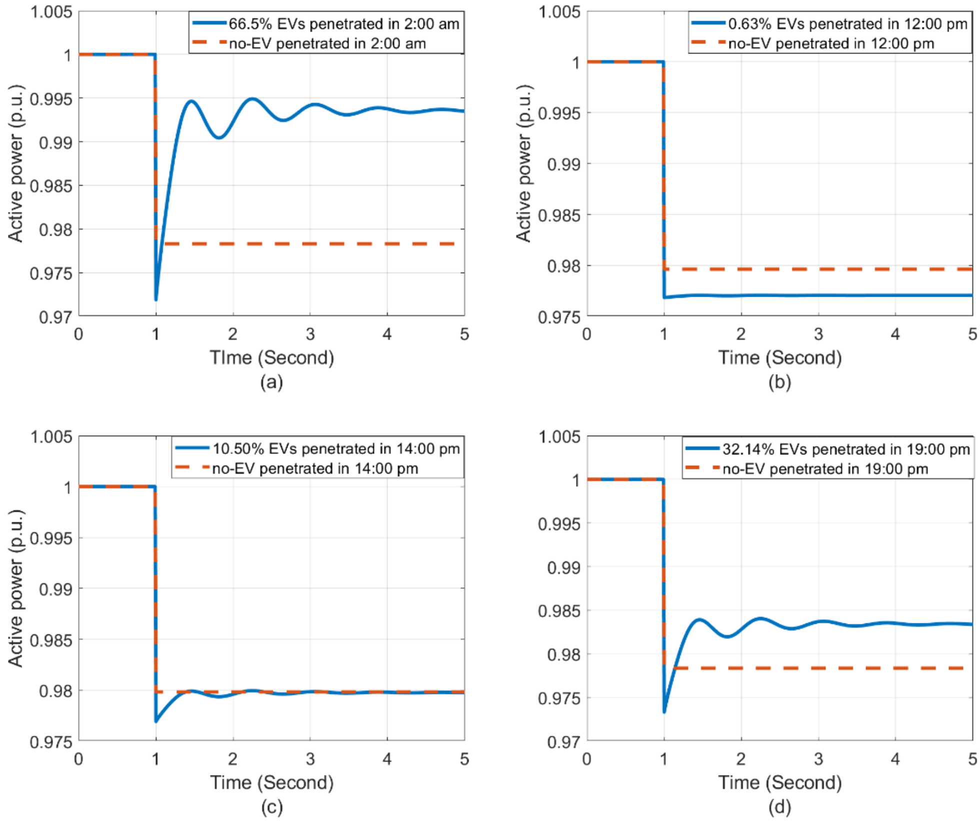

Figure 4. 11 Comparison of composite of EV penetration P_{EV} and $P_{No,EV}$ responses for S5 scenario during a -2.17% voltage disturbance. Time instance (a) T_1 (b) T_2 (c) T_3 (d) T_4.

Comparing the results shown in Figure 4. 10 and Figure 4. 11, a notable similarity emerges, particularly in the context of a larger recovery process when the penetration level of EVs increases. The system exhibits greater oscillation recovery following a voltage step change with higher EV penetration. In this scenario, the DN behaves more like a constant power load. On the other hand, a system with EV penetration invariably exhibits a larger overshoot error. Interestingly, this overshoot error is more pronounced than that observed in Figure 4. 10. This is why the result in Figure 4. 11(c) appears more similar to the no-EV scenario than the result from Figure 4. 11(b), despite the higher penetration of EVs into the DNs. To facilitate a more intuitive observation of the differences post-EV penetration, the indicator expressed in Section 3.4.5 is used to quantify the difference between the grid with and without EV penetration for these four typical scenarios. The results are shown in Table 4. 4.

Table 4. 4. Quantified the difference among 4 simulation scenarios with composite type EV load.

Time	EV penetration	$RMSE$	R^2	$SSE(\%)$	$OE(\%)$
2:00	66.56%	0.0122	0.5422	1.5378	0.6728
12:00	0.63%	0.0022	0.9998	0.3211	0.3431
14:00	10.50%	4.67E-04	0.9979	0.0050	0.3427
19:00	32.14%	0.0040	0.9639	0.5509	0.5627

The results bear a strong resemblance to the indicators presented in Table 4. 3. At 2:00 am, the greatest disparity between the EV and no-EV scenarios is observed. This discrepancy corresponds to the highest $RMSE$ value and the lowest R^2 value. This scenario also has a larger SSE which can be discerned from Figure 4. 7. Furthermore, increased EV penetration results in more pronounced dynamic characteristics in the response, leading to a heavier overshoot at the instant of disturbance occurrence. Consequently, the data at 02:00 also records the largest OE value.

Based on the R^2 values, the R^2 at (a) T_2 (c) T_3 (d) T_4. are relatively small and around 1 as shown in Table 4. 4. Meanwhile, the R^2 at T_1 still close to 0.5. This suggests that, the R^2 can also be influenced by the different types of EV model penetration, but this is only valid in scenarios without very high EV penetration. On the other hand, during the maximum EV penetration time, the DN's dynamic response is dominated by the EV, which results in significant differences from the no-EV scenarios, that R^2 will always be smaller.

An intriguing phenomenon emerges upon comparing the results from 12:00 and 14:00. The results at 14:00, which have a larger EV penetration and are more oscillatory but get better fitting quality on $RMSE$, R^2 and SSE. That is because the complex EV dynamic load model has a relatively larger overshoot, but is close to a constant power load. As the penetration of EV load increases, the worse overshoot results in a worse OE. On the other hand, the slightly larger power recovery can make a more similar steady-state which can result in better fitting quality.

4.5.2. Statistical analysis of error metrics

To provide further insights concerning the impact of EVs on DN dynamics, error metrics for all examined cases are computed and statistically analysed by means of boxplots. The corresponding results for single type EV penetration are summarized in Figure 4. 12. Additionally, in Figure 4. 13 the error metrics are presented as a function of the single type of EV penetration level for all the examined cases, i.e., for all examined time instances and scenarios.

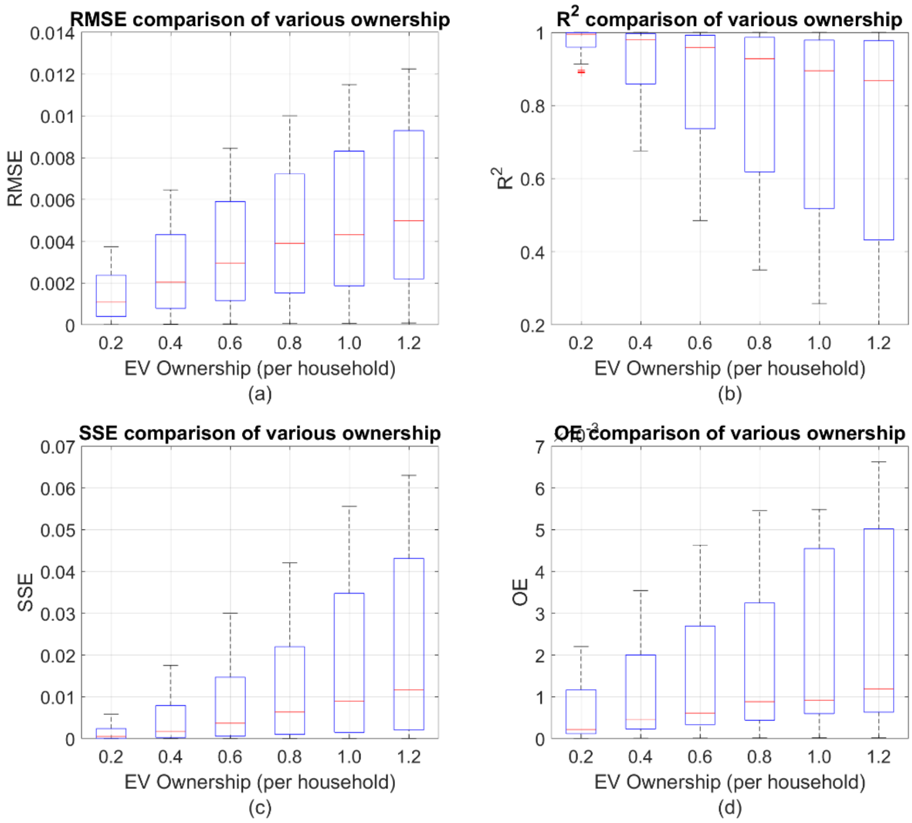

Figure 4. 12. Statistical analysis of error metrics using boxplots with single type EV penetration. (a) $RMSE$, (b) R^2, (c) SSE, and (d) OE

The four indicators used to quantify the differences are shown in Figure 4. 12, which illustrates the trend of EVs connecting to the power system. The $RMSE$ results indicate that increased EV penetration in power systems will lead to greater deviations in dynamic response under the same conditions. A similar conclusion can be drawn from the R^2 results. However, due to the length of the analysis window, the resulting difference is magnified. It is important to note that the best-fitting data, with an R^2 value close to 1, which is the data captured by the time of 12:00, with the lowest EV penetration. The

SSE results indicate that as more EVs are connected to the network, the steady-state value after a disturbance will change more significantly.

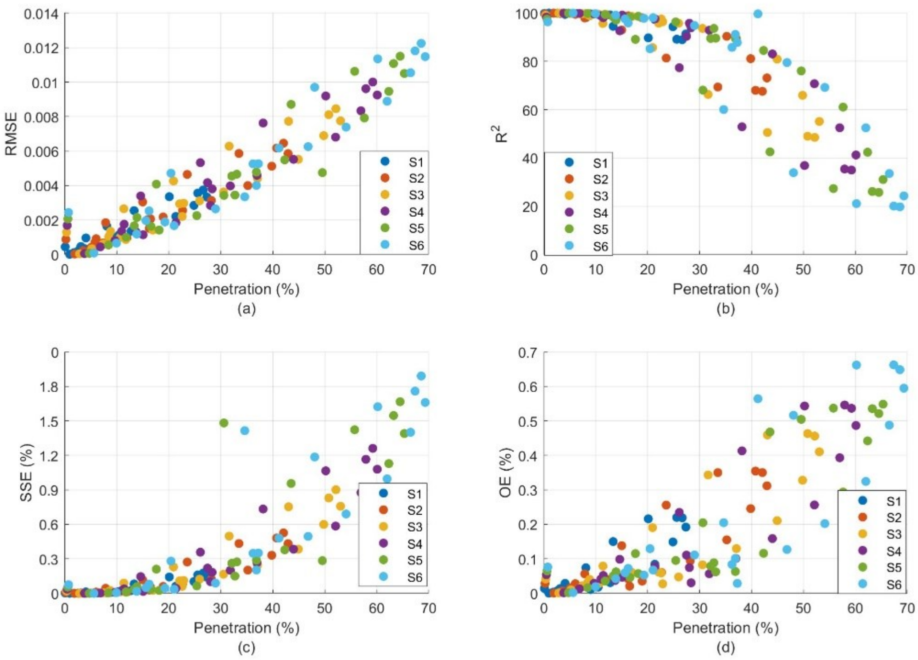

Figure 4. 13. Error metrics as a function of single type of EV ownership and EV penetration level. (a) $RMSE$; (b) R^2; (c) SSE; (d) OE.

Results of Figure 4. 12 and Figure 4. 13 reveal that as the EV penetration increases, $RMSE$, SSE, and OE generally increase, thus R^2 is reduced. It is evident that EVs have a clear impact on the dynamic characteristics of DNs.

On the other aspects, the four indicators also show some monotonicity with the increasing of EV penetration in Figure 4. 13. However, the same EV penetration does not mean other loads in this system are also in the same scenario. Which results in this monotonicity is not absolute. Further, this is also the reason that this study does not provide a precise number or fit these results via functions to represent the relationship between the EVs penetration and the number of indicators.

For the composite EV penetration, an evident pattern discernible from Table 4. 4 is that the scenario with more EV penetration always exhibits a larger oscillatory. However, when the EV penetration is minimal, a marginal increase in EV penetration can enhance the fitting quality. The results of the error metric for the composite type of EV penetration are presented in Figure 4. 14 and Figure 4. 15.

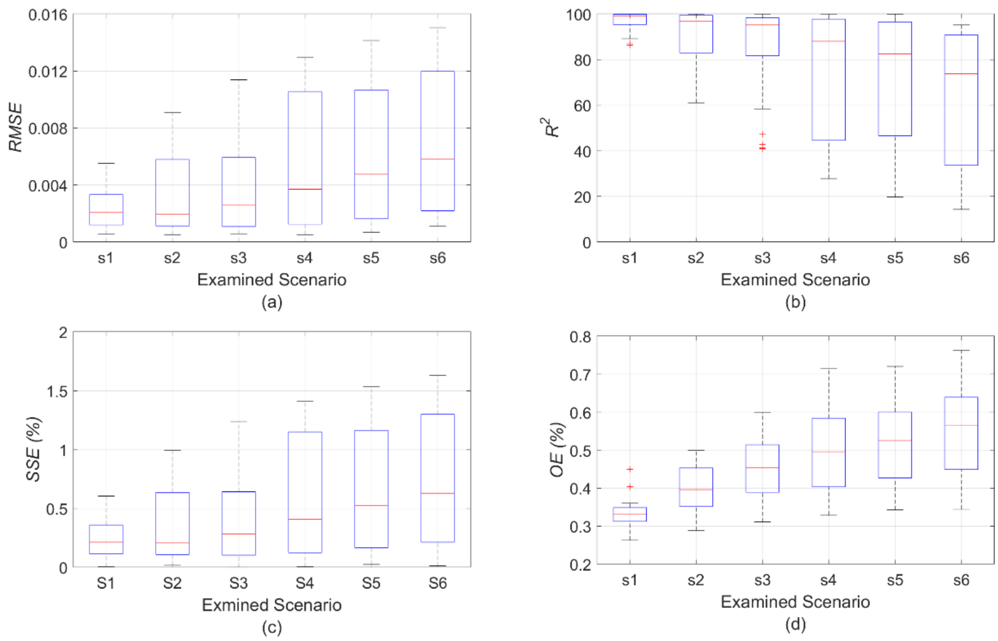

Figure 4. 14 Statical analysis of error metrics with composite EV penetration using boxplot. (a)$RMSE$, (b) R^2, (c) SSE, and (d) OE

The results of this study are quantified using four indicators, which are presented in Figure 4. 14. These indicators provide a general trend of the impact of EVs on power systems. The $RMSE$ results show that an increase in EV penetration levels can lead to higher deviations in the dynamic response under similar conditions. Similarly, the R^2 results demonstrate a similar trend, although the difference is magnified due to the length of the analysis window. It is worth noting that the best fitting data, captured at 12:00 with the lowest EV penetration, has an R^2 value close to 1, which indicates that the difference is likely caused by the penetration of EVs. The SSE results suggest that an increase in EVs connected to the power network will result in greater changes in the steady-state value following a disturbance. This is further supported by Figure 4. 14, which shows that the integrated load becomes closer to a constant power load with increased EV penetration levels. Finally, the OE results suggest that the connection of EVs will also result in more overshoot errors.

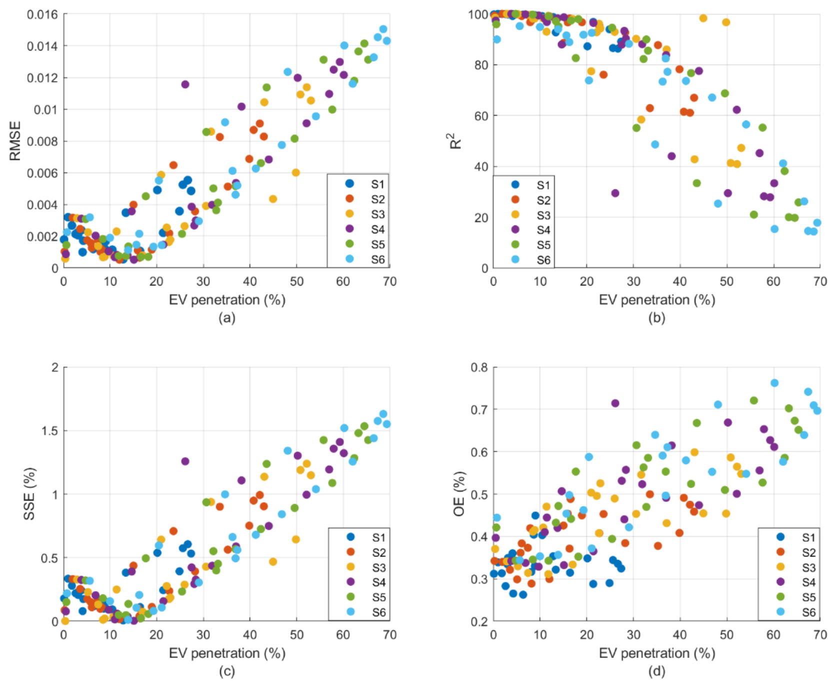

Figure 4. 15 Error metrics as a function of composite type EV ownership and EV penetration level. By complex EV penetration scenario (a) $RMSE$; (b) R^2; (c) SSE; (d) OE.

In summary, despite the apparent similarity between Figure 4. 12 and Figure 4. 14, there are significant differences in the dynamic response between the two scenarios compared in Figure 4. 10 and Figure 4. 11.

The variations observed in these four indicators for composite EV penetration align with the trends identified for single-type EV penetration. As EV penetration increases, the $RMSE$, SSE and OE increase, and the R^2 decreases. However, the application of this complex dynamic model yielded some notable distinctions. Specifically, it can be observed that the relationship between EV penetration levels and the indicators is not as robust as indicated by Figure 4. 13, due to the model's more intricate dynamic recovery process. Additionally, this analysis indicates that marginal increases in EV penetration levels can enhance fitting quality when EV penetration is low. From Figure 4. 15(b), it can be observed that there is a trend where higher EV penetration results in a smaller $RMSE$, this also confirms the inference made in Section 4.5.1.

This observation suggests that the indicators employed in this study may lack the precision necessary to comprehensively encapsulate the influence of EVs on DN in complex scenarios. Consequently, a more robust methodology is needed to overcome these limitations, which will be expressed in Chapter 4.

4.6 Summaries

In this chapter, the impact of EVs on the dynamic performance of DNs is investigated. Several test cases are examined, assuming different EV penetration levels and loading conditions. To replicate realistic loading and operational conditions, typical residential, industrial, as well as EV consumption profiles are used, and RMS simulations are performed on the benchmark MV DN of CIGRE using the DIgSILENT software. Moreover, the influence of PI parameters of EV chargers on network dynamics is analysed by performing parametric analysis. A subsequent evaluation is carried out to ascertain the network load capacity is sufficient to accommodate a scenario where all vehicles are replaced by EVs.

The dynamic characteristics derived from four typical time points demonstrate that DN penetrated by EVs exhibits varying dynamic behaviours at different times of daily operation. Generally, compared to the no-EV penetration scenario, the higher EV penetration level makes the DN have a worse OE but a smaller steady SSE. Overall, this study provides a general direction of change for the four quantification indicators ($RMSE$, R^2, SSE, and OE).

The result from the dynamic characteristics from the four typical time points illustrates that the higher EV penetration scenarios lead to larger overshoots and oscillations.

By comparing the results from single and composite types of EV penetration, this study finds that the differences cannot be distinctly illustrated through the four indicators. Therefore, a more precise quantification methodology is required for a detailed analysis.

Future research will focus on the PI parameters, these factors may have a significant impact on the penetration level of EVs, since they can affect the tripping of protection devices during voltage sags. Thus, the determination of the maximum EV penetration level, under different types of chargers and PI values, considering also dynamic constraints is another interesting topic for future research. Additionally, more sophisticated techniques shall be developed to provide further insights regarding the relation between EV penetration level and model parameters.

Chapter 5
Indicating the Dynamic Recovery Characteristics through Pole-Zero Analysis

5.1 Introduction

5.1.1 Motivation

As the market share of EVs continues to grow, an increasing number of EVs connect to the power system for battery charging. Beyond merely quantifying the differences among various EVs integrated into the system, it is crucial to explore the detailed impact on the system active power recovery. In the preceding Chapter, this thesis introduces the concept of an EV dynamic load model, which is integrated into the power network using four indicators. While these indicators effectively quantify different levels of EV penetration, they fall short of capturing the nuanced differences during the recovery process. For instance, composite types of EV penetration resulted in more complex oscillatory behaviour during recovery. This prompts the question of which method could be employed to reinforce the insight of the dynamic response.

Consequently, a type of indicating methodology is necessitated to fulfil this gap, that incorporates not only the comprehensive attributes of the two curves but also the characteristic points that are not subject to artificial selection.

The complexity of the dynamic response is primarily governed by the transfer function, a critical component of the dynamic equivalent model. Therefore, the method to quantify the characteristics of the transfer function would be a way to reinforce the insight of the dynamic response. The Pole-Zero representation can encompass the entirety of the transfer function, condensing its features into a handful of straightforward parameters [188]. As a result, this study introduces an analysis based on Pole-Zeros of the dynamic equivalent model of the entire DN hosting EVs. This approach will be employed to quantify and emphasize the dynamic characteristics.

5.1.2 Contributions

This chapter focuses on the dynamic recovery process and proposes a methodology to meticulously indicate the characteristics of dynamic recovery. To accomplish this, there are some tasks that need to be analysed:

- The simulation results from the preceding chapter have been presented using Pole-Zeros to highlight the characteristics of the complex dynamic response.

- These numerous Pole-Zeros are analysed using statistical methods, investigating their characteristics across various scenarios, such as EV ownership and operation time.
- This study has explored the optimal fitting order for the equivalent model across a range of operational scenarios. The optimal order is determined using the indicator R^2.

Fundamentally, this chapter builds upon the work of the preceding chapter. Its contributions extend beyond the scope of EV penetration into DNs, encompassing the analysis of complex dynamic characteristics. This broadens its application scenarios and benefits the power system dynamic stability analysis.

5.2 Pole-Zero Methodology

Pole-Zero analysis is a fundamental tool in control systems and power system stability analysis. It helps in understanding the behaviour of a system by examining its poles and zeros, which are derived from the system's transfer function. This implies that the transfer function, representing the dynamic characteristics of DNs with EV penetration, can be summarized using poles and zeros. Consequently, this approach facilitates the derivation of rules from a large number of response curves. The control system can be expressed to determine stability margins and transient response characteristics [190] This analysis is based on the transfer function obtained from the control loop, which is identical to the dynamic load model utilized in Chapter 3 [61][94][95]. This similarity between these two systems provides the inspiration for utilizing the Pole-Zero analysis in dynamic load modelling to investigate its dynamic characteristics and quantify its influence on system stability.

The transfer function has been expressed in the equation (2.9), to highlight its poles and zeros, this transfer function can be written as below:

$$G(s) = \frac{n(s)}{d(s)} = \frac{\beta_\nu s^\nu + \beta_{\nu-1} s^{\nu-1} + \cdots + \beta_0}{\alpha_\mu s^\mu + \alpha_{\mu-1} s^{\mu-1} + \cdots + \alpha_0} = K \frac{(s - z_1)(s - z_2) \ldots (s - z_\nu)}{(s - p_1)(s - p_2) \ldots (s - p_\mu)} \tag{5.1}$$

The coefficient $n(s)$ is the number polynomial of degree ν, and $d(s)$ is the denominator polynomial of degree μ. The poles of the system $G(s)$ are defined as the roots of the denominator polynomial equation, which $d(s) = 0$. The zeros of the system $G(s)$ are defined as the roots of the numerator polynomial equation, which $n(s) = 0$.

The zeros can be both real and complex numbers. If the zeros are complex, the zero locations will occur in complex conjugate pairs. The real and imaginary parts of the Pole-Zero can be defined by σ and ω, respectively.

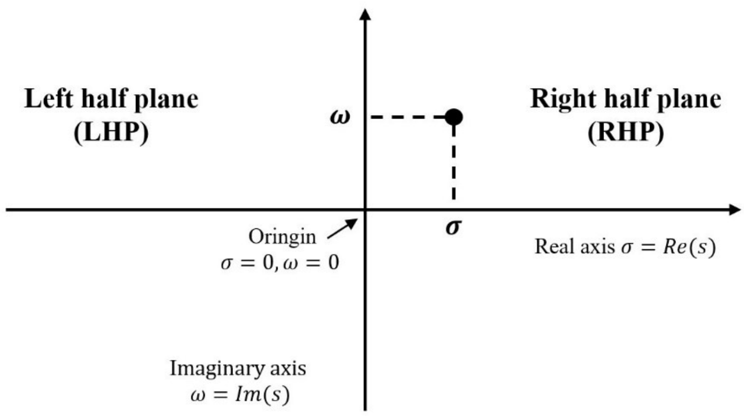

Figure 5. 1. s-plane for pole and zero location [190].

From Figure 5. 1 shown above, the complex Pole-Zero has been represented by the "Origin". The left of the imaginary axis is the Left Half Plane (LHP), and the region to the right of the imaginary axis is the Right Half Plane (RHP). Therefore, it can be identified, as a single pole in s-plane:

- If $\sigma = 0$, the response of the pole is a perfect oscillator.
- If $\omega = 0$, the response of the pole is a perfect exponential curve.
- If the pole is located in LHP, the exponential part of the response will decay towards zero, so the system becomes stable.
- If the pole is located in RHP, the exponential part of the response will rise towards infinity, and the system will be unstable.

In contrast to poles, modifications in the zeros do not directly and distinctly impact the dynamic response of the transfer function [190], except at certain specific points. Each zero indicates that the value of the transfer function equals zero at that point, resulting in an output of zero. An RHP zero introduces a phase lag in the system and terms characteristic to non-minimum phase systems, as the system's initial response to a step input is in the opposite direction of the final steady-state value [191].

In summary, the stable system means all the poles are located in the LHP, even if one of these poles lies in the RHP, the total response will be dominated by this pole and the system becomes unstable. There is no definitive criterion that dictates the role of zeros in determining the stable/unstable of a transfer function. An additional point that warrants emphasis is that, the characteristics of Pole-Zero analysis can primarily serve as a source of inspiration for dynamic stability analysis rather than being directly applicable. Given the potential issues that may arise from varying application scenarios, the characteristics of Pole-Zeros may not necessarily be relevant when analysing the characteristics of the dynamic equivalence model of DNs.

Because the distribution system under study is powered by an external grid, as illustrated in Figure 4. 5, and the only dynamic component is the EV dynamic load model, whose detailed dynamic characteristics are presented in Table 3. 3 and Table 3. 4, it is observed that the EV dynamic load model exhibits stable behaviour. Consequently, the distribution system under study does not experience any instability. The focus of the Pole-Zero analysis is to quantify the dynamic recovery characteristics, thereby providing a comprehensive analysis.

5.3 Analysis of dynamic recovery processes

The proposed modelling approach is used to derive dynamic equivalent models for entire DNs hosting EVs. The performance of the proposed method is evaluated under different loading conditions as well as under different EV penetration levels. For this purpose, the 144 cases of Section 4.5 are utilized. The composite type of EV load penetration which has been illustrated in Section 4.4.3 is utilized in this study. Moreover, the impact of the EV penetration level on the optimal order of the proposed model as well as on the required model parameters is assessed and recommendations for the derivation of generic equivalent model parameters are proposed. Furthermore, this chapter focuses on indicating the impact of EVs through Pole-Zero perspective, discusses the results predicated on Pole-Zero, and analyses their characteristics.

5.3.1 Fitting quality and target order of the transfer function

To derive reduced order equivalent models that represent the dynamic characteristics of the entire DN, the following procedure is adopted: dynamic responses of active power and voltage are recorded at the POI and forwarded as inputs to the developed method. Subsequently, the iterative procedure outlined in Section 3.4.1 is utilized for the determination of the optimal model order and for the identification of the required model parameters.

In order to maximize the dynamic characteristics from the response, this case study selects the time of 2 am in the morning with 1.2 EVs owned per household. The dynamic response fitted by the 1st 2nd and 3rd order transfer function based dynamic model is shown in Figure 5. 2 below.

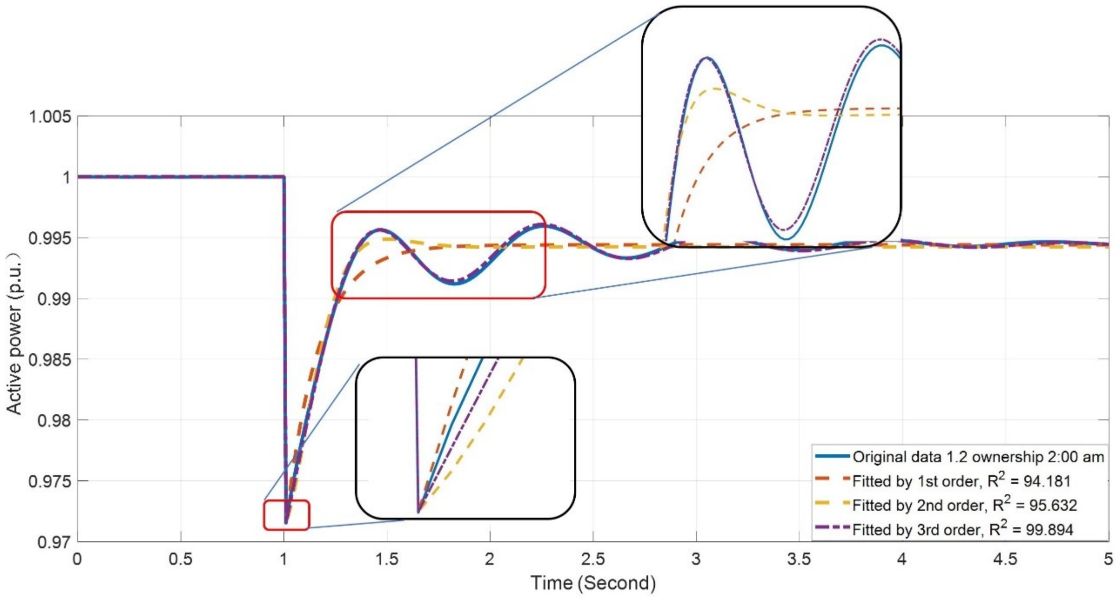

Figure 5. 2. Equivalencing of DNs. Convergence of the proposed modelling approach. Dynamic responses for S6, *T*=02:00 are used.

An indicative example is presented in Figure 5. 2, where the iterative procedure, used for the determination of the optimal model order, is illustrated. The ΔR^2 for the convergence of the iterative procedure is set to 1%. As shown, a 1st and a 2nd order model cannot capture accurately the oscillatory behaviour of the power. On the contrary, the 3rd order model provides very accurate results.

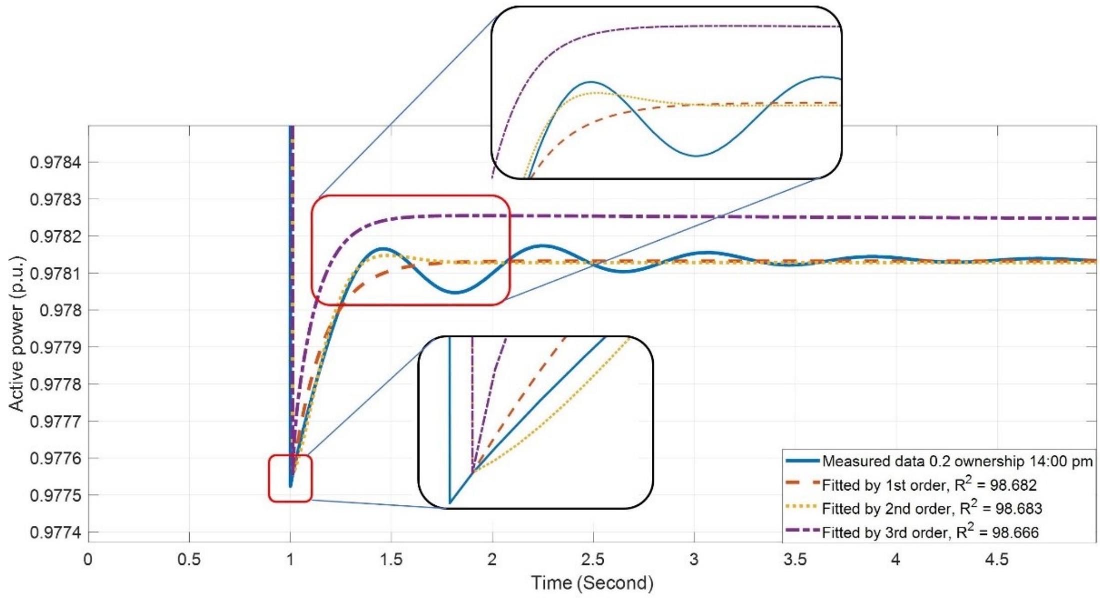

Figure 5. 3. Equivalencing of DNs. Convergence of the proposed modelling approach. Dynamic responses for S1, *T*=14:00 are used.

The dynamic data results, which correspond to a time of 14:00 and an EV ownership of 0.2 per household, represent the lowest EV penetration level, are illustrated in Figure 5. 3. The 3rd order transfer function does not exhibit a superior fitting quality in comparison to the others. Despite this, the result fitted by the 3rd transfer function exhibits a steady-state error, a characteristic absent in other results. On the other hand, the results from the 1st and 2nd transfer functions are similar. The sole distinction is the 2nd order function has an overshoot during the recovery process, which consequently enhances its fitting quality slightly over the 1st order transfer function.

5.3.2 Variability of model parameters - 5 seconds recorded

To thoroughly evaluate the performance of the proposed modelling approach, the dynamic responses of the 144 cases, as described in Section 3.4, are utilized. For each case, the proposed method is applied and equivalent models for the examined DN are derived. The original data is recorded 5 seconds after the disturbance occurs.

Table 5. 2. The fitting quality R^2 of the aggregated dynamic load modelling from the 1st order 2nd order and transfer functions.

Time	Ownership 0.2	Ownership 0.4	Ownership 0.6	Ownership 0.8	Ownership 1.0	Ownership 1.2
1:00	97.330	95.689	94.096	92.736	91.878	99.905
2:00	97.114	95.240	93.506	92.119	91.111	99.894
3:00	97.130	95.272	93.547	92.161	91.148	99.894
4:00	97.182	95.380	93.687	92.304	91.276	99.897
5:00	97.638	96.353	95.030	93.798	92.738	99.925
6:00	98.104	97.286	96.451	92.304	94.763	99.964
7:00	98.402	98.037	97.659	97.238	96.832	99.988
8:00	98.586	98.404	98.205	98.043	97.860	99.997
9:00	98.629	98.499	98.196	98.201	98.083	99.998
10:00	98.634	98.507	98.220	98.228	98.108	99.998
11:00	98.602	98.444	98.262	98.107	97.946	99.997
12:00	98.746	98.742	98.737	98.733	98.728	100.000
13:00	98.715	98.679	98.641	98.602	98.563	100.000
14:00	98.683	98.612	98.538	98.458	98.377	99.999
15:00	98.648	98.539	98.422	98.299	98.177	99.999
16:00	98.577	98.383	98.180	98.004	97.809	99.996
17:00	98.503	98.218	97.969	97.691	97.399	99.993
18:00	98.396	98.028	97.643	97.234	96.803	99.987
19:00	98.418	98.109	97.780	97.425	97.050	99.990
20:00	98.396	98.033	97.653	97.247	96.819	99.987
21:00	98.319	97.890	97.417	96.918	96.397	99.983
22:00	98.209	97.634	97.085	96.459	95.815	99.973
23:00	98.049	97.221	98.293	95.329	94.774	99.955
0:00	97.748	96.509	98.104	93.910	93.233	99.927

As delineated in Section 4.4.1, the EV essentially exhibits the highest penetration level around 02:00 am and the lowest penetration level around 14:00 pm. Furthermore, a higher EV ownership level can directly result in a higher penetration level of the EV dynamic load model. Consequently, a pattern can be discerned from Table 5. 2 indicating that the higher order, such as the 3rd order transfer function, typically exhibits superior fitting quality when the EV has a higher penetration level in DN.

However, this rule is not universally applicable, as the concept of 'Higher EV penetration' primarily centres on the independent value represented by EV charge demand. Even if the EV penetration level remains constant, the conditions of other loads, such as the residential and industrial loads in this study, might differ. This is why this study can only provide a rough rule. Combining the results from Figure 5. 2, Figure 5. 3 and Table 5. 2, when the EV penetration level is high, there is a significant complicated oscillatory recovery. The 1st and 2nd order transfer functions cannot adequately fit this oscillation, which is why the 3rd order transfer function normally has the best fitting quality. When the EV penetration level is low, the dynamic characteristics are not obvious, which is why the 3rd order transfer function has relatively worse fitting quality in this scenario.

The indicated Pole-Zeros will be incorporated within this section, and their evolving patterns under varying EV penetration levels will be exhibited and analysed.

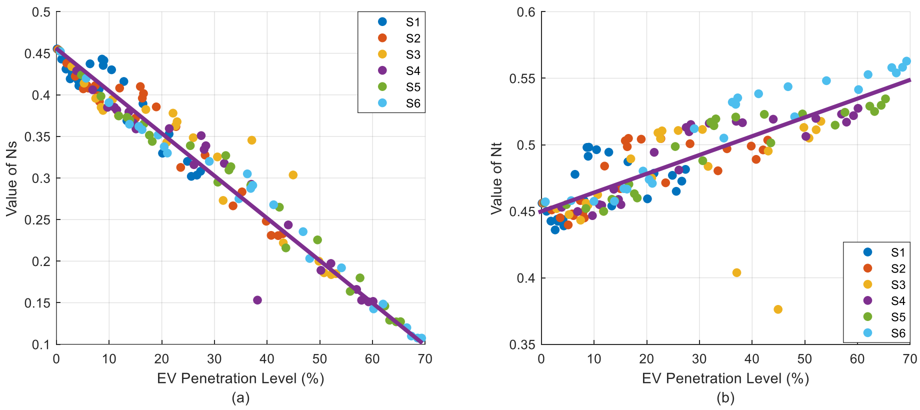

Figure 5. 4. Variations of (a) N_s and (b) N_t. across the 144 examined cases.

The S1 - S6 in Figure 5. 4 represent the nominal power of residential industrial and six examined EV load settings, as illustrated in Table 4. 1. It appears that there is a strong relationship between the value of N_s and the EV penetration level. As the EV penetration level increases, the static parameter N_s tends to decrease. This implies that the higher the EV penetration, the more the DN behaves as a constant power load a few seconds after a voltage disturbance. Additionally, as the EV penetration increases, voltage exponent N_t tends to increase. Thus, for higher EV penetration levels, larger power undershoots are expected. Finally, it is worth noting that the results of Figure 5. 4 reveal a strong linear relationship between the values of voltage exponents and the EV penetration level. This strong linear relationship can be used by DN operators to roughly predict the values of voltage exponents N_s and N_t based on the EV penetration level. This information can provide insights to the system operator regarding the expected power undershoot during a voltage disturbance as well as information regarding the new equilibrium point, i.e., the new steady-state of power after a voltage disturbance.

The poles fitted by 1st order transfer functions are presented in Figure 5. 5 below. Note that in this figure, the EV penetration on the x-axis is limited to 35%. It can be discerned that varying levels of EV penetration primarily influence the poles, indicative of stability, when few EVs penetrate this system. On the other hand, an interesting characteristic emerges in scenario S6, which represents 1.2 EVs owned per household, as it exhibits a deviation from the other scenarios.

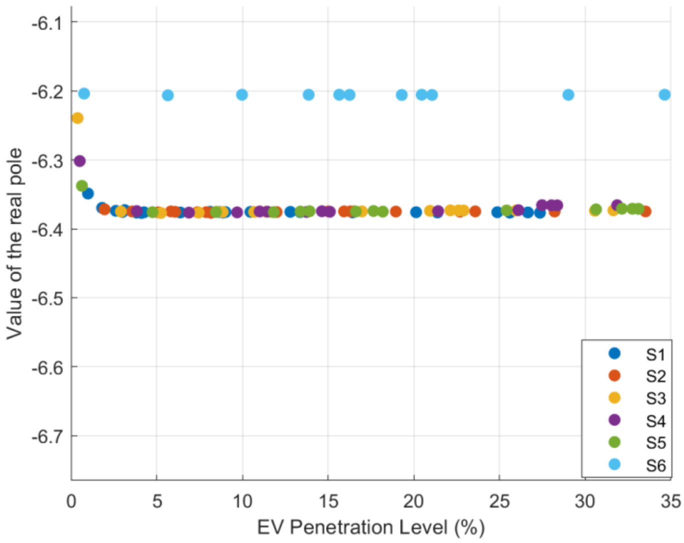

Figure 5. 5. Poles Variation for 1st order model.

This study conducted a detailed analysis of the characteristics of poles by separating them into real and imaginary parts. Figure 5. 6 presents the dynamic responses of DNs recorded under different EV ownership level settings. These results are fitted by 3rd order transfer functions using the methodology expressed in Section 3.4.3. Subsequently, the transfer functions from the equivalent dynamic model have been converted into Pole-Zero expressions.

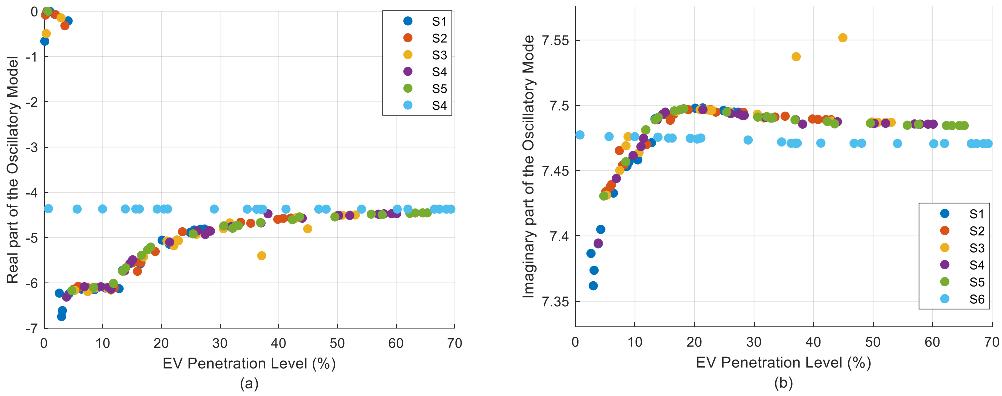

Figure 5. 6. Poles for third order models. (a): Real part of Pole; (b): Imaginary part of Pole;

As illustrated in Figure 5. 6, a robust correlation exists between the EV penetration level and EV ownership per household, as an increase in ownership signifies growth in EV penetration. Subsequently, when a low EV ownership level operates during low EV charging time, such as the scenario analysed in Figure 4. 11(b) there is not a clear dynamic recovery process. On this occasion, the fitted transfer function fails to accurately represent its dynamic response, which is why some poles are close to the coordinate zero point and the RHP area.

As the EV penetration level increases, the poles in the imaginary part also show a strong nonlinear relationship. However, similar to the results from the real part, the 1.2 EV ownership cases do not follow this relationship.

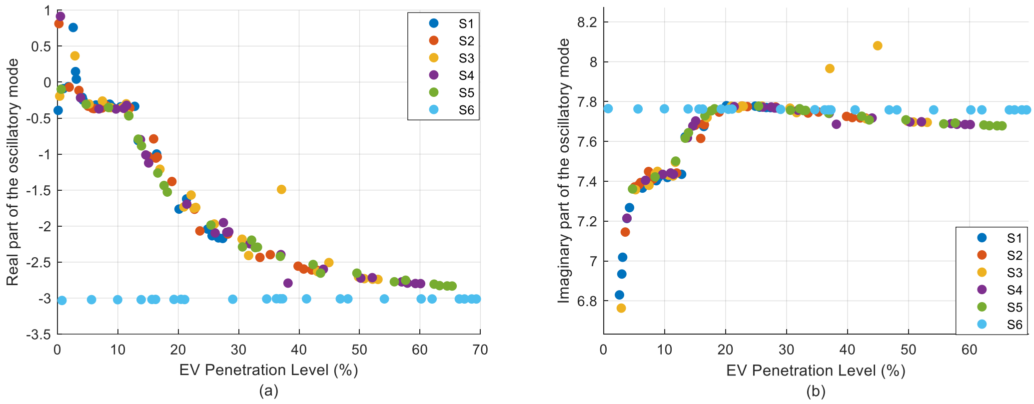

Figure 4. 7. Zeros for 3rd order model. (a): Real part of Zero; (b): Imaginary part of Zero;

Although the value of zeros does not directly determine whether the system is stable or not, it is still valuable to explore their changing patterns under different EV penetrations and ownership settings. Similar to the characteristics of poles, the values of zeros also show a strong relationship, except in 1.2 ownership scenarios.

5.3.3 Variability of model parameters - 0.3 second recorded

An interesting feature emerges from the results in Section 5.4.2. Not only does the EV penetration itself impact the poles and zeros of the dynamic response, but the EV ownership per household can also individually influence them in some cases. This section will use different fitting scales, guided by [189], rather than the 5 seconds, to identify results that differ from those in Section 5.4.2.

In this study, only 0.3 seconds after a disturbance occurs have been utilized in the fitting process of the equivalent function. To thoroughly evaluate the performance of the proposed modelling approach, the dynamic responses in the same cases as utilized in Section 5.4.2 are examined. For each case, the proposed method is applied, and equivalent models for the examined DN are derived. The resulting model order for each case is presented in Figure 5. 8, the corresponding R^2 values are summarized in Figure 5. 9. As shown, in all cases very high R^2 values (generally higher than 98%) are reported, demonstrating the accuracy of the proposed method.

The impact of EV penetration level on the required model order is analysed in Figure 5. 10. As shown, for low EV penetration scenarios, i.e., for EV penetration below 40%, 1st order models are adequate. On the other hand, for higher EV penetration levels (higher than 40%) 3rd order models are required.

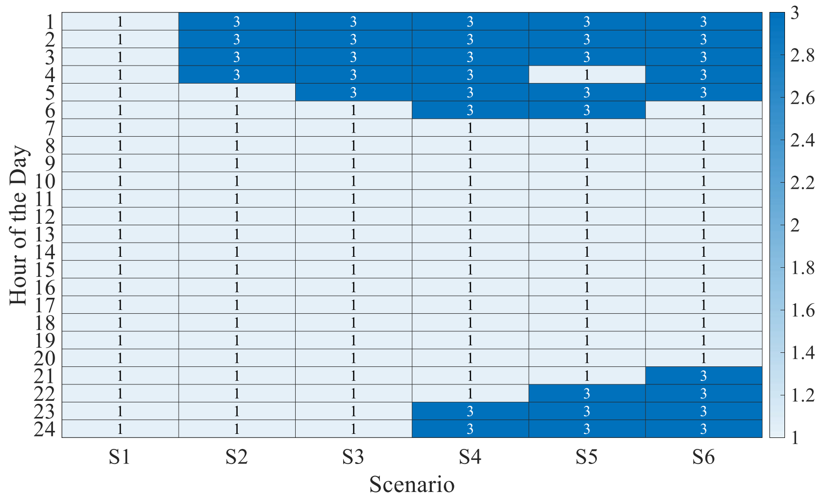

Figure 5. 8. Derivation of equivalent models for the examined DN under discrete loading conditions and EV penetration levels. Variability of model order.

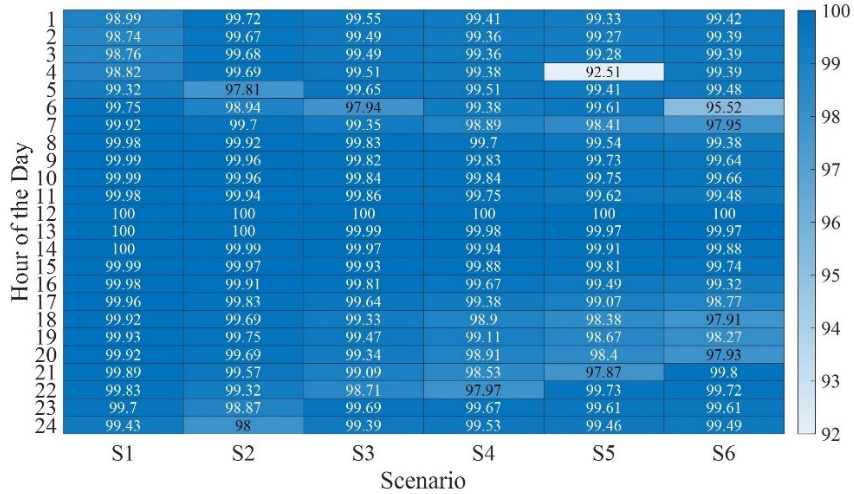

Figure 5. 9. Derivation of equivalent models for the examined DN under discrete loading conditions and EV penetration levels. Resulting R^2 values.

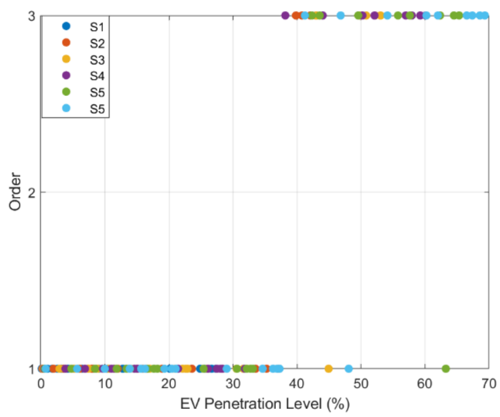

Figure 5. 10. Required model order for the dynamic analysis of DNs hosting EVs.

On the other hand, the static parameters N_s and N_t under the 0.3 second time scale fitting, are initially presented in Figure 5. 11.

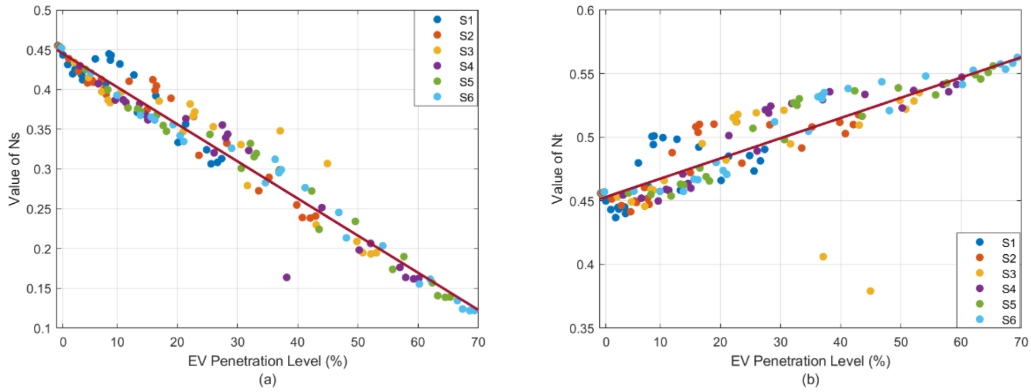

Figure 5. 11. Variation of (a): N_s and (b): N_t, fitted by the time range of 0.3 seconds after the disturbance occurred.

The result in Figure 5. 11 is very similar to the 5 second recording scenarios (Figure 5. 4). Both have a strong linear relationship between the value of voltage exponent and EV penetration level. Except, the high N_t in EV penetration scenarios is more concentrated. In general, the recording time scale almost no impact on the N_s and N_t.

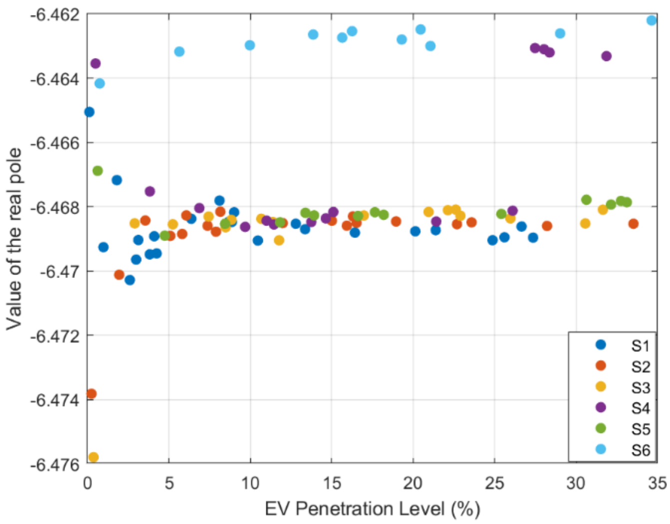

Figure 5. 12. Poles Variation for 1st order model.

To discern the variation in the value of the Pole between different recording scales, this study compared the outcomes in 5s (Figure 5. 5) and 0.3s (Figure 5. 12). Notably, the fitted results at the 0.3-second scale exhibit a higher concentration, particularly in scenarios with high EV penetration.

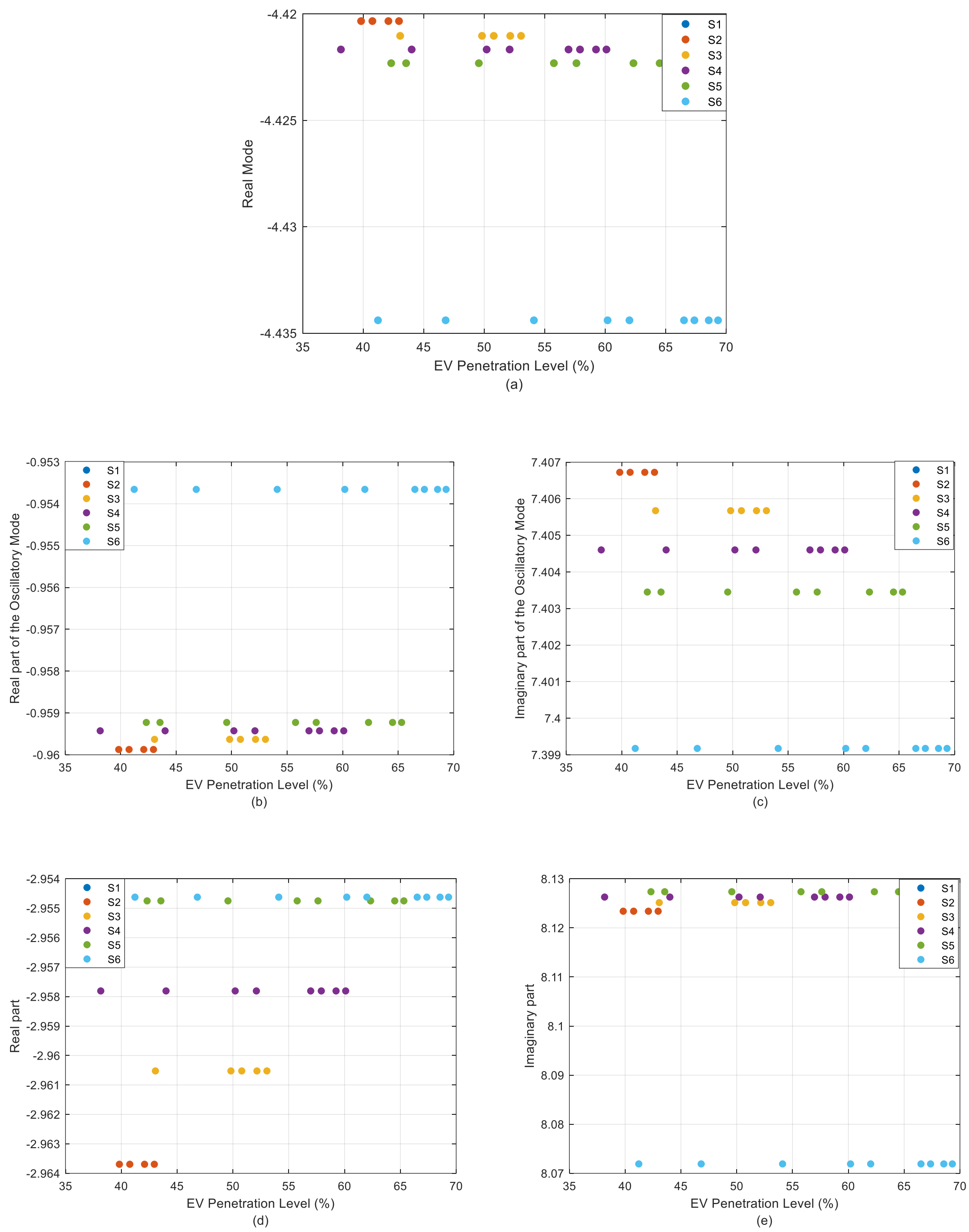

Figure 5. 13. Poles and Zeros for third order models. (a): Real Pole; (b): Real part of the oscillatory mode; (c): Imaginary part of the oscillatory mode; (d): Real part of Zeros; (e): Imaginary part of Zeros.

Concerning the 3rd order transfer functions, the variability of their parameters is presented in Figure 5. 13(a)-(e) As already explained, 3rd order transfer functions are used to simulate DN dynamics when EV penetration is relatively high, typically exceeding 40%. As shown in Figure 5. 13(a)-(e), the poles and zeros of these transfer functions do not vary considerably across the examined cases. In fact, only trivial differences are observed. As discussed in Section 2, the parameters of the developed transfer functions are mainly affected by the PI settings of the EV chargers. Therefore, since these settings do not change during the day, the variability of model parameters is rather limited.

Based on the aforementioned remarks, it can be deduced that when the transfer function is fitted by the 0.3 second time scale, the EV penetration level mainly affects the order of the required transfer functions. Nevertheless, the EV penetration level does not have a significant impact on the parameters of the transfer functions. Therefore, the system operator can use 1st order transfer functions for the modelling of DNs that present relatively low EV penetration levels, i.e., lower than 40%; 3rd order transfer functions shall be used for DNs with EV penetration levels. For both cases, since the variability of the parameters is restricted, typical parameters can be identified via a limited number of measurements/responses.

5.4 Summaries

This chapter employs the Pole-Zero concept to indicate the complex dynamic characteristics of DNs accommodating EVs, and the interesting attributes from the results.

The outcome is markedly influenced by the duration of the recording time. This chapter encompasses two distinct recording durations, such as, 0.3 seconds and 5 seconds. However, an interesting characteristic emerges unexpectedly, wherein the scenario of 1.2 EV ownership exhibits unique patterns of change, particularly during the 5-second recording duration.

Moreover, the impact of the EV penetration level on the order of the required transfer functions is analysed. Results reveal that for low EV penetration levels, 1st order transfer functions are generally needed, but for high EV penetration levels (higher than 40%), 3rd order transfer functions are required. Note that the 40% EV penetration level is an indicative value, determined by the analysis conducted in this thesis. This value can differ in cases where the PI parameters of fast and slow EV chargers differ considerably compared to those used in this study. Finally, the variability of model parameters is also assessed, and general guidelines are provided to facilitate the derivation of generic sets of parameters.

Future studies will concentrate on enhancing the robustness of Pole-Zero analysis, which may include proposing an optimal duration for data acquisition. Furthermore, for the interesting results, the 1.2 ownership exhibits a different role and should be deeply researched to identify the hidden reason.

Chapter 6
Stability of Electric Vehicle Charging Influenced by Battery State-of-Charge

6.1 Introduction

6.1.1 Motivation

In the preceding chapters, various aspects of EV charging within the power network have been investigated. In this chapter, this thesis will delve into the terminal stage of the charging process, specifically focusing on the EV's battery.

The battery is a critical component of EVs, and currently poses a significant technological challenge. The objective of this study is to shed light on the influence of the battery on EV load modelling. To address this question, this study undertakes a comprehensive review of EV battery modelling in this chapter, with a particular emphasis on the construction and control of the charging circuit, inclusive of the DC/DC converter briefly discussed in Chapter 2. Subsequently, this chapter introduced a representative battery charging terminal model to depict charging scenarios across a spectrum of State-of-Charge (SoC) levels. This model will be employed in subsequent simulations to examine the impact of varying SoC values on EV static load modelling.

6.1.2 Contributions

Building upon the established dynamic load modelling for EVs, this chapter introduces an electronic circuit-based battery charging model that can be incorporated into the existing modelling framework. In view of this independent component, this chapter will examine its impact on the current EV load model. The key contributions of this chapter are the following:

- A review of the typical electronic circuit-based battery model that can be employed in EV load modelling, along with an investigation of battery characteristics under different SoC conditions.
- An exploration of the phenomenon where the charging speed decreases as the battery approaches full charge. This chapter will focus on identifying which parameters of the battery model change and how these changes influence the EV charging model.
- The application of the EV model, adjusted for different SoC settings, to load modelling in order to observe deviations from the standard charging scenario

EV load model. This will address the question of whether a new load model is required to accurately represent the EV nearing a fully charged state.

6.2 Methodology

6.2.1 Characteristics and performance of batteries

Instead of the basic principles of chemistry, this study emphasizes the electrical characteristics of the battery. The initial challenge in this field is the representation of the energy stored in the battery. The unit "Ampere-hour (Ah)" can be employed to articulate this characteristic, which signifies the total power that can be discharged from a fully charged battery under specified conditions [109]. The rated Ah capacity is the nominal capacity of a fully charged battery, as predefined by the manufacturer. Furthermore, the unit "Watt-hour (Wh)" (or kWh) is also utilized to represent a battery capacity, which is defined as:

$$Rated\ Capacity_{Wh} = Rated\ Capacity_{Ah} \times Rated\ Voltage_{Battery} \tag{6.1}$$

On the other hand, the SoC is utilized to define the remaining capacity of battery. It is also affected by operating conditions, for example, battery temperature and load current.

$$SoC = \frac{Remaining\ Capacity}{Rated\ Capacity} \tag{6.2}$$

The change of SoC can be also expressed as the equation shown below if it is defined by Ah capacity.

$$\Delta SoC = SoC(t) - SoC(t_0) = \frac{1}{Ah}Capacity \int_{t_0}^{t} i(\tau)d\tau \tag{6.3}$$

In summary, the SoC serves as a parameter for quantifying the amount of electricity in the battery and for representing the battery's state during the charging process. From the perspective of EV charging, the End of Charge (EoC) characteristic is also a crucial consideration in electronic circuit-based battery modelling, although its relevance is contingent on the type of battery.

The Li-ion battery, which is extensively employed in EV manufacturing, exhibits EoC characteristics wherein the voltage increases rapidly as the battery nears full charge [87]. This phenomenon can be modelled by the polarisation resistance term. In the model, the polarisation resistance increases abruptly when the battery is almost fully charged.

$$R_{Pol} = K\frac{Q}{\int idt} \tag{6.4}$$

Where the $\int$ idt is actual battery charge (Ah), K is polarisation constant (V/Ah) or polarisation resistance R_{Pol}, and Q is battery capacity (Ah). Theoretically, if the battery is fully charged, the $\int idt$ should be 0. And at this moment, the R_{Pol} is infinite. On the other hand, there are some experimental results illustrating that the R_{Pol} is shifted by about 10% of the capacity of the battery [87][192], therefore, the equation (6.4) can be re-written as:

$$R_{Pol} = K\frac{Q}{\int idt - 0.1Q} \tag{6.5}$$

In this chapter, the battery modelling will be built based on the Li-Ion model. The battery voltage (V_{batt}) can be defined through the equation (6.6) shown below.

$$V_{batt} = E_0 - R \cdot i - R_{Pol} \cdot i^* - R_{Pol} \cdot \int idt + A \cdot exp(-B \cdot \int idt) \tag{6.6}$$

In this equation, E_0 is the battery constant voltage, R is the internal resistance, i^* is the filtered current. The parameters A and B are exponential zone amplitude (V) and exponential zone time constant inverse ($1/Ah$) respectively.

The electronic circuit-based battery model to be employed in this chapter is predicated on the aforementioned equation. It is important to underscore that this modelling is oriented towards power system stability studies, and as such, certain detailed characteristics of the battery will be disregarded. For instance, this study does not consider the influence of temperature or the memory effect of the battery. Furthermore, the internal resistance R remains invariant for the amplitude of the current.

6.2.2 Equivalent circuit models of batteries

The battery model employed in this study is based on an electronic circuit-based framework. This Li-ion EV battery model has been presented in [153], since the Li-ion battery is the most prevalent choice [192]. When compared to other battery types, Li-ion batteries exhibit superior energy density, diminished memory effect, and reduced power wastage. In relation to the battery characteristics outlined in Section 6.2.1, the electronic circuit-based battery model utilized in this Chapter is depicted below.

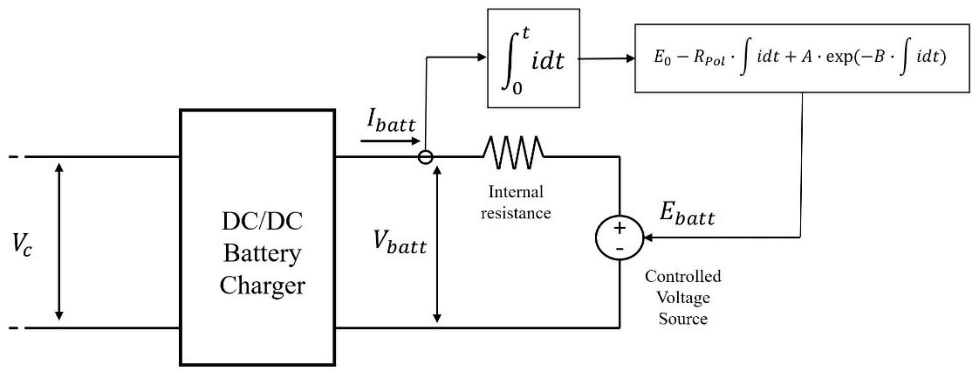

Figure 6. 1. Structure of electronic circuit based battery model [192].

The model illustrated in Figure 6. 1, represents a battery that comprises an equivalent voltage source, denoted as E_{batt} in series with an internal resistance. After passing through the DC/DC battery charger, the battery voltage V_{batt} is directly charging the battery. The equivalent voltage source is dictated by the battery's characteristics and its SoC. The E_{batt} can be calculated through the integration of the battery current I_{batt} over time and it consists of polarisation resistance R_{Pol}, which is defined in Equation (6.4) and (6.5). This term represents the non-linear voltage changes with the amplitude of the I_{batt}, and the SoC.

Typically, there are two main charging control strategies for the DC/DC battery charger - constant current control and constant voltage control. The constant current control maintains I_{batt} constant. The advantage of this charging strategy is that it maintains the charging speed within a safe and stable range. On the other hand, the E_{batt} can be changed by the charge state, which is shown in Figure 6. 2. When the battery is close to being fully charged, the charge state will cross the Q_{exp}, and enter an exponential zone. In this zone, the E_{batt} will increase rapidly. If the DC/DC charge controller continues to employ the constant current charge strategy, the V_{batt} will continue to increase which makes it dangerous.

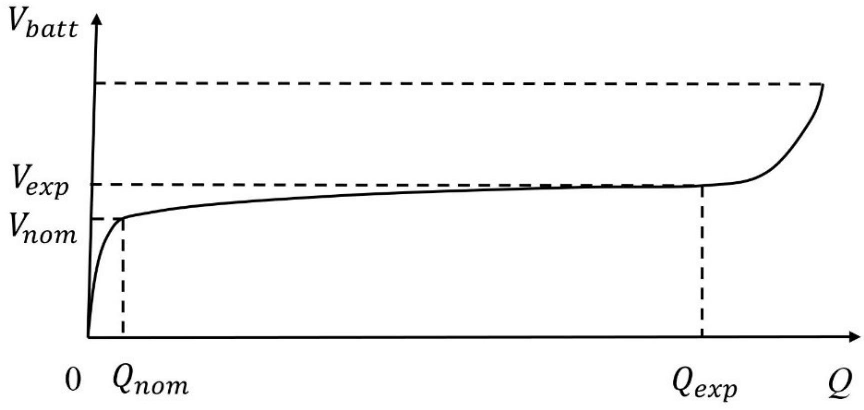

Figure 6. 2. Relationship between battery voltage V_{batt} and Battery electricity Q.

To circumvent potential hazards, the constant voltage charge strategy is employed in DC/DC charge control as the battery nears full charge. In this scenario, the V_{batt} remains constant, while the I_{batt} gradually decreases as E_{batt} increases. This is also why the charge speed slows down as the battery approaches full charge. When E_{batt} equals V_{batt}, there is no voltage drop across the internal resistance, resulting in I_{batt} becoming zero and consequently terminating the charge. The research conducted in [87][194] revealed that battery equivalent voltage (i.e., the internal voltage source E_{batt}) increased significantly in a high SoC. The power flow into the battery decreased with the DC/DC converter operating in constant voltage control.

In summary, the E_{batt} will remain relatively stable between nominal voltage V_{nom} and exponential voltage zone V_{exp} if the charge state keeps between the nominal capacity Q_{nom} and exponential capacity zone Q_{exp}.

From the perspective of this study, it is crucial to discern the differences among various SoC levels and ascertain whether these differences influence the load modelling of EVs. These variations can be reflected in different E_{batt}. This study will not consider the temperature affection, self-discharge of battery, and battery memory effect. More detailed explanations will be presented in Section 6.4.

6.3 Converter-based model with integrated batteries

The study presented in this chapter extends the research conducted in Chapter 3 by adding an electronic circuit-based battery model to the existing EV power electronic model. In the aforementioned Chapter 3, the EV charging model was divided into two approaches – single-phase slow charge (~7.4 kW, level-2) and DC fast charge (~50 kW). Both approaches deliver a stable DC charging power to the battery. Moreover, both methodologies share a common structure for the DC/DC converter and battery component, as illustrated in Figure 6. 3.

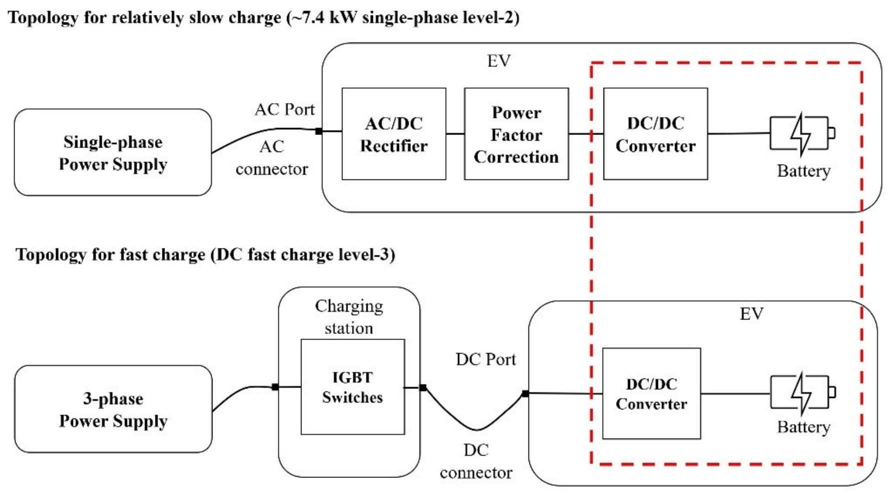

Figure 6. 3. Comparing both two charging approaches

The focus of the extended work in this section is on the battery component. As outlined in Section 6.2.2, the electronic circuit-based battery model can be constructed as depicted in Figure 6. 1. Consequently, the extended EV power electronic model, which will be utilized in this chapter, is established by replacing the battery component with the battery model described in [192]. It is important to emphasize that the objective of this study is to present a representative outcome of the characteristics of EV load modelling, including the battery component. Therefore, there is no need to extend both charging approaches individually.

The simulation model used in this study extends the DC fast charge model (~50 kW) by incorporating the electronic circuit-based battery model. This model will be crucial for investigating the characteristics of the battery as it nears full charge. It will enable a comparison of the load modelling results with the parameters outlined in Chapter 3. Furthermore, it will facilitate an analysis to determine whether a distinct load model needs to be developed separately for EVs approaching full charge.

6.4 Investigation of how battery SoC level affects EV equivalent model parameters

As presented in Chapter 3, the EV load model for power system stability studies encompasses both static and dynamic information. This model illustrates load characteristics through algebraic functions at any given instant and the dynamic response to small or large disturbances over time. However, it is important to note that once established, the components of the load model, such as $\theta = [N_s, N_t, \beta_\nu, \beta_{\nu-1}, \dots\ \beta_0, \alpha_{\mu-1}, \dots\ \alpha_0]$ illustrated from Section 2.3.2, remain invariant over time. This suggests that the existing load model structure may be insufficient in representing the dynamic characteristic changes as the battery approaches full charge, because these variables are predefined and remain constant in equations (3.5) – (3.9). This chapter focuses on the process when the EV is fully charged, examining whether the deceleration of the charging speed necessitates adjustments to the EV load model derived in Chapter 3. This section conducts multiple case studies at various stages during this process and compares the resulting load model with the conclusions drawn from Chapter 3.

In this study, high SoC scenarios have been modelled by increasing the battery equivalent voltage. A series of simulations were conducted, considering different levels of battery equivalent voltage (e.g., 420 V under normal conditions, 440 V, 460 V, and 480 V), which correspond to higher SoC. The same DC fast charge model used in Section 6.4.1 is considered for these studies. The results for active power at different voltage levels are presented in Figure 6. 4 below. These results reveal that, while the actual power level changes, the overall static load behaviour remains close to constant power (dependent on the battery voltage).

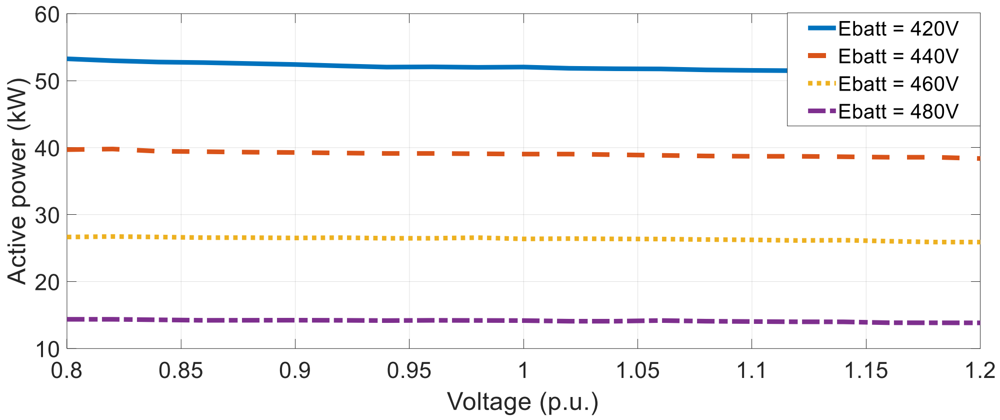

Figure 6. 4. Active power consumption for different battery equivalent voltage (E_{batt}) and voltage supplies.

In the preceding chapter, the exponential and ZIP models are selected to describe the static characteristics of the EV load model. In this section, by applying the curve fitting approach described previously to the results presented in Figure 6. 4, model parameters were extracted for the exponential and ZIP models. The numerical results for different SoC levels are presented in Table 6. 1. The parameter sets for both exponential and ZIP load models continue to indicate a near-constant power static behaviour from the EV charger.

Table 6. 1 Curve fitting parameters for DC fast charging approach for different battery equivalent voltage (E_{batt}) levels.

DC fast charge model				
E_{batt}	Exponential parameter	Z	I	P
420 V	−0.0921	0.062	−0.2199	1.156
440 V	−0.0764	0.044	−0.1651	1.12
460 V	−0.0683	−0.1440	0.218	0.9283
480 V	−0.0821	−0.1326	0.1816	0.9495

6.5 Summaries

In this study, to investigate whether the high SoC can impact the EV static modelling, the power electronic model of EV charging is extended by incorporating an electronic circuit-based battery model. This enhanced model can accurately represent the characteristics of the battery as it is near full charge. Subsequently, based on this implemented model, the study explores the process of charge termination. As SoC increases with more electricity flowing into the battery, the nominal equivalent voltage, E_{batt} also increases. On the other hand, the charge current decreases as the voltage drop across the internal resistance is reduced. When E_{batt} equals to V_{batt}, which is supplied via constant voltage control, the charging process stops.

Through a series of case studies that represent the battery charge at different SoC by adjusting E_{batt}. Based on the discussions and results presented, it is evident that the static load model does not need to account for varying SoC scenarios. In this study, the SoC is not directly a component in the circuit-based battery model but rather affects the battery excitation voltage. To simplify the process, a higher excitation voltage scenario is used to represent a higher SoC. This approach effectively achieves the study's objective.

Chapter 7
Conclusions and Future Work

7.1 Conclusions

This thesis investigates the impact of EV charging on power network dynamics, addressing several key aspects and providing comprehensive insights into the modelling and integration of EVs within power systems.

Dynamic Load Modelling - The study meticulously assesses the performance of dynamic load models, focusing on their ability to accurately represent the dynamic characteristics of EVs under voltage disturbances. It demonstrates that EV charging loads, both for slow & fast charging approaches, can be effectively represented as constant power loads in static scenarios. However, dynamic equivalent load models, derived using parameter estimation algorithms, reveal that control parameters significantly influence the dynamic response of EV chargers. The necessity of higher-order transfer functions (2^{nd} and 3^{rd} order) for accurate dynamic representation under varying control settings is highlighted, offering valuable information for system operators in stability studies.

Impact on Distribution Networks - The dynamic performance of DNs with varying levels of EV penetration is analysed using residential, industrial, and EV consumption profiles. This study performs RMS Simulations on the CIGRE benchmark MV DN to quantify the impact of different EV penetration scenarios, revealing that higher penetration levels lead to increased overshoot and oscillation in dynamic responses. The influence of PI parameters on network dynamics is also examined, with results statistically analysed through metrics such as $RMSE$, R^2, SSE and OE. The findings underscore the necessity of identifying detailed differences in the recovery process for comprehensive analysis and future research on the impact of PI parameters on EV penetration levels.

Pole-Zero Analysis - The study employs the Pole-Zero concept to analyse the complex dynamic characteristics of DNs accommodating EVs. It finds that the required order of transfer functions varies with EV penetration levels, with higher levels necessitating 3^{rd} order functions. This analysis provides general guidelines for deriving generic parameter sets and suggests future research directions to further explore the application of Pole-Zero analysis and investigate unique patterns observed at specific EV ownership scenarios.

State of Charge Influence - The power electronic model of EV charging is extended by incorporating an electronic circuit-based battery model to investigate the impact of high SoC on EV static modelling. The study concludes that while SoC affects the battery excitation voltage (E_{batt}), it does not necessitate adjustments to the EV static load model. This finding is based on a series of case studies and discussions, demonstrating that the implemented static load model remains valid across varying SoC scenarios.

Overall, this thesis provides contributions to the understanding of EV charging dynamics within power networks. It highlights the importance of accurate dynamic load modelling, the use of appropriate analysis techniques, and the potential effects of EV penetration on network stability.

7.2 Future work

This thesis has already outlined the scope of EV load modelling for power system dynamic stability, the impact of EV charging on power system distribution and transmission levels respectively, and some basic extensions about charge modelling influenced by battery charge states. Naturally, there are still numerous interesting aspects in these areas. Future areas of activity, which logically follow from the activities and outcomes reported in this thesis, are analysed in this section.

From the perspective of EV modelling, potential extensions include measuring real-world EVs to derive load models from actual data, as the current converter-based control model differs from real-world EVs. Additionally, the EV dynamic load model, derived from small voltage step disturbances, may not accurately represent EV behaviour under large voltage disturbances or other events. Collecting data from various event tests could enhance the model's generality and versatility. Furthermore, the extended EV model should incorporate more characteristics, such as frequency, rotor angle, and inertia for V2G scenarios, while remaining simple enough for integration into system-level studies.

For the system-level studies hosting EV charging. Potential extensions include improving EV demand estimation by using more accurate and reasonable EV charging demand distribution data, which can be implemented using the Monte-Carlo methodology, as the current study only considers the average EV load demand profile and estimated EV ownership per household. Additionally, applying the EV load model to other power networks beyond the CIGRE benchmark MV network could provide more typical results regarding the impact of EV charging on dynamic voltage stability.

This thesis uses Pole-Zero analysis to compare different scenarios in the dynamic recovery process. These scenarios include varying levels of EV ownership and EV penetration level. Interestingly, while both EV ownership and penetration levels are expected to affect the DN dynamic equivalent model similarly, the results show that in extreme cases (e.g., all vehicles are EVs), only EV ownership levels influence the model's parameters, with no change from different EV penetration levels. Future work should investigate the reasons behind this phenomenon and provide a theoretical explanation.

Appendix A - The explanation of the fitting result with negative R^2

The R^2 is defined in equation (2.13), which is utilized to quantify the fitting quality. It also implies that the R^2 should always be a positive value when the coefficient R is not an imaginary or complex number. However, the negative value of R^2 can be observed from some results. The purpose of this Appendix is to investigate and discuss the reasons for this occurrence.

In addition to illustrating the R^2 through the calculation equation, but from the definition equation, which is shown in $(A.1)$. The R^2 is a parameter to represent the relationship between RSS, TSS and ESS. Where the RSS, TSS and ESS represent the residual sum of squares, tot sum of squares, and explained sum of squares, respectively.

$$R^2 = 1 - \frac{RSS}{TSS} = \frac{ESS}{TSS} \tag{A.1}$$

Where:

$$RSS = \sum_{n=1}^{N} (y[n] - \hat{y}[n])^2 \tag{A.2}$$

$$TSS = \sum_{n=1}^{N} (y[n] - \bar{y})^2 \tag{A.3}$$

$$ESS = \sum_{n=1}^{N} (\hat{y}[n] - \bar{y})^2 \tag{A.4}$$

$\bar{y}$ is the mean value of the response, $\hat{y}$ is the estimated value. Transfer the equation $(D.3)$ into:

$$TSS = \sum_{n=1}^{N} (y[n] - \hat{y}[n] + \hat{y}[n] - \bar{y})^2 \tag{A.5}$$

And then:

$$TSS = \sum_{n=1}^{N} (y[n] - \hat{y}[n])^2 + \sum_{n=1}^{N} (\hat{y}[n] - \bar{y})^2 + 2 \cdot \sum_{n=1}^{N} (y[n] - \hat{y}[n])(\hat{y}[n] - \bar{y}) \tag{A.6}$$

$$TSS = SS + ESS + 2 \cdot \sum_{n=1}^{N} (y[n] - \hat{y}[n])(\hat{y}[n] - \bar{y}) \tag{A.7}$$

Finally, another equation for R^2 can be obtained.

$$R^2 = \frac{ESS + 2 \cdot \sum_{n=1}^{N}(y[n] - \hat{y}[n])(\hat{y}[n] - \bar{y})}{TSS} \qquad (A.8)$$

By focusing on the component $\sum_{n=1}^{N}(y[n] - \hat{y}[n])(\hat{y}[n] - \bar{y})$. It can be seen that if the estimated data is significantly different from the original data, the signs of these two parts may become opposite. In this case, this component can become a large negative value, which can result in a negative R^2.

Bibliography

[1] John Cook, Nuccitelli Dana, Green Sarah, "Quantifying the consensus on anthropogenic global warming in the scientific lecture," Environ Res Lett, vol. 8, no. 2, p. 024024, 2013.

[2] X. Xia, P. Li, Z. Xia, R. Wu, and Y. Cheng, "Life cycle carbon footprint of electric vehicles in different countries: A review," Separation and Purification Technology, vol. 301, Nov. 2022.

[3] N. Wang, and G. Tang, "A review on environmental efficiency evaluation of new energy vehicles using life cycle analysis", Sustainability, vol. 14, 2022.

[4] European Commission. (2020). A European strategy for low-emission mobility. https://ec.europa.eu/clima/policies/transport _ en , accessed 09.07.2020

[5] Y. A. Wu, A. W. Ng, Z. Yu, J. Huang, K. Meng, and Z. Y. Dong, "A review of evolutionary policy incentives for sustainable development of electric vehicles in China: Strategic implications," Energy Policy, vol. 148, Jan. 2021.

[6] N. Wang, L. Tang, and H. Pan, "A global comparison and assessment of incentive policy on electric vehicle promotion," Sustainable Cities and Society, vol. 44, pp. 597-603, Jan. 2019.

[7] J.A. Sanguesa, V. Torres-Sanz, P. Garrido, F. J. Martinez, and J. M. Marquez-Barja, "A Review on Electric Vehicles: Technologies and Challenges," Smart Cities, vol. 4, no. 1, pp. 372-404, 2021

[8] U. Tietge, P. Mock, N. Lutsey, and A. Campestrini. "Comparison of leading electric vehicle policy and deployment in Europe." ICCT The international council on clean transportation, 2016. [Online]. Available: https://theicct.org/node/1209.

[9] IEA, World energy outlook 2021, (2021). https://iea.blob.core.windows.net/ass ets/4ed140c1-c3f3-4fd9-acae-789a4e14a23c/WorldEnergyOutlook2021.pdf.

[10] IEA, Global EV outlook 2022, (2022). https://iea.blob.core.windows.net/assets /ad8fb04c-4f75-42fc-973a-6e54c8a4449a/GlobalElectricVehicleOutlook2022. pdf

[11] IEA (2023), Global EV Outlook 2023, IEA, Paris https://www.iea.org/reports/global-ev-outlook-2023, Licence: CC BY 4.0

[12] European Commission, “Press release: European Commission proposes a Digital Compass to translate the EU’s digital ambitions for 2030 into concrete action,”, Dec. 15, 2021.

[13] International Energy Agency (IEA). Global EV Outlook 201: scaling up the transition to electrical mobility. Paris. 2019. Available at: https://www.iea.org/reports/global-ev-outlook-2019

[14] R R. Kumar and K. Alok, “Adoption of electric vehicle: A literature review and prospects for sustainability,” Journal of Cleaner Production, vol. 253, p. 119911, 2020. Available: https://doi.org/10.1016/j.jclepro.2019.119911

[15] Department for Transport, "Decarbonising Transport: A Better, Greener Britain," UK Government, London, UK, Jul. 2021. [Online]. Available: https://assets.publishing.service.gov.uk/media/610d63ffe90e0706d92fa282/decarbonising-transport-a-better-greener-britain.pdf

[16] European Commission, "Delivering the European Green Deal," European Union, Brussels, Belgium, Jul. 2021. [Online]. Available: https://ec.europa.eu/clima/eu-action/european-green-deal/delivering-european-green-deal_en

[17] International Energy Agency, "Global EV Outlook 2021: Policies to Promote Electric Vehicle Deployment," IEA, Paris, France, Apr. 2021. [Online]. Available: https://www.iea.org/reports/global-ev-outlook-2021/policies-to-promote-electric-vehicle-deployment

[18] Z. Yang, "Beyond Europe: Are there ambitious electrification targets across major markets?," International Council on Clean Transportation, Nov. 2022. [Online]. Available: https://theicct.org/global-oem-targets-cars-ldvs-nov22/

[19] E. Pipitone, S. Caltabellotta, and L. Occhipinti, “A Life Cycle Environmental Impact Comparison between Traditional, Hybrid, and Electric Vehicles in the European Context,” Sustainability, vol. 13, no. 19, p. 10992, 2021. Available:. https://doi.org/10.3390/su131910992

[20] M. Nour, J. P. Chaves-Avila, G. Magdy, and A. Sanchez-Miralles, “Review of positive and negative impacts of electric vehicles charging on electric power systems,” Energies, vol. 13, no. 18, Sep. 2020.

[21] S. Habib, M. M. Khan, F. Abbas, L. Sang, M. U. Shahid, and H. Tang, “A comprehensive study of implemented standards, technical challenges, impacts and prospects for electric vehicles,” IEEE Access, vol. 6, pp. 13866-13890, 2018.

[22] Z. Guo, J. Zhang, R. Zhang and X. Zhang, "Aviation-to-Grid Flexibility Through Electric Aircraft Charging," in *IEEE Transactions on Industrial Informatics*, vol. 18, no. 11, pp. 8149-8159, Nov. 2022, doi: 10.1109/TII.2021.3128252.

[23] H. Tian, D. Tzelepis, P. N. Papadopoulos. “Electric Vehicle Charger Static and Dynamic Modelling for Power System Studies.” Energies 2021, 14, 1801.

[24] D. Pandit, N. Nguyen and J. Mitra, "Reliability of EV-Integrated Systems Considering Inertia and Primary Frequency Regulation," 2022 North American Power Symposium (NAPS), Salt Lake City, UT, USA, 2022, pp. 1-6, doi: 10.1109/NAPS56150.2022.10012175

[25] H. W. Qazi, D. Flynn and Z. H. Rather, "Impact of electric vehicle load response variation on frequency stability," 2016 IEEE PES Innovative Smart Grid Technologies Conference Europe (ISGT-Europe), Ljubljana, Slovenia, 2016, pp. 1-6, doi: 10.1109/ISGTEurope.2016.7856268.

[26] S. Huang, J. R. Pillai, B. Bak-Jensen and P. Thøgersen, "Voltage support from electric vehicles in distribution grid," 2013 15th European Conference on Power Electronics and Applications (EPE), Lille, France, 2013, pp. 1-8, doi: 10.1109/EPE.2013.6634344.

[27] J. Miret, M. Castilla and À. Borrell, "Optimizing Voltage Support using Electric Vehicles in an Islanded Microgrid under Voltage Sags," 2022 IEEE 31st International Symposium on Industrial Electronics (ISIE), Anchorage, AK, USA, 2022, pp. 24-31, doi: 10.1109/ISIE51582.2022.9831738.

[28] Gorner and L. Paoli, “Nearly half of all prospective new car buyers are thinking of going electric,” IEA Commentary, 2021. Available:. https://www.weforum.org/agenda/2021/08/coronavirus-increased-ev-sales/

[29] M. Gorner,L. Paoli, “How global electric car sales defied Covid-19 in 2020,” IEA Commentary, 2021. Available: https://www.iea.org/commentaries/how-global-electric-car-sales-defied-covid-19-in-2020

[30] T. Gersdorf, R. Hensley, P. Hertzke, and P. Schaufuss, "Electric mobility after the crisis: Why an auto slowdown won't hurt EV demand," Single-resource - Digital Library on Green Mobility – DLGM, 2020. Available:https://greenmobility-library.org/public/index.php/single-resource/SkZBUW54MGNEWlo3RnBxelVwUjNiQT09

[31] T. Gersdorf, R. Hensley, P. Hertzke, and P. Schaufuss, "Challenges and opportunities for EV manufacturers during the pandemic," Journal of Electric Vehicle Technology, 2020. Available https://spectrum.ieee.org/the-ev-transition-explained-2659602311

[32] International Electrotechnical Commission, IEC 62196-1:2014, https://webstore.iec.ch/publication/6582

[33] International Electrotechnical Commission, IEC 61851-1:2017, https://webstore.iec.ch/publication/33644

[34] T. Braunl, "EV charging standards," University of Western Australia, Perth, Australia, 2012, pp. 1-5.

[35] ICF Consulting Services. Overview of Electric Vehicle Market and the Potential of Points for Demand Response; ICF Consulting Service: Fairfax, VA, USA, 2016; pp. 1–32.

[36] Scottish Power website, Electric Vehicle charger installation. https://www.scottishpower.co.uk/electric-vehicles/chargers

[37] SSE website, Electric vehicle charger installation. https://www.sseairtricity.com/ie/home/home-services/electric-vehicle-charger-installation/

[38] ABB Terra CE53–JCG. Available online: https://new.abb.com/products/4EPY410071R1/terrace53-cjg-terra-50-kw-charger-ccs-chademo-ac-cable-ce

[39] J2954-202010 , "Ground Vehicle Standard, Wireless Power Transfer for Light-Duty Plug-in/Electric Vehicles and Alignment Methodology," SAE Standard, Warrendale, PA, USA, 2020. Available: https://www.sae.org/standards/content/j2954_202010/.

[40] EV Database, “Useable battery capacity of full electric vehicles,” [Online]. Available: https://ev-database.org/cheatsheet/useable-battery-capacity-electric-car.

[41] Tesla Model Y (2022-2024) price and specifications,” [Online]. Available: https://ev-database.org/car/1743/Tesla-Model-Y. [Accessed: 04-Oct-2024]

[42] M. Chen, D. Zhou, A. Tayyebi, E. Prieto-Araujo, F. Dörfler and F. Blaabjerg, "On Power Control of Grid-Forming Converters: Modeling, Controllability, and Full-State Feedback Design," in IEEE Transactions on Sustainable Energy, vol. 15, no. 1, pp. 68-80, Jan. 2024, doi: 10.1109/TSTE.2023.3271317

[43] F. Blaabjerg, H. Wang, I. Vernica, B. Liu and P. Davari, "Reliability of Power Electronic Systems for EV/HEV Applications," in *Proceedings of the IEEE*, vol. 109, no. 6, pp. 1060-1076, June 2021, doi: 10.1109/JPROC.2020.3031041.

[44] D. K. Singh and A. K. Bohre, "Planning of EV Fast Charging Station Including DG in Distribution System Using Optimization Technique," 2020 IEEE International Conference on Power Electronics, Drives and Energy Systems (PEDES), Jaipur, India, 2020, pp. 1-6, doi: 10.1109/PEDES49360.2020.9379351.

[45] B. Faujdar and R. K. Pandey, "Overview of EV Charging Smart Control Architecture-Recent Developments," 2023 International Conference on Power, Instrumentation, Energy and Control (PIECON), Aligarh, India, 2023, pp. 1-6, doi: 10.1109/PIECON56912.2023.10085827.

[46] P. Xue et al., "Robust Joint Planning of Electric Vehicle Charging Infrastructures and Distribution Networks," 2022 7th Asia Conference on Power and Electrical Engineering (ACPEE), Hangzhou, China, 2022, pp. 135-139, doi: 10.1109/ACPEE53904.2022.9783920.

[47] C . H. Dharmakeerthi, N. Mithulananthan, and T. K. Saha, “Impact of electric vehicle fast charging on power system voltage stability,” Int. J. Electr. Power Energy Syst., vol. 57, pp. 241–249, 2014. doi:10.1016/j.ijepes.2013.12.005.

[48] K. M. S. Y. Konara and M. L. Kolhe, "Charging Coordination of Opportunistic EV Users at Fast Charging Station with Adaptive Charging," 2021 IEEE Transportation Electrification Conference (ITEC-India), New Delhi, India, 2021, pp. 1-6, doi: 10.1109/ITEC-India53713.2021.9932507.

[49] A. P. Sidharthan and S. A. Arefi, "Optimization of Charging in a Multi-Port EV Charging Station for Emergency Vehicle Priority Fast Charging," 2021 IEEE International Women in Engineering (WIE) Conference on Electrical and Computer Engineering (WIECON-ECE), Dhaka, Bangladesh, 2021, pp. 192-195, doi: 10.1109/WIECON-ECE54711.2021.9829632.

[50] M. Garau and B. N. Torsæter, "Agent-Based Analysis of Spatial Flexibility in EV Charging Demand at Public Fast Charging Stations," 2021 IEEE Madrid PowerTech, Madrid, Spain, 2021, pp. 1-6, doi: 10.1109/PowerTech46648.2021.9494818.

[51] M. Ehsani, K. V. Singh, H. O. Bansal and R. T. Mehrjardi, "State of the Art and Trends in Electric and Hybrid Electric Vehicles," in Proceedings of the IEEE, vol. 109, no. 6, pp. 967-984, June 2021, doi: 10.1109/JPROC.2021.3072788.

[52] F. Marra, G. Y. Yang, C. Træholt, E. Larsen, C. N. Rasmussen and S. You, "Demand profile study of battery electric vehicle under different charging options," 2012 IEEE Power and Energy Society General Meeting, 2012, pp. 1-7, doi: 10.1109/PESGM.2012.6345063.

[53] Omar Hanafy Abdalla, "Dynamic load modelling and aggregation in power system simulation studies", 12th international Middle-East Power System Conference, 2008.

[54] I. F. Visconti, D. A. Lima, J. M. C. d. S. Costa and N. R. d. B. C. Sobrinho, "Measurement-Based Load Modeling Using Transfer Functions for Dynamic Simulations," in IEEE Transactions on Power Systems, vol. 29, no. 1, pp. 111-120, Jan. 2014, doi: 10.1109/TPWRS.2013.2279759

[55] S. L. Rani and V. V. R. Raju, "V2G and G2V Technology in Micro-Grid Using Bidirectional Charger: A Review," 2022 Second International Conference on Power, Control and Computing Technologies (ICPC2T), Raipur, India, 2022, pp. 1-5, doi: 10.1109/ICPC2T53885.2022.9777085.

[56] U. Chukwu and S. Mahajan, "The Modeling of V2G Component for Power Flow Studies," 2018 Clemson University Power Systems Conference (PSC), Charleston, SC, USA, 2018, pp. 1-5, doi: 10.1109/PSC.2018.8664049.

[57] S. Sahoo, D. R. Pullaguram and S. Mishra, "A consensus priority algorithm based V2G charging framework for frequency response," 2016

IEEE 7th Power India International Conference (PIICON), Bikaner, India, 2016, pp. 1-6, doi: 10.1109/POWERI.2016.8077297.

[58] F. R. Islam and H. R. Pota, "V2G technology to improve wind power quality and stability," 2011 Australian Control Conference, Melbourne, VIC, Australia, 2011, pp. 452-457.

[59] Kundur. Power system load in Power System Stability and Control. Balu, N.J., Lauby, M.G., Eds, McGraw-Hill, New York, NY, USA, 1994, pp. 271–312.

[60] P. Kundur et al., "Definition and classification of power system stability IEEE/CIGRE joint task force on stability terms and definitions," in IEEE Transactions on Power Systems, vol. 19, no. 3, pp. 1387-1401, Aug. 2004, doi: 10.1109/TPWRS.2004.825981.

[61] Volkswagen, "ID.3", 2019 [Online]. Available: https://bit.ly/32eAnAv

[62] Tesla, "Model 3", 2019. [Online]. Available: http://bit.ly/2WhRK3y

[63] J. Dixon, P. B. Andersen, K. Bell, and C. Træholt, "On the ease of being green: An investigation of the inconvenience of electric vehicle charging," Applied Energy, vol. 258, p. 114090, 2020. Available: https://doi.org/10.1016/j.apenergy.2019.114090.

[64] J . Dixon, W. Bukhsh, C. Edmunds, and K. Bell, "Scheduling electric vehicle charging to minimise carbon emissions and wind curtailment," Renewable Energy, vol. 161, p. 114090, 2020. Available: https://doi.org/10.1016/j.renene.2020.07.017.

[65] J. Dixon, "Keeping the Car Clean: on the Electrification of Private Transport: Summary Report," University of Strathclyde, Glasgow, 2020, 26 p. Available: https://pureportal.strath.ac.uk/en/studentTheses/keeping-the-car-clean-on-the-electrification-of-private-transport-2.

[66] P. W. Sauer and M. A. Pai, Power System Dynamics and Stability. Department of Electrical and Computer Engineering, University of Illinois at Urbana-Champaign, 1406 W. Green St., 2007

[67] S. Meikap, D. Das, C. Kumar and G. Buticchi, "A Multi-Port Converter System for Grid Tied Electric Vehicle Charging Station," 2022 IEEE 13th International Symposium on Power Electronics for Distributed Generation Systems (PEDG), Kiel, Germany, 2022, pp. 1-6, doi: 10.1109/PEDG54999.2022.9923228.

[68] M. Vasiladiotis and A. Rufer, "A Modular Multiport Power Electronic Transformer With Integrated Split Battery Energy Storage for Versatile Ultrafast EV Charging Stations," in IEEE Transactions on Industrial Electronics, vol. 62, no. 5, pp. 3213-3222, May 2015, doi: 10.1109/TIE.2014.2367237

[69] W. -C. Hsu, J. -F. Chen, Y. -P. Hsieh and Y. -M. Wu, "Design and Steady-State Analysis of Parallel Resonant DC–DC Converter for High-Voltage Power Generator," in IEEE Transactions on Power Electronics, vol. 32, no. 2, pp. 957-966, Feb. 2017, doi: 10.1109/TPEL.2016.2543506.

[70] S. Narula, G. Bhuvaneswari and B. Singh, "Power factor corrected bridgeless modular zeta converter based SMPS," 2016 IEEE 7th Power India International Conference (PIICON), Bikaner, India, 2016, pp. 1-5, doi: 10.1109/POWERI.2016.8077322.

[71] R. Almazmomi and A. A. Arkadan, "EM Based Modeling of EV Dynamic Charging Systems," 2023 International Applied Computational Electromagnetics Society Symposium (ACES), Monterey/Seaside, CA, USA, 2023, pp. 1-2, doi: 10.23919/ACES57841.2023.10114772.

[72] J. Yang, H. Chen, X. Meng, T. Ge, X. Guan and Y. Luo, "Electromagnetic Transient Simulation Modelling and Analysis of Electric Vehicle Charging Stations," 2023 IEEE International Conference on Advanced Power System Automation and Protection (APAP), Xuchang, China, 2023, pp. 604-607, doi: 10.1109/APAP59666.2023.10348422.

[73] T. N. Le, S. Al-Rubaye, H. Liang and B. J. Choi, "Dynamic charging and discharging for electric vehicles in microgrids," 2015 IEEE International Conference on Communication Workshop (ICCW), London, UK, 2015, pp. 2018-2022, doi: 10.1109/ICCW.2015.7247477.

[74] P. Palensky, A. A. Van Der Meer, C. D. Lopez, A. Joseph and K. Pan, "Cosimulation of Intelligent Power Systems: Fundamentals, Software Architecture, Numerics, and Coupling," in IEEE Industrial Electronics Magazine, vol. 11, no. 1, pp. 34-50, March 2017, doi: 10.1109/MIE.2016.2639825.

[75] C. Gomes, C. Thule, J. Deantoni, P. G. Larsen, and H. Vangheluwe, "Co-simulation: The Past, Future, and Open Challenges," in Leveraging Applications of Formal Methods, Verification and Validation. Distributed Systems, vol. 11246, T. Margaria and B. Steffen, Eds. Cham: Springer, 2018, pp. 504-520. doi: 10.1007/978-3-030-03424-5_34

[76] A. Akkermann, B. Å. Hjøllo, and M. Siegel, "Maritime Co-simulation Framework: Challenges and Results," in Validation and Verification of

Automated Systems, vol. 1, S. G. Lee, Ed. Cham: Springer, 2019, pp. 251-269. doi: 10.1007/978-3-030-14628-3_19.

[77] X. Wang, Z. He, and J. Yang, "Electric vehicle fast-charging station unified modelling and stability analysis in the dq frame," Energies, vol. 11, no. 5; May 2018.

[78] L. Wang, Z. Qin, L. B. Larumbe, and P. Bauer, "Multi-timescale modelling of fast charging stations for power quality analysis," 2021 23rd European Conference of Power Electronics and Applications. Ghent, Belgium; 2021.

[79] C. H. Dharmakeerthi, N. Mithulananthan and A. Atputharajah, "Development of dynamic EV load model for power system oscillatory stability studies," 2014 Australasian Universities Power Engineering Conference (AUPEC), Perth, WA, Australia; 2014.

[80] K . Qian, C. Zhou, M. Allan and Y. Yuan, "Modeling of Load Demand Due to EV Battery Charging in Distribution Systems," in IEEE Transactions on Power Systems, vol. 26, no. 2, pp. 802-810, May 2011, doi: 10.1109/TPWRS.2010.2057456.

[81] M . Yilmaz and P. T. Krein, "Review of charging power levels and infrastructure for plug-in electric and hybrid vehicles," 2012 IEEE International Electric Vehicle Conference, Greenville, SC, USA, 2012, pp. 1-8, doi: 10.1109/IEVC.2012.6183208.

[82] S. Amjad, S. Neelakrishnan, and R. Rudramoorthy, "Review of design considerations and technological challenges for successful development and deployment of plug-in hybrid electric vehicles", Renewable and Sustainable Energy Reviews 14, pp. 1104–1110, 2010.

[83] S . Bohn, M. Agsten, A. Dubey, and S. Santoso, "A comparative analysis of PEV charging impacts: An international perspective," SAE Technical Paper, Detroit, MI, USA, 2015. Available: https://www.sae.org/publications/technical-papers/content/2015-01-0300/.

[84] B.-R . Lin, T. L. Hung, and C.-H. Huang, "Bi-directional single-phase half-bridge rectifier for power quality compensation," IEE Proceedings - Electric Power Applications, vol. 150, pp. 397–406, 2003. Available: https://doi.org/10.1049/ip-epa:20030261.

[85] W. Kempton and J. Tomic, "Vehicle-to-grid power fundamentals: Calculating capacity and net revenue," J. Power Sources, vol. 144, pp. 268–279, 2005 doi:10.1016/j.jpowsour.2004.12.025.

[86] M. C. Kisacikoglu, B. Ozpineci and L. M. Tolbert, "EV/PHEV Bidirectional Charger Assessment for V2G Reactive Power Operation," in

IEEE Transactions on Power Electronics, vol. 28, no. 12, pp. 5717-5727, Dec. 2013, doi: 10.1109/TPEL.2013.2251007..

[87] O . Tremblay and L.A. Dessaint, “Experimental Validation of a Battery Dynamic Model for EV applications,” World Electric Vehicle Journal, vol. 3, pp. 289–298, 2009. Available: doi:10.3390/wevj3020289.

[88] N. Minorsky, “Directional stability of automatically steered bodies,” Journal of the American Society of Naval Engineers, vol. 34, no. 2, pp. 280-309, May 1922.

[89] S. Rastgoo, Z. Mahdavi, M. Azimi Nasab, M. Zand, and S. Padmanaban, “Using an Intelligent Control Method for Electric Vehicle Charging in Microgrids,” World Electric Vehicle Journal, vol. 13, no. 12, p. 222, Dec. 2022. [Online]. Available: https://doi.org/10.3390/wevj13120222.

[90] M. A. S. T. Ireshika, R. Lliuyacc-Blas, and P. Kepplinger, “Voltage-Based Droop Control of Electric Vehicles in Distribution Grids under Different Charging Power Levels,” Energies, vol. 14, no. 13, p. 3905, Jun. 2021. [Online]. Available: https://doi.org/10.3390/en14133905

[91] NERC Resources Subcommittee, “Balancing and Frequency Control,” North American Electric Reliability Corporation, Jan. 2011. [Online]. Available: https://www.nerc.com/comm/OC/BAL0031_Supporting_Documents_2017_DL/NERC%20Balancing%20and%20Frequency%20Control%20040520111.pdf.

[92] J. W. Heron and H. Sun, "Smart Electric Vehicle Charging with Ideal and Practical Communications in Smart Grids," 2019 IEEE Global Communications Conference (GLOBECOM), Waikoloa, HI, USA, 2019, pp. 1-6, doi: 10.1109/GLOBECOM38437.2019.9013481.

[93] D. Karlsson and D. J. Hill, "Modelling and identification of nonlinear dynamic loads in power systems," in IEEE Transactions on Power Systems, vol. 9, no. 1, pp. 157-166, Feb. 1994, doi: 10.1109/59.317546

[94] D.P. Stojanović, L. M. Korunović, and J. V. Milanović, “Dynamic load modelling based on measurements in medium voltage distribution network,” Electric Power Systems Research, vol. 78,]]]]]=]=no. 2, pp. 228–238, Feb. 2008. Available: https://doi.org/10.1016/j.epsr.2007.02.003.

[95] D J. Hill and I. A. Hiskens, "Dynamic analysis of voltage collapse in power systems," Proceedings of the 31st IEEE Conference on Decision and Control, Tucson, AZ, USA, 1992, pp. 2904-2909 vol.3, doi: 10.1109/CDC.1992.371279.

[96] W. Krajewski, A. Lepschy and U. Viaro, "Designing PI controllers for robust stability and performance," in IEEE Transactions on Control Systems Technology, vol. 12, no. 6, pp. 973-983, Nov. 2004, doi: 10.1109/TCST.2004.833619.

[97] E. O. Kontis, T. A. Papadopoulos, M. H. Syed, E. Guillo-Sansano, G. M. Burt and G. K. Papagiannis, "Artificial-Intelligence Method for the Derivation of Generic Aggregated Dynamic Equivalent Models," in IEEE Transactions on Power Systems, vol. 34, no. 4, pp. 2947-2956, July 2019, doi: 10.1109/TPWRS.2019.2894185.

[98] T. Hiyama, M. Tokieda, W. Hubbi and H. Andou, "Artificial neural network based dynamic load modeling," in IEEE Transactions on Power Systems, vol. 12, no. 4, pp. 1576-1583, Nov. 1997, doi: 10.1109/59.627861.

[99] C. Zhang *et al.*, "Appropriate Evaluation of Primary Frequency Response and Its Applications," *2023 IEEE PES GTD International Conference and Exposition (GTD)*, Istanbul, Turkiye, 2023, pp. 119-123, doi: 10.1109/GTD49768.2023.00049.

[100] B. Gustavsen, A. Semlyen. "Rational approximation of frequency domain responses by vector fitting." in IEEE Transactions on Power Delivery, vol. 14, no. 3, pp. 1052-1061. July 1999, doi: 10.1109/61.772353.

[101] The MathWorks, Inc. (2004). Curve Fitting Toolbox for Use with MATLAB. Accessed: January 01, 2023. Available:http://cda.psych.uiuc.edu/matlab_pdf/curvefit.pdf

[102] E. O. Kontis, A. I. Chrysochos, G. K. Papagiannis and T. A. Papadopoulos. "Development of measurement-based generic load models for dynamic simulations," In Proceedings of the 2015 IEEE Eindhoven PowerTech, Eindhoven, The Netherlands, 29 June–2 July 2015, pp. 1–6, doi:10.1109/PTC.2015.7232800.

[103] E. O. Kontis, T. A. Papadopoulos, A. I. Chrysochos and G. K. Papagiannis. "Measurement-Based Dynamic Load Modeling Using the Vector Fitting Technique". in IEEE Transactions on Power Systems, vol. 33, no. 1, pp. 338-351, Jan. 2018, doi: 10.1109/TPWRS.2017.2697004

[104] G. Zhang and J. McCalley, "Optimal power flow with primary and secondary frequency constraint," *2014 North American Power Symposium (NAPS)*, Pullman, WA, USA, 2014, pp. 1-6, doi: 10.1109/NAPS.2014.6965392.

[105] Chih-Wen Liu and J. S. Thorp, "New methods for computing power system dynamic response for real-time transient stability prediction," in *IEEE Transactions on Circuits and Systems I: Fundamental Theory and Applications*, vol. 47, no. 3, pp. 324-337, March 2000, doi: 10.1109/81.841915

[106] B. Zhou, T. Littler and L. Meegahapola, "Assessment of transient stability support for electric vehicle integration," *2016 IEEE Power and Energy Society General Meeting (PESGM)*, Boston, MA, USA, 2016, pp. 1-5, doi: 10.1109/PESGM.2016.7741347.

[107] E. Jong, "A Framework for Incorporation of Infeed Uncertainty in Power System Risk-Based Security Assessment," IEEE Transactions on Power Systems, vol. 33, no. 1, pp. 1-10, Jan. 2018.

[108] C. Palensky, "Impedance-Based Analysis for Power Electronics-Based Systems," CIGRE Science & Engineering, no. 29, pp. 1-8, Nov. 2019.

[109] J. A. P. Lopes, F. J. Soares, P. M. R. Almeida. "Integration of Electric Vehicles in the Electric Power System." in Proceedings of the IEEE, vol. 99, no. 1, pp. 168-183, Jan. 2011, doi: 10.1109/JPROC.2010.2066250.

[110] R. Freire, J. Delgado, J. M. Santos and A. T. de Almeida, "Integration of renewable energy generation with EV charging strategies to optimize grid load balancing," 13th International IEEE Conference on Intelligent Transportation Systems, Funchal, Portugal, 2010, pp. 392-396, doi: 10.1109/ITSC.2010.5625071.

[111] Brenna, Morris, Federica Foiadelli, Carola Leone and Michela Longo. "Electric Vehicles Charging Technology Review and Optimal Size Estimation." Journal of Electrical Engineering & Technology 15 (2020): 2539 - 2552.

[112] H. Padullaparti, A. Pratt, I. Mendoza, S. Tiwari, M. Baggu, C. Bilby, and Y. Ngo, "Peak Demand Management and Voltage Regulation Using Coordinated Virtual Power Plant Controls," National Renewable Energy Laboratory, Golden, CO, USA, Tech. Rep. NREL/TP-5D00-81105, Sep. 2023. [Online]. Available: https://www.nrel.gov/docs/fy24osti/81105.pdf

[113] S. Abdelkader, J. Amissah, and O. Abdel-Rahim, "Virtual power plants: an in-depth analysis of their advancements and importance as crucial players in modern power systems," *Energy, Sustainability and Society*, vol. 14, no. 52, Aug. 2024. [Online]. Available: https://energsustainsoc.biomedcentral.com/articles/10.1186/s13705-024-00483-y

[114] Hu, Z., Song, Y., Xu, Z. (2015). Hierarchical Coordinated Control Strategies for Plug-in Electric Vehicle Charging. In: Rajakaruna, S., Shahnia, F., Ghosh, A. (eds) Plug In Electric Vehicles in Smart Grids. Power Systems. Springer, Singapore. https://doi.org/10.1007/978-981-287-317-0_3

[115] M. K. Das and S. K. Jain, "Review on Optimization Techniques used for Scheduling of Electric Vehicle Charging," 2021 International Conference on

Control, Automation, Power and Signal Processing (CAPS), Jabalpur, India, 2021, pp. 1-6, doi: 10.1109/CAPS52117.2021.9730621.

[116] M. A. del Cacho Estil-les, M. Pia Fanti, A. M. Mangini and M. Roccotelli, "Electric Vehicles Routing Including Smart-Charging Method and Energy Constraints," 2022 IEEE 18th International Conference on Automation Science and Engineering (CASE), Mexico City, Mexico, 2022, pp. 1735-1740, doi: 10.1109/CASE49997.2022.9926492.

[117] M. Chen, J. Shen, F. Wu, F. Zhao, Q. Zhang and S. Zhang, "Coordination and Optimization Scheduling Strategy for Distribution Network Based on Composite Demand Side Response," 2022 IEEE/IAS Industrial and Commercial Power System Asia (I&CPS Asia), Shanghai, China, 2022, pp. 1327-1332, doi: 10.1109/ICPSAsia55496.2022.9949624.

[118] H. Ma, L. Lai and J. Sun, "A New Coordinated Distribution Network Planning Method Considering Demand Response," 2021 IEEE 5th Conference on Energy Internet and Energy System Integration (EI2), Taiyuan, China, 2021, pp. 1254-1259, doi: 10.1109/EI252483.2021.9713468.

[119] L. Gong, Y. Guo, H. Sun and W. Deng, "Model Predictive Control-Based Real-Time Optimal Charging of Electric Vehicle Aggregators," 2022 IEEE Power & Energy Society General Meeting (PESGM), Denver, CO, USA, 2022, pp. 1-5, doi: 10.1109/PESGM48719.2022.9916951.

[120] H. Ali, B. Francois, L. Brotcorne, Z. Foroozandeh and J. P. Soares, "Model predictive control for smart grid charging of autonomous electric vehicle fleet using local renewable energy generation," 27th International Conference on Electricity Distribution (CIRED 2023), Rome, Italy, 2023, pp. 1889-1893, doi: 10.1049/icp.2023.1063.

[121] T. Chen, X. Zhang, and J. Wang, "A Review on Electric Vehicle Charging Infrastructure Development in the UK," J. Mod. Power Syst. Clean Energy, vol. 8, pp. 193–205, 2020, doi:10.35833/MPCE.2018.000374.

[122] R. Garcia-Valle, J.A.P. Lopes, "Electric Vehicle Integration into Modern Power Networks," Springer Science & Business Media, New York, NY, USA, 2013, vol. 4, pp. 87–107, pp. 155–203, doi:10.1007/978-1-4614-0134-6.

[123] G. A. Putrus, P. Suwanapingkarl, D. Johnston, E. C. Bentley, and M. Narayana, "Impact of electric vehicles on power distribution networks," 5th IEEE Vehicle Power and Propulsion Conference, VPPC '09, pp. 827–831, 2009. [Online]. Available: https://doi.org/10.1109/VPPC.2009.5289760

[124] S. Shao, M. Pipattanasomporn, and S. Rahman, "Challenges of PHEV penetration to the residential distribution network," 2009 IEEE Power and Energy Society General Meeting, PES '09, pp. 1–8, 2009. [Online]. Available: https://doi.org/10.1109/PES.2009.5275806.

[125] L. Pieltain Fernández, T. Gómez San Román, R. Cossent, C. Mateo Domingo, and P. Frías, “Assessment of the impact of plug-in electric vehicles on distribution networks,” IEEE Transactions on Power Systems, vol. 26, no. 1, pp. 206–213, 2011. [Online]. Available: https://doi.org/10.1109/TPWRS.2010.2049133

[126] P. Richardson, D. Flynn, and A. Keane, “Impact assessment of varying penetrations of electric vehicles on low voltage distribution systems,” IEEE PES General Meeting, PES 2010, pp. 1–6, 2010. [Online]. Available: https://doi.org/10.1109/PES.2010.5589940.

[127] A. Ihekwaba, C. Kim, Analysis of electric vehicle charging impact on grid voltage regulation, 2017 North American Power Symposium (NAPS), pp. 1-6, 2017

[128] A.G. Anastasiadis, G.P. Kondylis, A. Polyzakis, G. Vokas, “Effects of increased electric vehicles into a distribution network,” Energy Procedia, Vol. 157, pp. 586-593, 2019.

[129] C.C. Mendoza, A.M. Quintero, F. Santamaria, A. Alarcon, “Coordinated recharge of electric vehicles in real time.” DYNA, Vol. 83, No. 197, pp. 222-231, 2016.

[130] S. Gao, H. Jia, J. Liu, C. Liu, “Integrated configuration and charging optimization of aggregated electric vehicles with renewable energy sources.” Energy Procedia, Vol. 158, pp. 2986-2993, 2019

[131] Hugo Morais, Tiago Sousa, Zita Vale, Pedro Faria. “Evaluation of the electric vehicle impact in the power demand curve in a smart grid environment. Energy Conversion and Management.” Volume 82, 2014, Pages 268-282, ISSN 0196-8904, https://doi.org/10.1016/j.enconman.2014.03.032.

[132] M. Gilleran, E. Bonnema, J. Woods, P. Mishra, I. Doebber, C. Hunter, M. Mitchell, and M. Mann, “Impact of electric vehicle charging on the power demand of retail buildings,” Advances in Applied Energy, vol. 4, 2021, article 100062, ISSN 2666-7924, https://doi.org/10.1016/j.adapen.2021.100062.

[133] S. Bae and A. Kwasinski, "Spatial and Temporal Model of Electric Vehicle Charging Demand," in IEEE Transactions on Smart Grid, vol. 3, no. 1, pp. 394-403, March 2012, doi: 10.1109/TSG.2011.2159278.

[134] C. H. Stephan and J. Sullivan, “Environmental and energy implications of plug-in hybrid-electric vehicles,” Environ. Sci. Tech, vol. 42, no. 4, pp. 1185–1190, Feb. 2008

[135] M. Kintner-Meyer, K. P. Schneider, and R. G. Pratt, “Impacts assessment of plug-in hybrid vehicles on electric utilities and regional US power grids: Part

1: Technical analysis." Pacific Northwest National Laboratory, Richland, WA, Tech. Rep. PNNL-SA-61669, 2007

[136] P. Zhang, K. Qian, C. Zhou, B. G. Stewart and D. M. Hepburn, "A Methodology for Optimization of Power Systems Demand Due to Electric Vehicle Charging Load," in *IEEE Transactions on Power Systems*, vol. 27, no. 3, pp. 1628-1636, Aug. 2012, doi: 10.1109/TPWRS.2012.2186595.

[137] J. Dunckley and G. Tal, "Plug-In Electric Vehicle Multi-State Market and Charging Survey," Electric Power Research Institute, Palo Alto, CA, Tech. Rep

[138] UK Data Service. UK National travel survey, Aug 2020, https://www.gov.uk/government/statistical-data-sets/nts02-driving-licence-holders

[139] R. C. Leou, C. L. Su, and C. N. Lu, "Stochastic analyses of electric vehicle charging impacts on distribution network," IEEE Transactions on Power Systems, vol. 29, no. 3, pp. 1055–1063, 2014. [Online]. Available: https://doi.org/10.1109/TPWRS.2013.2291556

[140] E. Veldman and R. A. Verzijlbergh, "Distribution grid impacts of smart electric vehicle charging from different perspectives," IEEE Transactions on Smart Grid, vol. 6, no. 1, pp. 333–342, 2015. [Online]. Available: https://doi.org/10.1109/TSG.2014.2355494

[141] A. Lojowska, D. Kurowicka, G. Papaefthymiou, and L. Van Der Sluis, "Stochastic Modeling of Power Demand due to EVs Using Copula," IEEE Transactions on Power Systems, vol. 27, no. 4, pp. 1960–1968, 2012. [Online]. Available: https://doi.org/10.1109/TPWRS.2012.2192139

[142] J.-C. Walter and G. T. Barkema, "An introduction to Monte Carlo methods," Physica A, 2014.

[143] P.-C.G. Vassiliou and A. C. Georgiou, "Markov and Semi-Markov Chains, Processes, Systems, and Emerging Related Fields," *Mathematics*, vol. 9, no. 19, p. 2490, 2021. [Online]. Available: https://doi.org/10.3390/math9192490.

[144] S. Brooks, A. Gelman, G. Jones, and X.-L. Meng, "A conceptual introduction to Markov Chain Monte Carlo methods," arXiv preprint, 2011

[145] Y. Iwafune, K. Ogimoto, Y. Kobayashi and K. Murai, "Driving Simulator for Electric Vehicles Using the Markov Chain Monte Carlo Method and Evaluation of the Demand Response Effect in Residential Houses," in *IEEE Access*, vol. 8, pp. 47654-47663, 2020, doi: 10.1109/

[146] H. Tayarani, T. V. Ramadoss, V. Karanam, G. Tal, and C. Nitta, "Forecasting Battery Electric Vehicle Charging Behavior: A Deep Learning

Approach Equipped with Micro-Clustering and SMOTE Techniques," arXiv:2307.10588, 2023. [Online]. Available: https://arxiv.org/pdf/2307.10588.

[147] Y. Wang and D. Infield, "Markov Chain Monte Carlo simulation of electric vehicle use for network integration studies," Int. J. Electr. Power Energy Syst., vol. 99, pp. 85-94, 2018.

[148] M. Shibl, L. Ismail, and A. Massoud, "Electric Vehicles Charging Management Using Machine Learning Considering Fast Charging and Vehicle-to-Grid Operation," Energies, vol. 14, no. 19, p. 6199, 2021. [Online]. Available: https://doi.org/10.3390/en14196199

[149] A. Zhang, Q. Liu, J. Liu, and L. Cheng, "CASA: cost-effective EV charging scheduling based on deep reinforcement learning," Neural Computing and Applications, vol. 36, pp. 8355–8370, 2024.

[150] K. Rudion, A. Orths, Z. A. Styczynski,K. Strunz. "Design of benchmark of medium voltage distribution network for investigation of DG integration." 2006 IEEE Power Engineering Society General Meeting, 2006, pp. 6 pp.-, doi: 10.1109/PES.2006.1709447

[151] Buchhholz, H. Frey, N. Lewald, T. Stephanblome, Z. Styczynki. "Advanced planning and operation of dispersed generation ensuring power quality security and efficiency in distribution systems." Cigre 2004 session, Paris, France August September 2004.

[152] J. V. Milanovic, Julija. Matevosyan, Anish. Gaikwad, "Modelling and Aggregation of Loads in Flexible Power Networks.", 2014, Scope and Status of the Work of CIGRE WG C4.605.

[153] Durr Matthias, Cruden Andrew, Gair Sinclair, McDonald J.R, "Dynamic model of a lead acid battery for use in a domestic fuel cell system," Journal of Power Sources, Volume 161, n 2, October 27, 2006, pp 1400-1411

[154] Corrigan D, Masis A, Batteries foe electric and hybrid vehicles, 2011, In: Reddy TB (ed) Linden's handbook of batteries, 4th edn, McGraw Hill, New York.

[155] E. Kuhn, C. Forgez, P. Lagonotte, G. Friedrich, "Modelling Ni-mH battery using Cauer and Foster structures," Journal of Power Sources, v 158, n 2 SPEC. ISS., Aug 25, 2006, pp 1490-1497

[156] M. A Fetcenko, S. R. Ovshinsky, B. Reichman, K. Young, C. Fierro, J. Koch, A. Zallen, W. Mays, and T. Ouchi, "Recent advances in NiMH battery technology," Journal of Power Sources, vol. 165, no. 2, pp. 544–551, 2007

[157] G. Zubi, R. Dufo-López, M. Carvalho, and G. Pasaoglu, "The lithium-ion battery: State of the art and future perspectives," Renewable and

Sustainable Energy Reviews, vol. 89, pp. 292-308, 2018. Available: https://doi.org/10.1016/j.rser.2018.03.002.

[158] S. Dhameja, Electric Vehicle Battery Systems. Boston, MA, USA: Newnes, 2002..

[159] Musavi, F.; Edington, M.; Eberle, W.; Dunford, W.G. "Evaluation and Efficiency Comparison of Front End AC-DC Plug-in Hybrid Charger Topologies." IEEE Trans. Smart Grid 2012, 3, 413–421, doi:10.1109/TSG.2011.2166413.

[160] J.-S Kim, G.-Y. Choe, H.-M. Jung, B.-K. Lee, Y.-J. Cho, and K.-B. Han, "Design and implementation of a high-efficiency on-board battery charger for electric vehicles with frequency control strategy," in Proceedings of the 2010 IEEE Vehicle Power and Propulsion Conference, Lille, France, 1–3 September 2010, pp. 1–6. Available: doi:10.1109/VPPC.2010.5729042.

[161] Xu Xiao et al., "Component-based modelling of EV battery chargers," 2015 IEEE Eindhoven PowerTech, Eindhoven, 2015, pp. 1-6, doi: 10.1109/PTC.2015.7232690.

[162] M Restrepo, J. Morris, M. Kazerani, and C. A. Cañizares, "Modelling and testing of a bidirectional smart charger for distribution system EV integration," IEEE Transactions on Smart Grid, vol. 9, pp. 152–162, 2016. Available: doi:10.1109/TSG. 2016.2547178.

[163] Delta Electronics, Inc. Delta EV DC Quick Charger for EU. Available online: https://chademo.com/portfolios/delta-electronics1-2/.

[164] V. Caliskan, D. J. Perreault, T. M. Jahns and J. G. Kassakian, "Analysis of three-phase rectifiers with constant-voltage loads," 30th Annual IEEE Power Electronics Specialists Conference. Record. (Cat. No.99CH36321), Charleston, SC, USA, 1999, pp. 715-720 vol.2, doi: 10.1109/PESC.1999.785588.

[165] David J. McLaughlin. Applied Electrical Engineering Fundamentals. Chapter 4.4: Rectifier Diode. 2003, University of Massachusetts at Amherst https://openbooks.library.umass.edu/funee/

[166] V. M. Rao, A. K. Jain, K. K. Reddy and A. Behal, "Experimental Comparison of Digital Implementations of Single-Phase PFC Controllers," in IEEE Transactions on Industrial Electronics, vol. 55, no. 1, pp. 67-78, Jan. 2008, doi: 10.1109/TIE.2007.904016

[167] M. Chen, A. Mathew and J. Sun, "Nonlinear Current Control of Single-Phase PFC Converters," in IEEE Transactions on Power Electronics, vol. 22, no. 6, pp. 2187-2194, Nov. 2007, doi: 10.1109/TPEL.2007.909410.

[168] B. Singh, B. N. Singh, A. Chandra, K. Al-Haddad, A. Pandey and D. P. Kothari, "A review of single-phase improved power quality AC-DC converters," in IEEE Transactions on Industrial Electronics, vol. 50, no. 5, pp. 962-981, Oct. 2003, doi: 10.1109/TIE.2003.817609.

[169] A. Collin, S. Djokic, H. Thomas, and J. Meyer, "Modelling of electric vehicle chargers for power system analysis," in Proceedings of the 11th International Conference on Electrical Power Quality and Utilisation, Lisbon, Portugal, 17–19 October 2011, pp. 1–6, doi:10.1109/EPQU.2011.6128816.

[170] C.S Lee, J.B. Jeong, B.H. Lee, and J. Hur, "Study on 1.5 kW battery chargers for neighbourhood electric vehicles," in Proceedings of the 2011 IEEE Vehicle Power and Propulsion Conference, Chicago, IL, USA, 6–9 September 2011, pp. 1–4, doi:10.1109/VPPC.2011.6043129.

[171] R . Horton, J.A. Taylor, A. Maitra, and J. Halliwell, "A time-domain model of a plug-in electric vehicle battery charger," in Proceedings of the 2012 PES T & D, Orlando, FL, USA, 7–10 May 2012, pp. 1–5doi:10.1109/TDC.2012.6281409.

[172] B. Singh, B. N. Singh, A. Chandra, K. Al-Haddad, A. Pandey and D. P. Kothari, "A review of three-phase improved power quality AC-DC converters," in IEEE Transactions on Industrial Electronics, vol. 51, no. 3, pp. 641-660, June 2004, doi: 10.1109/TIE.2004.825341

[173] S. Habib, M. M. Khan, F. Abbas, and H. J. Tang, "Assessment of electric vehicles concerning impacts, charging infrastructure with unidirectional and bidirectional chargers and power flow comparisons," International Journal of Energy Research. vol. 42, no. 11, pp. 3416– 3441, Sep. 2018

[174] IEEE Task Force report, "Load representation for dynamic performance analysis." Paper 92WM126-3 PWRD, presented at the IEEE pES winter Meeting, New York, January 26-30, 1992.

[175] L.M. Korunović, J.V. Milanović, S.Z. Djokic, K. Yamashita, S.M. Villanueva, and S. Sterpu, "Recommended Parameter Values and Ranges of Most Frequently Used Static Load Models," IEEE Trans. Power Syst., vol. 33, pp. 5923–5934, 2018 doi:10.1109/TPWRS.2018.2834725.

[176] A . Bokhari, A. Alkan, and R. Dogan, "Experimental determination of the ZIP coefficients for modern residential, commercial, and industrial loads," IEEE Trans. Power Deliv., vol. 29, pp. 1372–1381, 2013, doi:10.1109/TPWRD. 2013. 2285096.

[177] A. C. Melhorn, K. McKenna, A. Keane, D. Flynn, and A. Dimitrovski, "Autonomous plug and play electric vehicle charging scenarios including reactive power provision: a probabilistic load flow analysis," IET Generation, Transmission & Distribution, vol. 11, no. 3, pp. 768–775, Feb. 2017

[178] J. Dixon. 2021. Code for EV Charging. [Online]. Available at: https://github.com/jamesjhdixon/EVCharging.

[179] Google, Google maps [Online]. Available: https://www.google.co.uk/maps, 2019.

[180] UK Data Service, UK national travel survey 2002-2016 [Online]. Available: https://goo.gl/LgtfDd, 2019.

[181] Technical Reference Documentation – General Load "ElmLod", "TypLod", DgiSILENT PowerFactory User Manual 2021.

[182] J. Rotman, Galois Theory, 1st ed. New York, NY, USA: Springer New York, 1990

[183] T. W. Hungerford, Algebra, 1st ed. New York, NY, USA: Springer New York, 1974.

[184] D. Mandic and V. S. L. Goh, "The Magic of Complex Numbers," Imperial College London, 2009.

[185] Mirzaee, F., Samadyar, N. & Alipour, S. Numerical solution of high order linear complex differential equations via complex operational matrix method. SeMA 76, 1–13 (2019). https://doi.org/10.1007/s40324-018-0151-7

[186] Department for Business, Energy and Industrial Strategy (BEIS). (2021). Domestic Electricity Consumption in Great Britain [Report]. Retrieved from https://www.gov.uk/government/statistics/energy-consumption-in-the-uk-2022

[187] G. A. Barzegkar-Ntovom, T. A. Papadopoulos, E. O. Kontis. "Robust Framework for Online Parameter Estimation of Dynamic Equivalent Models Using Measurements." *in IEEE Transactions on Power Systems*, vol. 36, no. 3, pp. 2380-2389, May 2021, doi: 10.1109/TPWRS.2020.3033385

[188] A. M. Perdon and B. Wyman, "On the zeros and poles of a transfer function," Linear Algebra and its Applications, 1989.

[189] E. O. Kontis, S. P. Dimitrakopoulos, A. I. Chrysochos, G. K. Papagiannis and T. A. Papadopoulos. "Dynamic equivalencing of active distribution grids." 2017 IEEE Manchester PowerTech, 2017, pp. 1-6, doi: 10.1109/PTC.2017.7981103.

[190] Jacqueline Wilkie, Michael johnson, Reza Katebi. Control engineering – an introductory course. RED GLOBAL PRESS, London, UK, 2002.

[191] MASSACHUSETTS INSTITUTE OF TECHNOLOGY, "Understanding Poles and Zeros," Department of Mechanical Engineering, 2.14 Analysis and Design of Feedback Control Systems

[192] Frost & Sullivan, public report “M5B6-Global Electric Vehicles Lithium-ion Battery Second Life and Recycling Market Analysis”, online, 2010.

[193] O. Tremblay, L. Dessaint and A. Dekkiche, "A Generic Battery Model for the Dynamic Simulation of Hybrid Electric Vehicles," 2007 IEEE Vehicle Power and Propulsion Conference, 2007, pp. 284-289, doi: 10.1109/VPPC.2007.4544139.

[194] S. Tong, M.P. Klein, and J.W. Park, “On-line optimization of battery open circuit voltage for improved state-of-charge and state-of-health estimation,” J. Power Sources, vol. 293, pp. 416–428, 2015,, doi:10.1016/j.jpowsour.2015.03.157.